Massachusetts Institute of Technology
Department of Civil Engineering
Constructed Facilities Division
Cambridge, Massachusetts 02139

Evaluation of Seismic Safety of Buildings

Report No. 11

INELASTIC DYNAMIC DESIGN OF STEEL FRAMES TO RESIST SEISMIC LOADS

by

JAMES HERBERT ROBINSON, JR.

Supervised by

John M. Biggs

July 1977

Sponsored by National Science Foundation
Division of Advanced Environmental Research
and Technology
Grants ATA 74-06935 and ENV 76-19021

Publication No. R77-23 Order No. 574

SHEET	MIT-CE-R77-23	2.	3. Recipient's Accession No.

4. Title and Subtitle

INELASTIC DYNAMIC DESIGN OF STEEL FRAMES TO RESIST SEISMIC LOADS (Evaluation of Seismic Safety of Buildings)

5. Report Date: July 1977

6.

7. Author(s): James H. Robinson, Supervised by Prof. John M. Biggs

8. Performing Organization Rept. No. R77-23, No. 574

9. Performing Organization Name and Address

Massachusetts Institute of Technology
Dept. of Civil Engineering
77 Massachusetts Avenue
Cambridge, Massachusetts 02139

10. Project/Task/Work Unit No.

11. Contract/Grant No.
ATA 74-06935 and
ENV 76-19021

12. Sponsoring Organization Name and Address

National Science Foundation
1800 "G" St., N.W.
Washington, D.C. 20550

13. Type of Report & Period Covered
Research. 10/76 to present

14.

15. Supplementary Notes

This is report No. 11 of a series begun under NSF GRANT ATA 74-06935 and continued under NSF Grant ENV 76-19021.

16. Abstracts

The reliability of an inelastic design procedure based upon elastic modal analysis using an inelastic response spectrum proposed by Newmark and Hall is investigated. This was accomplished by computing the inelastic response in terms of local member ductilities, of three st eel moment-resisting frames, to simulated earthquake motions derived from the design response spectrum. The effects of P-Δ forces, earthquake motion details, assumed damping level, and earthquake intensity were examined.

The results indicate that the unmodified inelastic seismic design procedure is unconservative, probably because modal responses cannot be combined according to SRSS to compute the total inelastic response, although it is felt that there is a great deal of promise in the use of inelastic spectra in the seismic design of structures.

17. Key Words and Document Analysis. 17a. Descriptors

structural dynamics
inelastic response
frames
seismic design
inelastic spectra
P-Δ effect
Ductility

17b. Identifiers/Open-Ended Terms

17c. COSATI Field/Group 13 02 Civil Engineering 13 13 Structural Engineering

18. Availability Statement	19. Security Class (This Report)	21. No. of Pages
Release Unlimited	UNCLASSIFIED	143
	20. Security Class (This Page) UNCLASSIFIED	22. Price PC A07-A01

ABSTRACT

This report details an investigation designed to determine the reliability of an inelastic design procedure based upon elastic modal analysis using an inelastic response spectrum proposed by Newmark and Hall. This was accomplished by computing the inelastic response, in terms of local member ductilities, of three steel moment-resisting frames to simulated earthquake motions derived from the design response spectrum. The effects of P-Δ forces, earthquake motion details, assumed damping level, and earthquake intensity were examined.

The results indicate that the unmodified inelastic seismic design procedure is unconservative, most likely because individual modal responses, based on elastic modal properties, cannot be combined according to SRSS to compute total inelastic response with sufficient accuracy. However, it is possible to achieve the desired inelastic response, with respect to both level of yielding and distribution of yielding throughout the structure, by increasing member strength or design forces.

It is felt that in spite of the design difficulties demonstrated herein, there is a great deal of promise in the use of inelastic spectra in the seismic design of structures. More research is necessary to determine necessary modifications to the inelastic design spectrum.

PREFACE

This is the eleventh report prepared under the research project entitled "Evaluation of Seismic Safety of Buildings," supported by National Science Foundation Grant ATA 74-06935 and its continuation Grant ENV 76-19021. This report is derived from a thesis written by James H. Robinson in partial fulfillment of the requirements for the degree of Master of Science in the Department of Civil Engineering at the Massachusetts Institute of Technology.

The purpose of the supporting project is to evaluate the effectiveness of the total seismic design process, which consists of steps beginning with seismic risk analysis through dynamic analysis and the design of structural components. The project seeks to answer the question: "Given a set of procedures for these steps, what is the actual degree of protection against earthquake damage provided?" Alternative methods of analysis and design are being considered. Specifically, these alternatives are built around three methods of dynamic analysis: (1) time-history analysis, (2) response spectrum modal analysis, and (3) random vibration analysis.

The formal reports produced thus far are:

1. Arnold, Peter, Vanmarcke, Erik H., and Gazetas, George, "Frequency Content of Ground Motions during the 1971 San Fernando Earthquake," M.I.T. Department of Civil Engineering Research Report R76-3, Order No. 526, January 1976.
2. Gasparini, Dario, and Vanmarcke, Erik H., "Simulated Earthquake Motion Compatible with Prescribed Response Spectra," M.I.T. Department of Civil Engineering Research Report R76-4, Order No. 527, January 1976.
3. Vanmarcke, Erik H., Biggs, J.M., Frank, Robert, Gazetas, George, Arnold, Peter, Gasparini, Dario A., and Luyties, William, "Comparison of Seismic Analysis Procedures for Elastic Multi-degree Systems," M.I.T. Department of Civil Engineering Research Report R76-5, Order No. 528, January 1976.
4. Frank, Robert, Anagnostopoulos, Stavros, Biggs, J.M., and Vanmarcke, Erik H., "Variability of Inelastic Structural Response Due to Real and Artificial Ground Motions," M.I.T. Department of Civil Engineering Research Report R76-6, Order No. 529, January 1976.

5. Haviland, Richard, "A Study of the Uncertainties in the Fundamental Translational Periods and Damping Values for Real Buildings," Supervised by Professors J. M. Biggs and Erik H. Vanmarcke, M.I.T. Department of Civil Engineering Research Report R76-12, Order No. 531, February 1976.

6. Luyties, William H. III, Anagnostopoulos, Stavros, and Biggs, John M., "Studies on the Inelastic Dynamic Analysis and Design of Multi-Story Frames," M.I.T. Department of Civil Engineering Research Report R76-29, Order No. 548, July 1976.

7. Gazetas, George, "Random Vibration Analysis of Inelastic Multi-Degree-of-Freedom Systems Subjected to Earthquake Ground Motions," Supervised by Professor Erik H. Vanmarcke, M.I.T. Department of Civil Engineering Research Report R76-39, Order No. 556, August 1976.

8. Haviland, Richard W., Biggs, John M., and Anagnostopoulos, Stavros A., "Inelastic Response Spectrum Design Procedures for Steel Frames," M.I.T. Department of Civil Engineering Research Report R76-40, Order No. 557, September 1976.

9. Gasparini, Dario A., "On the Safety Provided by Alternate Seismic Design Methods," Supervised by Professors J. M. Biggs and Erik H. Vanmarcke, M.I.T. Department of Civil Engineering Research Report R77-22, Order No. 573, July 1977.

10. Vanmarcke, Erik H., and Lai, Shih-sheng P., "Strong Motion Duration of Earthquakes," M.I.T. Department of Civil Engineering Research Report R77-16, Order No. 569, July 1977.

The project is supervised by Professors John M. Biggs and Erik H. Vanmarcke of the Civil Engineering Department. They have been assisted by Dr. Stavros Anagnostopoulos, a Research Associate in the Department. Research assistants, in addition to Mr. Robinson, who contributed to the work reported herein were Peter Arnold, Robert Frank, William Luyties, Dario Gasparini, Richard Haviland, George Gazetas, Shih-sheng P. Lai, and Ricardo Binder.

TABLE OF CONTENTS

TABLE OF CONTENTS
(continued)

LIST OF FIGURES

LIST OF FIGURES (Continued)

LIST OF FIGURES (Continued)

LIST OF FIGURES (Continued)

LIST OF TABLES

CHAPTER 1 - INTRODUCTION

1.1 RECENT SEISMIC DESIGN RESEARCH

Current seismic design is based on the calculation of a base shear force which reflects both frame and site seismic characteristics. The base shear is distributed as a static lateral load over the height of the frame. A static elastic analysis of the effect the seismic lateral loads coupled with various combinations of wind and dead and live loads is performed to determine necessary member strength. It is economically unfeasible to design most frames to behave elastically under all earthquake loads having a reasonable probability of occurring during the lifetime of the structure. Researchers in the past have investigated the possibility of designing frames to experience a certain amount of inelastic behavior under moderate earthquake loads (3,4,12,14,15), and most code provisions for seismic design implicitly assume that some inelastic behavior will occur should a code designed frame be subjected to a moderate or severe earthquake (3, 8).

Clough, Benuska, and Wilson (9) performed a study in which member moment yield strength in a twenty-story reinforced concrete frame was based on a static analysis of the effect of seismic lateral loads determined from the 1959 SEAOC Code combined with the effect of dead and live gravity loads. Girder yield moment was arbitrarily set at twice the design moment determined in the static analysis. Column yield moments were chosen to reflect axial load-moment interaction and ranged from five times the static analysis design moment in the upper stories to ten times

the design moment in the lower stories of the frame. A second more flexible frame was also studied in which column yield moment varied from two to six times the static analysis moments. Results of a step-by-step inelastic time integration seismic analysis of the response of the frames to four seconds of the 1940 El Centro earthquake indicated that most of the yielding in frames designed in this manner will occur in the girders. The only significant column yielding took place in the upper stories of the more flexible frame. These results are characteristic of the so-called strong column - weak girder design philosophy (2). Ductility demand, defined as the ratio of maximum end rotation to yield rotation under antisymmetric end moments, varied greatly throughout the frame. Ductility ranged from 1.0 to approximately 6.5. Clough et al. concluded that elastic static analysis of code lateral forces does not present an obvious direct method of calculating member ductility requirement. Furthermore, it is apparent that such an approach does not promote a uniform distribution of inelastic behavior throughout the structure.

In a second report, Clough and Benuska (8) again determined girder and column strength from the results of a static analysis of forces due to code lateral and gravity loads. Girder and column moment capacities were set at two times and six times the moments determined in the static analysis respectively. These member strengths were thought to be typical of the strength characteristics of many high-rise reinforced concrete frames. After reviewing the results of an inelastic time integration analysis of the response of the frame to earthquake motion, Clough

and Benuska again concluded that in typical reinforced concrete frames inelastic behavior is concentrated in the relatively weak girders in the frame. It was suggested that weak areas in a frame attract a major portion of any inelastic behavior which might occur during response to seismic motions.

In a similar study, Walpole and Shepherd (26) applied factors of 1.5 and 1.25 to design loads determined by static analysis for columns and girders respectively in a six-story reinforced concrete frame. The same frame was also studied with a load factor of 1.25 applied to column design loads. An inelastic dynamic analysis of each frame was performed in addition to an elastic dynamic analysis. The authors found that yielding was restricted to the beams in the frame with the larger column load factor, while yielding did occur in the columns of the second frame. A comparison of the results of the elastic dynamic analysis with those of the inelastic dynamic analysis indicated that the ratio of elastic maximum end moment to specified yield moment is useful in predicting the ductility requirements determined by inelastic analysis.

Anderson and Gupta (3) proposed determining seismic design forces from a modal analysis using an elastic response spectrum instead of determining design loads from a static analysis of code lateral loads. The authors attempted to restrict inelastic behavior to the girders. Plastic moment capacity in the girders was specified as the sum of the seismic loads from the modal analysis and the moments resulting from a static analysis of gravity loads. The calculated strength of columns

included the effects of column axial loads and strain hardening in the girders on the available moment capacity in the columns. Column strength was then set equal to the combined seismic and gravity loads. To ensure elastic behavior in the columns, a check was made at each joint to ensure that the sum of the plastic moment capacities of the girders intersecting at any joint was less than the sum of the moment capacities of the columns intersecting at the same joint. In analyzing the response of a 10-story steel frame designed in accordance with the above criteria, Anderson and Gupta found that the average girder ductilities were in the range of the design ductility level of 10, and that the columns did in fact behave elastically. When the same frame, designed to achieve a girder ductility demand of 7, was subjected to the same 40-second simulated earthquake motion used in the study of the first frame, the girder ductilities generally exceeded the design level. The authors believed that this in turn resulted in considerable inelastic behavior in the columns. The authors concluded that uniformly distributed inelastic behavior can be achieved through the use of a response spectrum modal analysis in the design process.

Recently the Applied Technology Council (4) proposed a seismic design methodology which is based on the use of seismic loads determined from a modal analysis using an inelastic response spectrum. The ATC suggested using rules proposed by Newmark and Hall (16) to determine inelastic design spectra from given elastic spectra. It was intended that the design procedure enable the designer to control inelastic behavior expressed in terms of local member ductility ratios. The ATC arranged to

have several consulting firms investigate the feasibility of such a design procedure by requesting that the firms redesign several existing structures in accordance with the procedure outlined by the ATC. Although no attempt was made to calculate the response of the redesigned frames through a time integration analysis or some other alternative to the response spectrum analysis used in the design process, the report generally concluded that incorporating an inelastic response spectrum analysis in the design process is a promising approach to seismic design. However, more research and development will be necessary before such a design methodology can be included in code design procedures.

Luyties (15) performed a time integration inelastic seismic analysis of two of the ATC redesigned frames. He concluded that although the ATC method in some instances failed to predict local member ductility accurately, in general the prediction of inelastic behavior was reasonable. He too expressed the need for additional research on the use of inelastic seismic design spectra.

Luyties (15) and Haviland (12) performed much of the early research on the design methodology which is presented herein. The procedure is based on a desire to control inelastic behavior in both the columns and the girders of steel frames subjected to earthquake motions having response spectra similar to the design spectrum. The design spectrum is an inelastic spectrum determined by the Newmark-Hall rules (16). Both Luyties and Haviland noted that local ductilities in frames subjected to design earthquakes exceeded the design level of ductility. Haviland performed a limited investigation of the use of "spectral factors" to modify

the design forces resulting from an inelastic response spectrum modal analysis, so that local ductilities might be limited to the design level.

1.2 OBJECTIVES AND OUTLINE OF THESIS

The topic of this thesis is the inelastic design of plane steel frames to resist seismic forces using inelastic response spectrum techniques. The main objective of this research effort was the development of a reliable inelastic design methodology which 1) limits local member inelastic behavior to a specified design level and which 2) results in a uniform distribution of inelastic behavior. The need for a strong column - weak girder design philosophy in the design of reinforced concrete frames is apparent because it is necessary to avoid the catastrophic brittle failures which can occur in overloaded reinforced concrete columns. Steel, however, is a highly ductile material capable of resisting tensile as well as compressive loads. The desirability of a strong column - weak girder design is less clear in the case of steel frames. Thus in this thesis an attempt is made to control inelastic behavior in all members, and no attempt is made to restrict yielding to the girders.

The use of an inelastic response spectrum in seismic design of frames was thought to be appealing for the following reasons. Modal analysis is both a simple and a relatively inexpensive method of dynamic analysis. Only as many modes as necessary to achieve the desired level of accuracy need be included in a modal analysis. Finally, it was felt that an inelastic spectrum derived for a given ductility level would

give a reasonable prediction of the level of frame inelastic behavior which could be expected to occur under design loading conditions.

Chapter 2 presents the inelastic design procedure used in this study. The preliminary selection and design of a 4-story, a 10-story and a 16-story frame is described. Next a description of the Newmark-Hall inelastic response spectrum used to determine seismic design loads is given. Its derivation is presented, and limitations on the theoretical justification of the use of an inelastic response spectrum are described. Rules for determining member strength based on the results of a modal analysis coupled with a static analysis of the effect of gravity loads are suggested. Finally, the general characteristics of the 4-, 10-, and 16-story frames with respect to member strength are described.

The procedure used to analyze the response of the frames described in Chapter 2 is presented in Chapter 3. A brief description is given of the program FRIEDA (Frame Inelastic Earthquake Dynamic Analysis), which was used to perform a step-by-step inelastic time integration analysis of the response of each frame to simulated earthquake motions having response spectra which match the design spectrum. The simulated earthquake motions and the method by which they were generated are described. Finally, the definition of ductility used to evaluate local member inelastic behavior is presented and other output parameters from the time integration analysis are described.

In Chapter 4 the results of the inelastic time integration analyses are presented and discussed. Results of a design using unfactored

design loads are presented first. These results are followed by an investigation of the use of strength factors to increase member capacity so that local member ductilities can be limited to the specified design level of 4. Next the importance of including the P-Δ effect in analysis is investigated, and a possible method of including the P-Δ effect in the design procedure is presented. The remainder of Chapter 4 contains a brief investigation of the effects of damping, earthquake motion details, and earthquake intensity on frame response. The final section of Chapter 4 reports on single degree of freedom system tests performed to gain some understanding of the nature of the discrepancy between response predicted by modal analysis and response calculated by time integration analysis.

Chapter 5 summarizes the major conclusions of this report and offers suggestions for further research on the use of inelastic response spectra in the seismic design of frames.

CHAPTER 2 - INELASTIC DYNAMIC DESIGN PROCEDURE

2.1 PRELIMINARY SELECTION AND DESIGN OF FRAMES

The stiffness characteristics of the 4-, 10-, and 16-story steel moment-resisting frames studied in this thesis were established in a preliminary design performed by Piqué and presented in his doctoral dissertation (19). The frames were designed using working stress principles according to the 1973 Uniform Building Code for dead plus live load (D+L); for a combination of dead, live, and wind loads (D+L+W); and for a combination of dead, live, and earthquake loads (D+L+Q). Drift limitations on total frame displacement and on interstory displacement of 1/350 and 1/500 were imposed for wind and seismic loads respectively. The decision was made to study these frames because of a desire to use frames having stiffness characteristics similar to those of actual existing frames. Strength characteristics were determined independently of stiffness characteristics according to a procedure which is detailed in a later section of this chapter. It was felt that heights of 4-, 10-, and 16-stories represent a fairly wide range of typical steel frames. Figures 2.1, 2.2, and 2.3 depict elevations of the three frames.

The dead load assumed for the preliminary design of all three frames was 80 psf. The live load used in designing the 10- and 16-story frames was 50 psf for typical floors and 20 psf for the roof. The 4-story frame was designed for a typical live load of 40 psf and for a roof live load of 20 psf. UBC seismic loads used in the preliminary design were computed for a building located in zone 3. A uniform wind load of 20 psf was

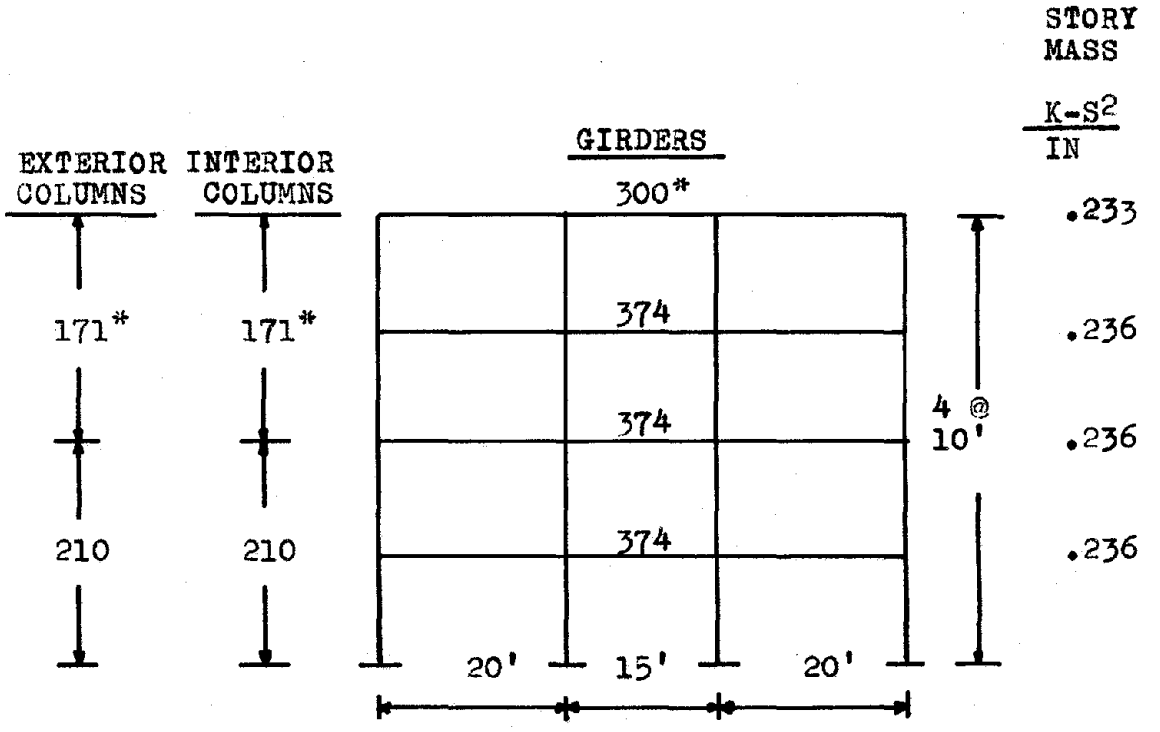

FIGURE 2.1 4-STORY FRAME

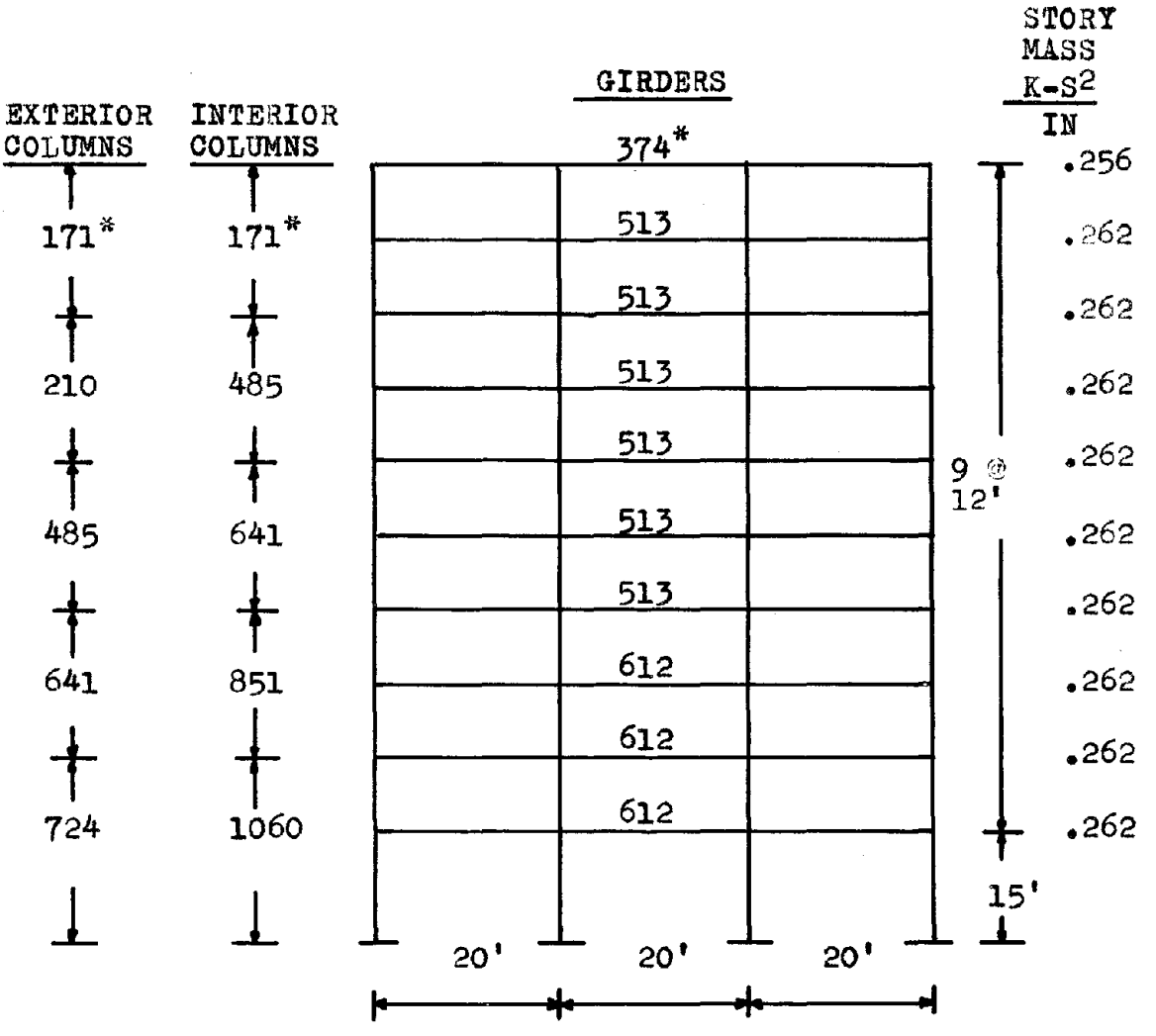

* - moment of inertia (IN^4)

FIGURE 2.2 - 10-STORY FRAME

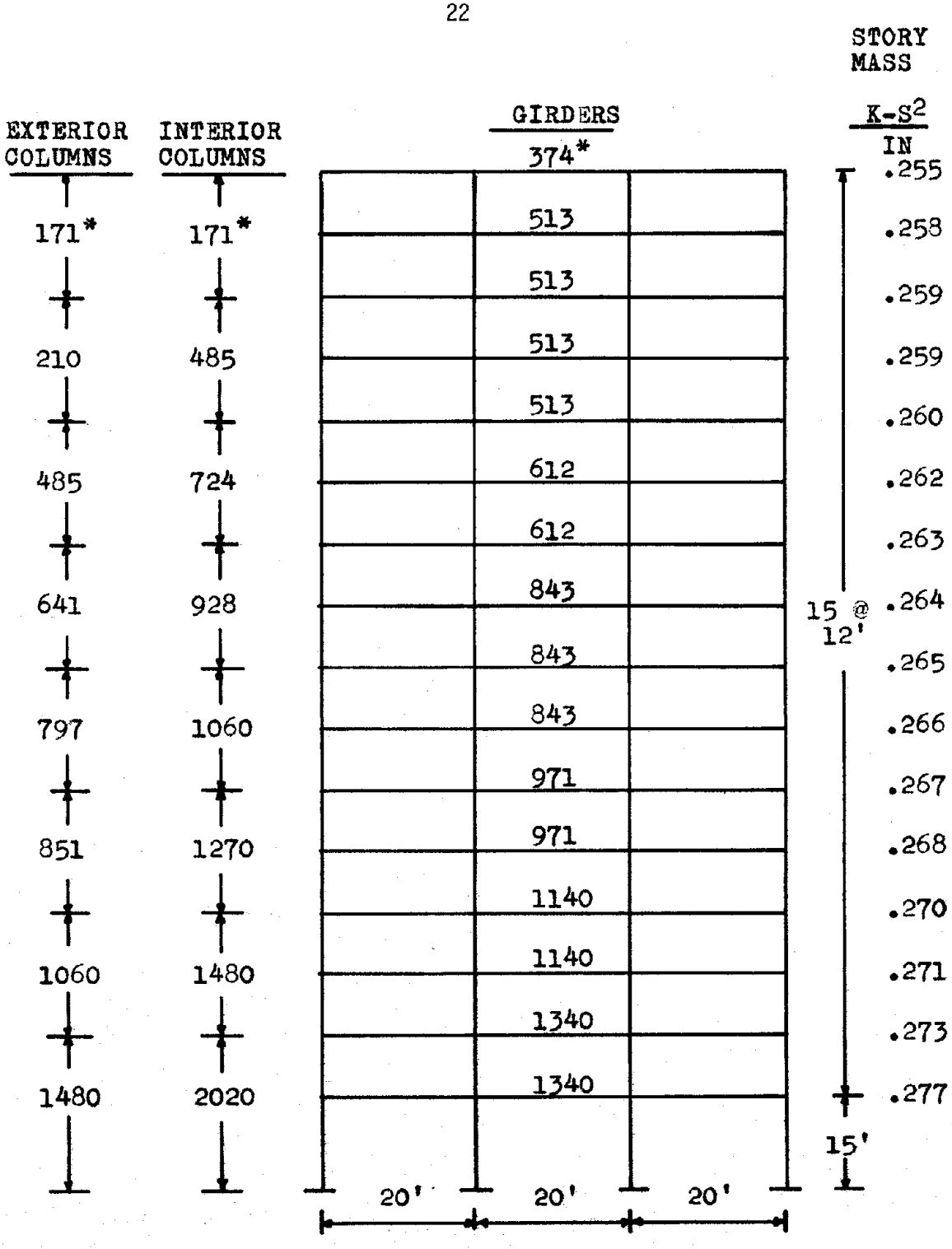

* - moment of inertia (IN^4)

FIGURE 2.3 - 16-STORY FRAME

used in the design of the 4- and 10-story frames. The design wind load for the 16-story frame was 20 psf for floors one through three, 25 psf for floors four through eight, and 30 psf for the remaining eight floors.

It was assumed that the frames designed above represent interior bents spaced at 20 feet, and that torsional effects in the entire building could be neglected. It was further assumed that the frames are braced against out of plane motion; thus only two-dimensional design and analysis was considered. Column sections were varied at two-story intervals to reflect present day practice which, for economic purposes, results in designs in which column sections are rarely varied more frequently. The same section, designed for the maximum force occurring in the story, was used for all girders in any given story. Again, the decision to choose girders in this manner reflects modern practice which attempts to minimize variations in sections while also minimizing overdesign of members.

The following is a brief description of the details of the design of the 4-, 10-, and 16-story frames. A more complete description of the design of each frame is presented in an appendix found in reference (19). The 4-story frame represents a frame found in a typical low-rise apartment building. Thus the story heights are 10 feet; the exterior spans are 20 feet, and the interior span is 15 feet. The 10- and 16-story frames are representative of common office building frames. The first floor is 15 feet high; the remaining floors are 12 feet in height. All spans are 20 feet in length.

Dead plus live loads controlled the design of all members in the 4-story frame with the exception of the first floor interior columns. Girders in the first seven stories of the 10-story frame were proportioned for a combination of dead plus live plus seismic loads; girder design in the remaining three stories was controlled by dead plus live loads. Column design was controlled by the combination of dead plus live plus earthquake loads in the first six stories of the 10-story frame, and by dead plus live loads in the upper four stories. No changes were necessary to satisfy drift requirements in either the 4- or the 10-story design.

The effect of wind loads was more pronounced in the design of the 16-story frame. Girder design in the top three floors was controlled by dead plus live loads, while girder design in the remaining thirteen stories was controlled by a combination of dead plus live plus wind loads. Dead plus live plus wind loads controlled the design of all columns except those in the top two stories where dead plus live loads controlled design. The girders in the first and second floors and the columns in the third and fourth stories were increased in size to satisfy wind load drift limitations.

2.2 DETERMINATION OF SEISMIC DESIGN LOADS

2.2.1 Newmark-Hall Inelastic Response Spectrum

The inelastic design response spectrum used in this report was determined from an elastic response spectrum for single degree of freedom systems having damping which is 5% of critical damping and respond-

ing to a motion with a peak acceleration of .33 g. Newmark and Hall (16) have proposed an elastic design spectrum for a ground motion characterized by a maximum displacement of 36 in., a maximum velocity of 48 in/sec., and a maximum acceleration of 1 g. In this study each of the above ground motion maxima was reduced by a factor of .33 and plotted on tripartite logarithmic paper. An elastic spectrum was obtained by applying Newmark-Hall (16) amplification factors of 1.4, 1.9, and 2.6 in the regions of amplified displacement, amplified velocity, and amplified acceleration respectively. Between the periods of .167 sec. and .06 sec., which define the transition region, the amplified acceleration region was connected by a straight line to the region in which maximum ground acceleration equals maximum response acceleration. Thus, in the amplified displacement region the assumed elastic displacement response was 16.63 in.; in the amplified velocity region the assumed elastic pseudo-velocity response was 30.1 in/sec; and in the amplified acceleration region the assumed pseudo-acceleration response was .86 g.

The inelastic acceleration and displacement spectra giving the response of a single degree of freedom elastic perfectly plastic system was determined from the elastic response spectrum according to the rules proposed by Newmark and Hall (16) as follows. In regions of amplified displacement and amplified velocity response, corresponding to relatively long periods, the inelastic displacement response is assumed to be identical to the elastic response. The acceleration spectrum at all periods differs from the displacement spectrum by a factor μ. This factor, termed the ductility factor, is the ratio of total displacement to yield

displacement in the elasto-plastic system. Thus it is apparent that the inelastic acceleration response spectrum can also be used to determine yield displacement.

In the region of amplified acceleration response, the location of the inelastic displacement and acceleration spectra relative to the elastic spectrum is determined by the conditions necessary to satisfy the requirement that the energy absorbed during the response of an elastic system equal the energy absorbed by the corresponding elasto-plastic system as measured by the area beneath the respective force-deformation curves.

Finally, in the region of very short periods where elastic response acceleration equals ground acceleration, it is assumed that the inelastic acceleration response is equal to the elastic response.

In general, at all periods in all regions of the spectrum the inelastic displacement spectrum and the inelastic acceleration spectrum differ by the ductility factor μ. The periods at the corners of the inelastic spectra are the periods which mark the corners of the elastic spectrum. The region of equivalent inelastic and elastic energy absorption and the region in which response acceleration equals ground acceleration are joined by a straight line passing through a transition zone. An examination of the elastic and elasto-plastic force deformation curves shown in figure 2.4 reveals that in the region of amplified elastic acceleration response, the elastic response differs by a factor of $(2\mu-1)^{1/2}$. Figure 2.5 shows the elastic and inelastic spectra used in this research. The inelastic spectra were selected to predict the response of systems having a maximum ductility of $\mu = 4$.

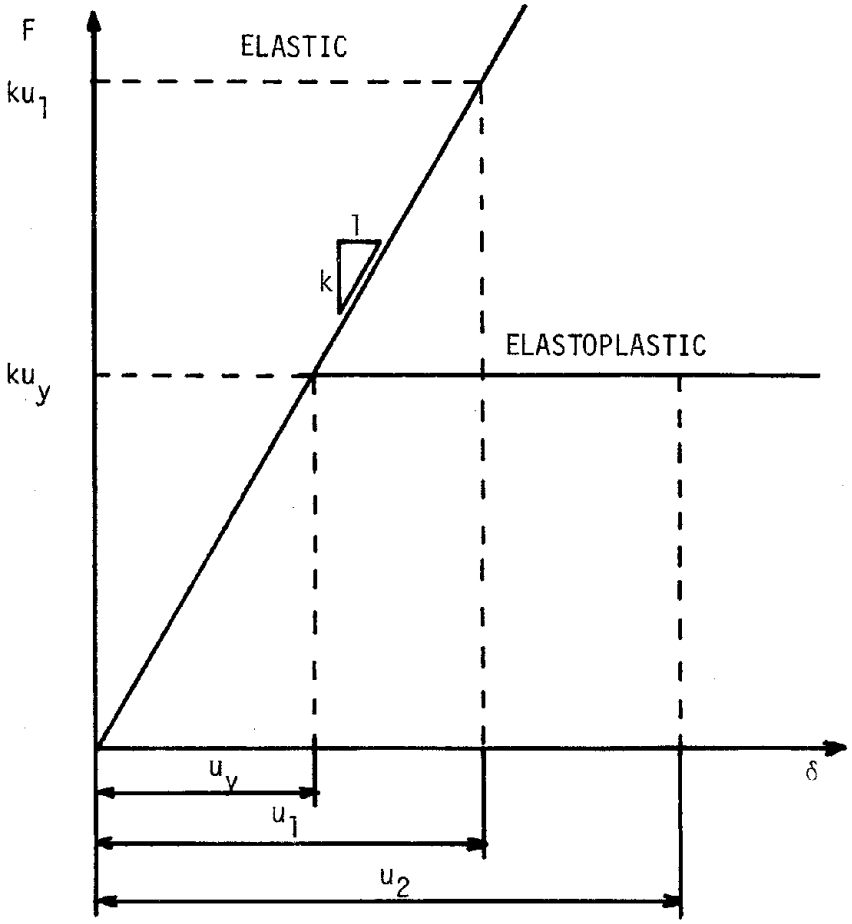

$$\frac{1}{2}(u_y)(ku_y) + (u_2-u_y)(ku_y) = \frac{1}{2}(u_1)(ku_1)$$

By definition $u_2 = \mu u_y$

Thus $$\frac{u_y}{u_1} = \frac{1}{\sqrt{2\mu-1}}$$

where: μ = ductility factor

k = initial stiffness

u_y = yield deformation of elastoplastic system

u_1 = maximum relative displacement of elastic system

u_2 = maximum relative displacement of elastoplastic system

FIGURE 2.4 - RELATIONSHIP BETWEEN ELASTIC AND ELASTO-PLASTIC FORCE-DEFORMATION CURVES (after Ref. (12))

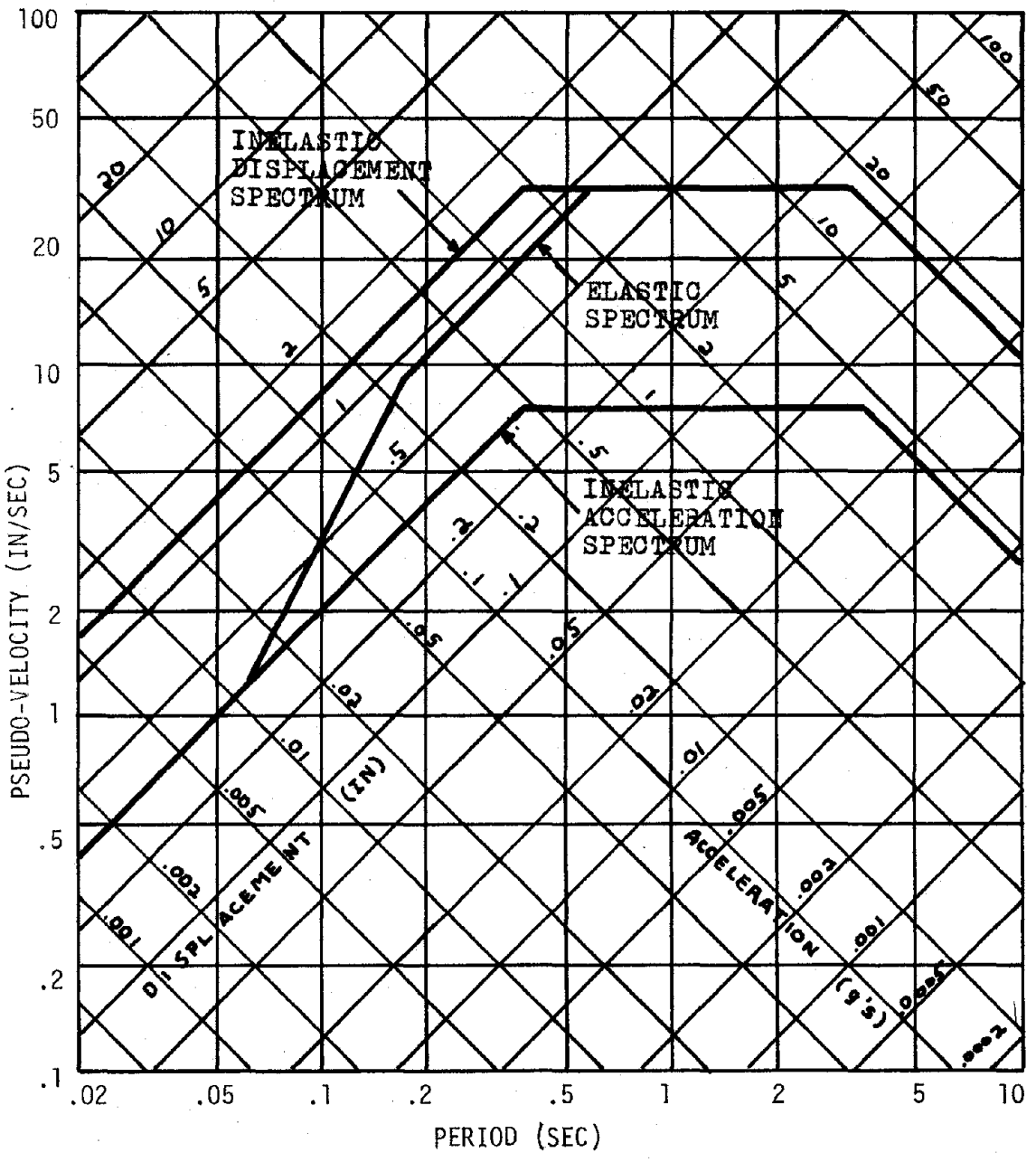

FIGURE 2.5 - ELASTIC AND INELASTIC DESIGN SPECTRA

2.2.2 Modal Analysis

The elastic modal properties of the frames under consideration in this report are presented in Appendix A. As previously noted, these elastic properties were determined by the preliminary design process. The modal frequencies were obtained by solving the eigenvalue problem:

$$\left([K]_L - \omega_n^2 [M]_D \right) \{a_n\} = 0$$

$[K]_L$ = lateral stiffness matrix

ω_n = natural frequency of n^{th} mode

$[M]_D$ = diagonal matrix of lumped story masses

$\{a_n\}$ = shape vector of n^{th} mode

The masses in the diagonal mass matrix correspond to frame mass lumped at each story level and determined from the frame weight coupled with an assumed uniform gravity load of 80 psf. The lateral stiffness matrix was obtained from well-known matrix transformations which reduce the frame under consideration from a plane frame having three degrees of freedom at each joint to an equivalent system with a single lateral degree of freedom located at each story level.

The program APPLEPIE (20) was used to perform a modal analysis of each frame based on elastic modal properties and using the inelastic response spectrum detailed in Section 2.2.1 as the input response spectrum. The modal displacements were obtained by applying the following equation:

$$\{u_n\} = \Gamma_n \frac{S_a}{\omega_n^2} \{a_n\}$$

$$\Gamma_n = \frac{\{a_n\}^T [M]_D}{\{a_n\}^T [M]_D \{a_n\}} = \text{modal participation factor}$$

$\{u_n\}$ = vector of lateral displacements for mode n

S_a = acceleration response corresponding to ω_n determined from inelastic response spectrum.

The program determines lateral displacements for each mode. The displacements are used to determine joint vertical and rotational displacements, and these displacements are in turn used to determine maximum member modal forces. Finally, member modal forces are combined according to the square root of the sum of the squares rule. Member forces determined in the manner described above were used to compute the seismic design loads used in the inelastic design procedure presented herein.

2.2.3 Limitations on the Use of Inelastic Response Spectra

The use of inelastic response spectra to perform modal analyses of multi-degree of freedom systems cannot be justified theoretically. The inelastic spectra used in this report were designed to predict the response of single degree of freedom elasto-plastic systems to seismic motions. The practice of combining individual modal responses to obtain total response, which is based upon the principle of superposition, is not valid for nonlinear analyses. During the course of inelastic

response of a given frame to an earthquake motion, modal characteristics (modal shapes and frequencies) change continually as hinges appear and disappear at various locations throughout the structure. In Chapter 4 the use of strength factors to modify member capacities obtained from the modal analyses and thereby improve response is discussed. Results of a series of tests with single degree of freedom elasto-plastic systems are also presented in Chapter 4. These results give a general indication of the source of the discrepancy between modal analysis and time integration analysis.

2.3 DETERMINATION OF GRAVITY FORCES

The importance of including gravity loads in seismic design procedures has been demonstrated in the past ([12,15]). Thus a gravity load of 80 psf was assumed in determining member forces due to static vertical loads. A static analysis (21) of vertical loads was performed, and the resulting end moments and axial loads were used in the process of determining member strength.

2.4 DETERMINATION OF MEMBER STRENGTH

The method used in determining member strength was proposed by Luyties et al. (15) and revised by Haviland et al. (12). Girder strength was established according to the following expression:

$$M_P \geq \frac{1}{2}(M_{EQ}^1 + M_{EQ}^2); \qquad M_P \geq \frac{wl^2}{8} \tag{2.1}$$

M_P is the plastic moment capacity of the member. M_{EQ}^1 and M_{EQ}^2 are

illustrated in figure 2.6a and are spectral design moments determined by a modal analysis using an inelastic response spectrum as detailed in Section 2.2. Luyties (15) found that design based on the maximum spectral end moment was not necessarily more conservative than design based on the average spectral moment given by equation (2.1). In many instances average spectral moment designs resulted in an improved distribution of inelastic behavior, possibly because such a design limits overdesign of one end of members in which there is a large difference in spectral end moments. Overdesign of one end of a member increases inelastic behavior in adjoining members. The second design strength condition found in equations (2.1) reflects a need to ensure that structural integrity is maintained under the influence of gravity loads which might lead to the formation of a plastic hinge at midspan. Assuming antisymmetric seismic bending moments M_p, and plastic hinges at both ends of a given girder, figure 2.7 illustrates that the midspan seismic internal moment is zero and that the maximum existing moment could be the internal moment due to the gravity load. Assuming that all available strength of the member ends is used to resist seismic loads, the beam is approximated as simply supported with respect to vertical loads. The maximum moment is given by $wl^2/8$, where w is a uniform gravity load and l is the member length.

Determination of column strength is a somewhat more complicated procedure than the process of determining girder strength because estimates of necessary column resistance must include the effect of axial loads in reducing available strength. The following AISC formula for

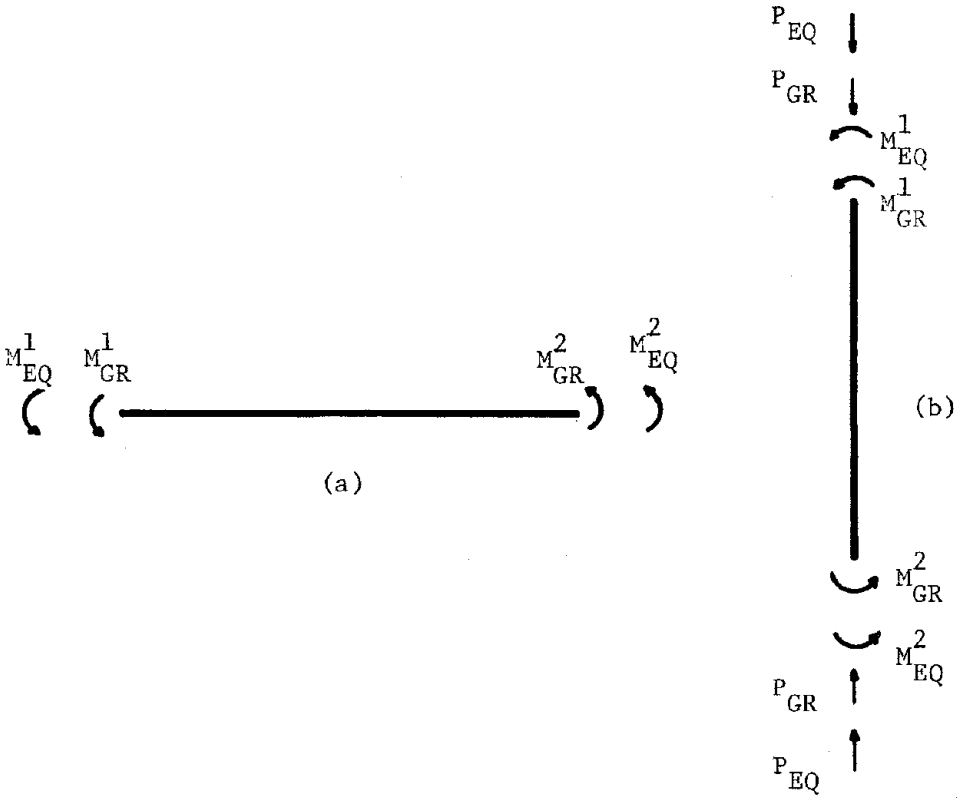

FIGURE 2.6 - MEMBER END FORCES DUE TO SEISMIC AND GRAVITY LOADS

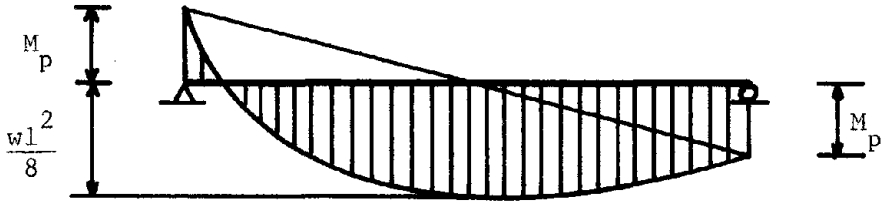

FIGURE 2.7 - MOMENT DIAGRAM FOR GIRDER WITH PLASTIC HINGES AT BOTH ENDS (after Reference (12))

column axial-flexural interaction in plastic design was used to develop an expression for determining column strength:

$$\frac{P}{P_y} + \frac{M}{1.18\ M_p} \geq 1; \quad M \leq M_p \tag{2.2}$$

In order to use the above expression to determine column plastic moment capacity M_p based on design forces P and M, the axial strength P_y must be eliminated from the equation. This was accomplished by noting that in general the ratio of plastic section modulus to area ranges from 5.1 to 7.7 for wide flange sections as size increases, and that the average ratio is approximately Z/A = 6. Thus assuming that Z/A = M_p/P_y = 6 and substituting, equation (2.2) becomes:

$$\frac{6P}{M_p} + \frac{M}{1.18\ M_p} \geq 1; \quad M \leq M_p$$

Upon rearranging terms the following expression for column strength was obtained:

$$M_p \geq 6P + M/1.18; \qquad M_p > M \tag{2.3}$$

Furthermore, the numerical value of P_y was determined from M_p, again assuming Z/A = 6:

$$P_y = M_p/6 \tag{2.4}$$

The design moment M was established as follows:

$$M = \frac{1}{2}(M^1_{EQ} + M^2_{EQ}) \; ; \; M \geq \frac{1}{2}(M^1_{GR} + M^2_{GR}) \tag{2.5}$$

The design axial load, P, was determined by the following equation:

$$P = P_{EQ} + P_{GR}$$

M^1_{EQ}, M^2_{EQ}, and P_{EQ}, shown in figure 2.6b, are seismic forces determined by modal analysis. M^1_{GR}, M^2_{GR} and P_{GR} also illustrated in figure 2.6b are the gravity end forces determined in the static analysis described in Section 2.3. In keeping with the philosophy used in the design of girders, the column design moments are average spectral values rather than maximum spectral forces in an attempt to improve the distribution of inelastic behavior. The second condition (2.5) involving gravity load moments was included to ensure adequate behavior under gravity loads.

As previously noted, the member strengths determined by equations (2.1) and (2.3) were established without regard for member stiffness. It was not necessary for analysis purposes to select actual steel members having the specified strength and stiffness properties, and in keeping with the basic nature of this research, no attempt was made to choose wide flange members.

Design moments were not increased to reflect the increased moment due to gravity loads, although design axial loads were determined from the sum of seismic and gravity axial forces because of a basic difference in the manner in which gravity moments and gravity axial loads effect member strength. This difference is illustrated in figure 2.8. Initial gravity moments alter column and girder behavior prior to first yield only. Their effect is to increase or decrease the initial available strength depending on the direction of initial lateral loading. After initial yielding has occurred, the full moment capacity, $2M_p$, is available for resisting lateral forces (figure 2.8b). Axial forces due

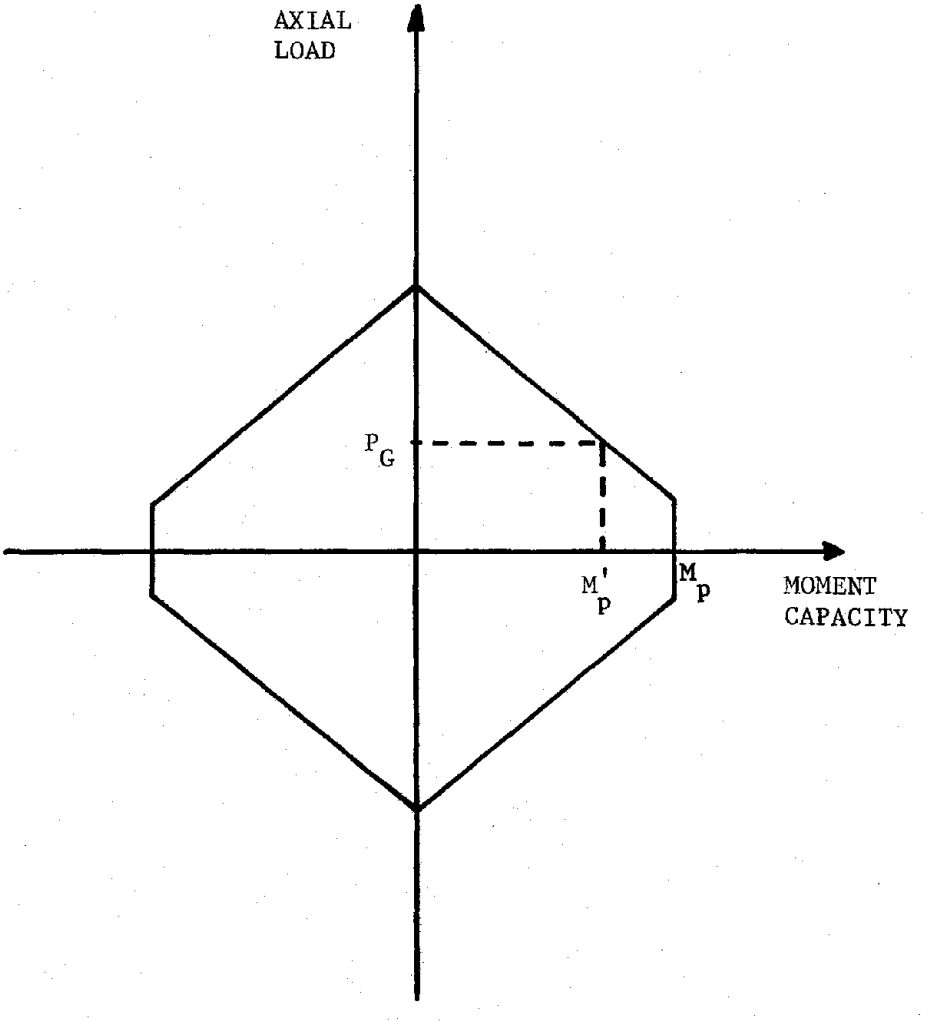

FIGURE 2.8a - THE EFFECT OF GRAVITY FORCES ON AVAILABLE MEMBER STRENGTH

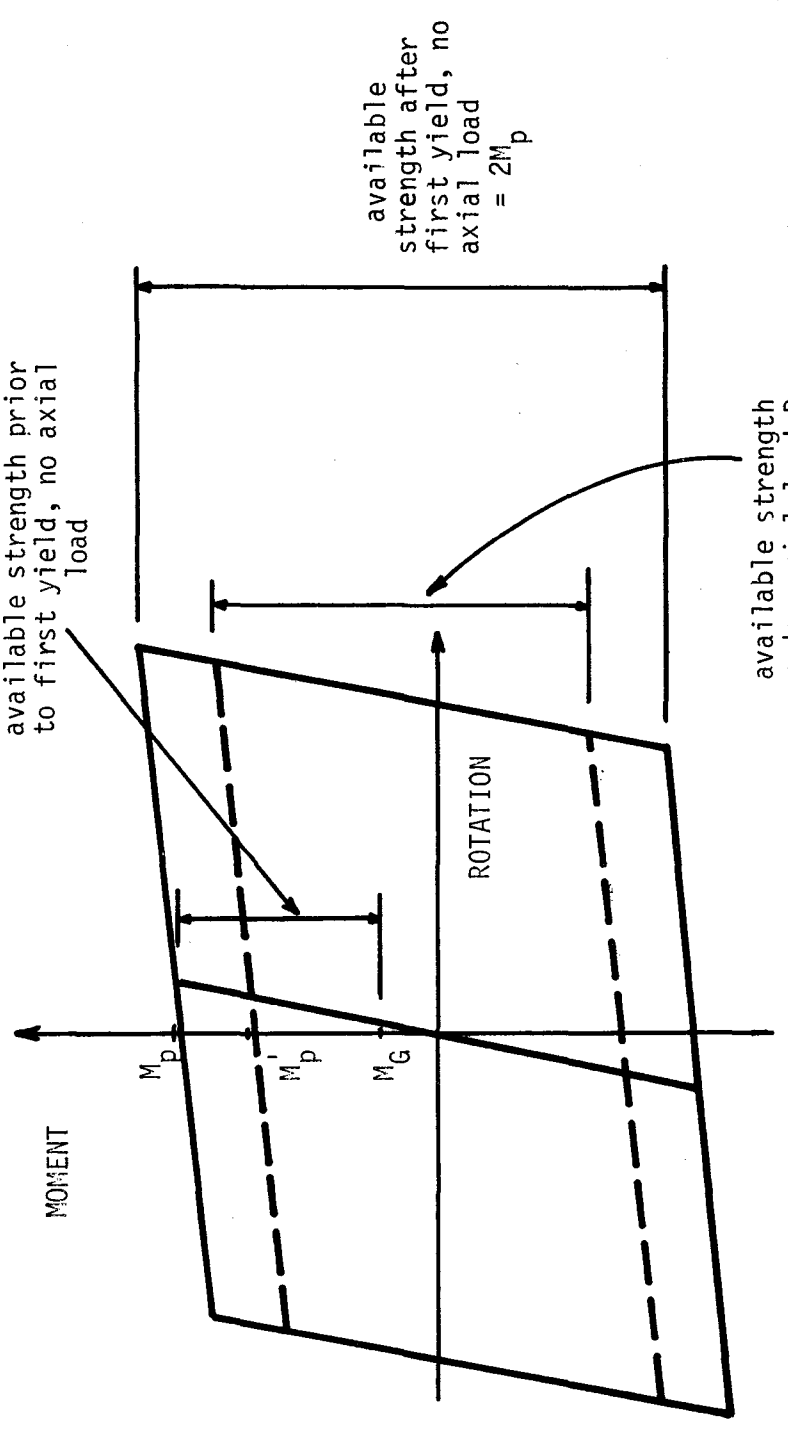

FIGURE 2.8b - THE EFFECT OF GRAVITY FORCES ON AVAILABLE MEMBER STRENGTH

to gravity loads, in contrast, permanently reduce column moment capacity. Figure 2.8a indicates how moment capacity M_p' is determined, given gravity axial load P_G. (Axial loads due to seismic loads should also be accounted for, but have been ignored here to simplify this explanation.) It is apparent from figure 2.8b that as long as an axial force due to gravity loads exists, available moment capacity after first yielding is reduced from $2M_p$ to $2M_p'$. Evidence supporting the contention that the effect of gravity moments is transitory is offered by Anderson and Gupta (3). Upon examining the behavior of a typical girder in a frame subjected to earthquake motion, they found that as seismic response progressed, plastic hinges formed simultaneously at both ends of the member in a manner which is characteristic of response to pure lateral loads. The authors further noted that moment-rotation behavior was hysteretic and shifted from the base position by an amount which corresponded to the initial rotation due to gravity loads. Luyties (15) observed that increasing design moments to reflect gravity moment effects resulted in "weak column" designs characterized by excessive amounts of inelastic behavior in columns. He concluded that columns were heavily "penalized" by axial loads, while, after initial yielding mechanisms formed, gravity moments had no effect on girders or columns. This resulted in girders which were overdesigned, because gravity design moments result in a greater increase in girder strength than in column strength.

In determining member resistance as detailed above, it was assumed that all members were adequately braced so that full plastic deformations

could be developed in frame members. Strain hardening, shear forces, axial forces in girders, and column buckling were not considered when determining member strength. No load factors were used to provide safety against failure, because it was felt that such factors might observe the results of the research.

The strengths of the members in the 4-, 10-, and 16-story frames are listed in tables 2.1 to 2.3. In general, column design was controlled by seismic forces in all but the upper stories of all three frames. Gravity forces tended to control girder design except in lower stories.

Gravity loads governed the design of exterior columns in the fourth floor, interior girders in the third and fourth floors, and all exterior girders of the four-story frame.

The only columns in the 10-story frame proportioned for gravity loads were those in the exterior of the eighth and tenth floors. All girders except for the exterior girders in the first floor and all girders in the second floor were designed to resist gravity loads.

Resistance of all columns in the 16-story frame was based on seismic forces with the exception of the exterior columns in the twelfth, fourteenth, and sixteenth stories. The exterior girders in the eighth and ninth floors and all girders above the ninth floor were proportioned for gravity loads.

TABLE 2.1 - MEMBER STRENGTH - 4-STORY FRAME - UNFACTORED DESIGN

	COLUMN M_p's (K-in)		GIRDER M_p's (K-in)*	
STORY	EXTERIOR	INTERIOR	EXTERIOR	INTERIOR
1	928.5	1333	993.6	666.5
2	670.8	1135	993.6	619.3
3	500.7	817.1	993.6	558.9
4	435.9	492.4	979.2	550.8

* w = .138 K/in assumed uniform gravity load floors 1-3.
w = .136 K/in assumed uniform gravity load floor 4.

TABLE 2.2 - MEMBER STRENGTH - 10-STORY FRAME - UNFACTORED DESIGN

	COLUMN M_p's (K-in)		GIRDER M_p's (K-in)**	
STORY	EXTERIOR	INTERIOR	EXTERIOR	INTERIOR
1	2018	3152	1033	1008
2	1635	2747	1024	1014
3	1488	2458	1008	1008
4	1298	2220	1008	1008
5	1140	1948	1008	1008
6	971.8	1678	1008	1008
7	753.7	1456	1008	1008
8	615.7	1172	1008	1008
9	500.8	783.8	1008	1008
10	426.5	482.6	986.4	986.4

** w = .140 K/in assumed uniform gravity load floors 1-9.
w = .137 K/in assumed uniform gravity load floor 10.

TABLE 2.3 - MEMBER STRENGTH - 16-STORY FRAME - UNFACTORED DESIGN

	COLUMN M_p's (K-in)		GIRDER M_p's (k-in)*	
STORY	EXTERIOR	INTERIOR	EXTERIOR	INTERIOR
1	3167	4553	1358	1305
2	2698	4142	1370	1364
3	2539	3864	1260	1278
4	2343	3632	1238	1287
5	2162	3392	1133	1211
6	1974	3163	1111	1191
7	1821	2895	1020	1095
8	1637	2662	986.4	1072
9	1457	2426	986.4	1054
10	1283	2180	986.4	986.4
11	1121	1926	986.4	986.4
12	974.9	1666	979.2	979.2
13	757.3	1440	979.2	979.2
14	635.7	1172	979.2	979.2
15	508.9	788.7	979.2	979.2
16	446.0	498.2	979.2	979.2

* w = uniform gravity load varies over height with frame mass.

CHAPTER 3 - INELASTIC DYNAMIC ANALYSIS

3.1 METHOD OF ANALYSIS

The response of the frames presented in Chapter 2 to design loading conditions was determined by performing a step-by-step inelastic dynamic analysis of each frame. The analysis was performed with the program FRIEDA (Frame Inelastic Earthquake Dynamic Analysis), which was originally written by Aziz (5) and extensively revised by Luyties et al. (15).

FRIEDA uses the point hinge two-component model suggested by Clough and Benuska (8) to model member inelastic behavior. All plastic deformation occurs at point hinges located at the ends of each member whenever member end moments exceed a specified yield level. Each member is comprised of an elastic component, which has constant stiffness regardless of the amount of member deformation which occurs. The elastic component is coupled with an elastic perfectly plastic component which contributes nothing to member stiffness once yielding is initiated, until a reversal in loading occurs. The result of combining the two components is the bilinear moment-rotation relationship illustrated in figure 3.1. The stiffness of the elastic component determines the stiffness of the second slope of the bilinear moment-rotation relationship. The assumed post yield stiffness for all members considered in this report was 5% of the initial member stiffness.

To perform an inelastic analysis with FRIEDA, the user must specify member stiffness and strength. Gravity loads are considered as initial

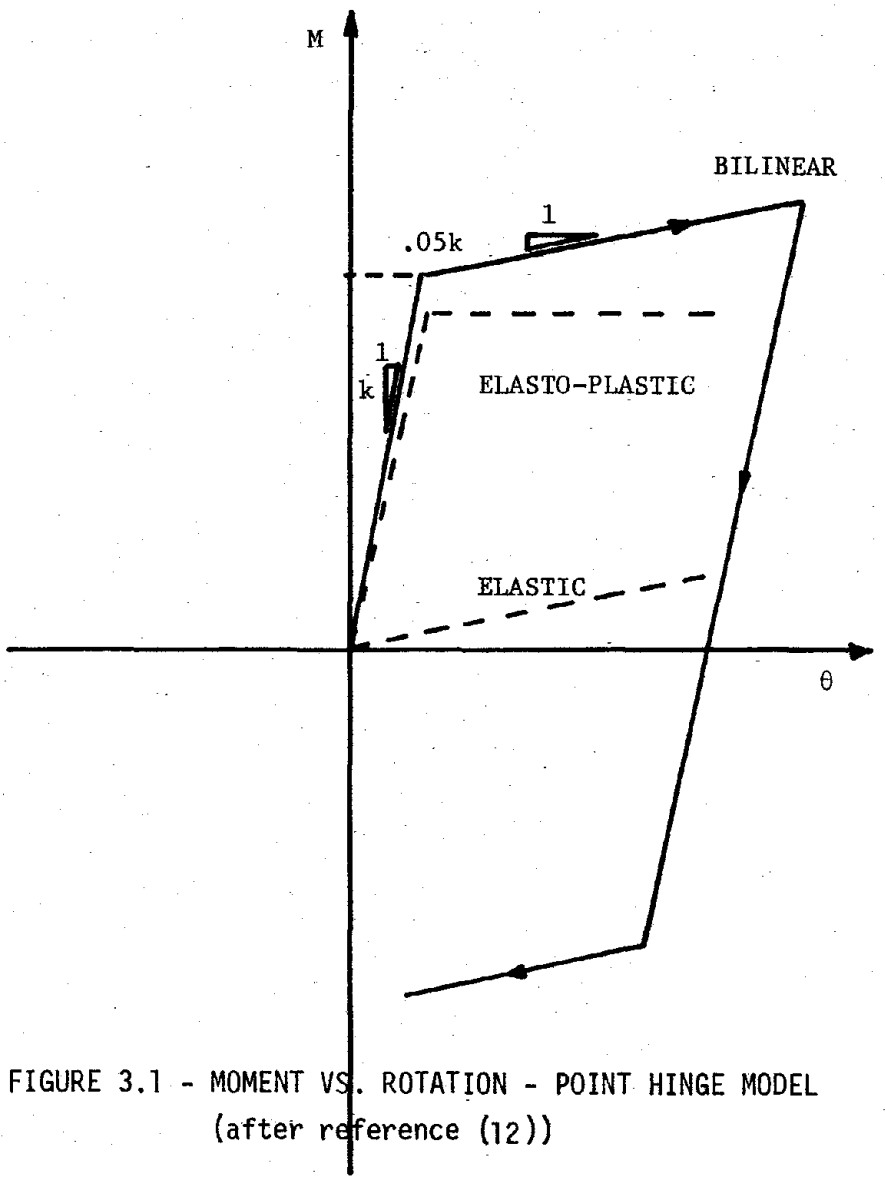

FIGURE 3.1 - MOMENT VS. ROTATION - POINT HINGE MODEL
(after reference (12))

end moments and axial forces specified by the user. The program also is capable of including axial-flexural interaction in determining column resistance. In the analyses performed for this research effort, a normalized interaction diagram (shown in figure 3.2) based on the AISC Manual was used. The final set of important data which must be included in the program input represents the earthquake motion in the form of a digitized accelerogram.

FRIEDA performs a numerical integration of the equations of motion using the constant velocity method. The time increment used in the digitized accelerogram defines the time step employed in the numerical integration scheme.

3.2 SIMULATED EARTHQUAKE ACCELEROGRAM

The purpose of the time integration analyses of each frame was to determine response under design loading conditions; thus, it was necessary that the earthquake motions used have response spectra which closely match the design spectrum. The program SIMQKE (10) was used to simulate earthquake motions having response spectra which match a specified spectrum.

To generate artificial seismic motions, SIMQKE uses the following expression to compute ground acceleration, z(t):

$$z(t) = I(t) \sum_{n} A_n \sin(\omega_n t + \phi_n)$$

Using random vibration theory, the program calculates a power spectral density function corresponding to the specified response spectrum.

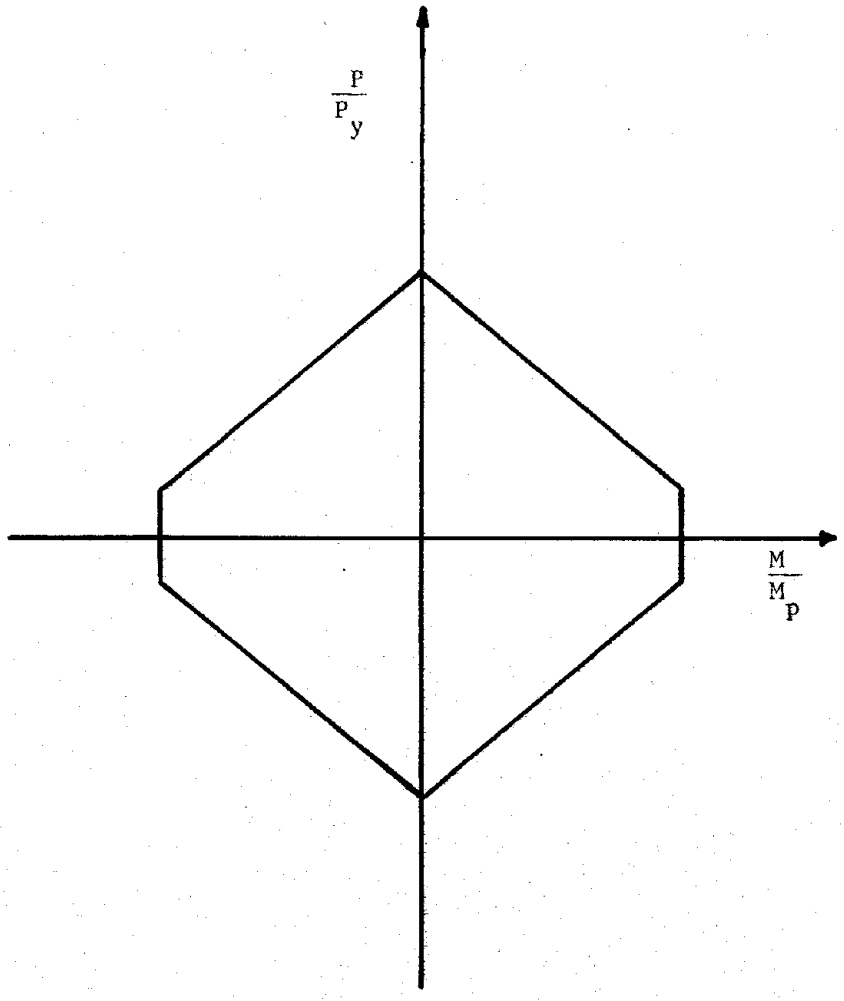

FIGURE 3.2 - NORMALIZED INTERACTION DIAGRAM

The spectral density function is then used to compute squared amplitudes, A_n^2, where the subscript indicates that the amplitude corresponds to frequency ω_n. The phase angle ϕ_n is determined by a random number generator and enables one to generate an unlimited number of different artificial motions, all matching a single target response spectrum. The intensity function I(t) represents the transient nature of the characteristics of any earthquake.

Three motions, #1, #2, and #3, were generated to have response spectra matching the elastic design spectrum from which the inelastic spectra were derived. These motions were used in the analysis of the 4-story frame. The time interval used in the digitized accelerogram is .01 seconds, and each motion has a duration of 10 seconds. Three different motions, #R1, #R2, and #R3, having a time increment of .02 seconds and a duration of 20 seconds, were used to analyze the 10- and 16-story frames. The longer records were generated to analyze the taller frames because their increased fundamental periods resulted in an increase in the amount of time necessary for structural response to reach maximum levels. It was felt that a time increment of .02 seconds would produce an accurate representation of earthquake motion and that such an increment would satisfy the numerical integration stability requirements of the constant velocity formula. The intensity functions used in generating the earthquakes used in this study are shown in figure 3.3. The calculated response spectra along with the target spectrum are shown in figures 3.4 through 3.9.

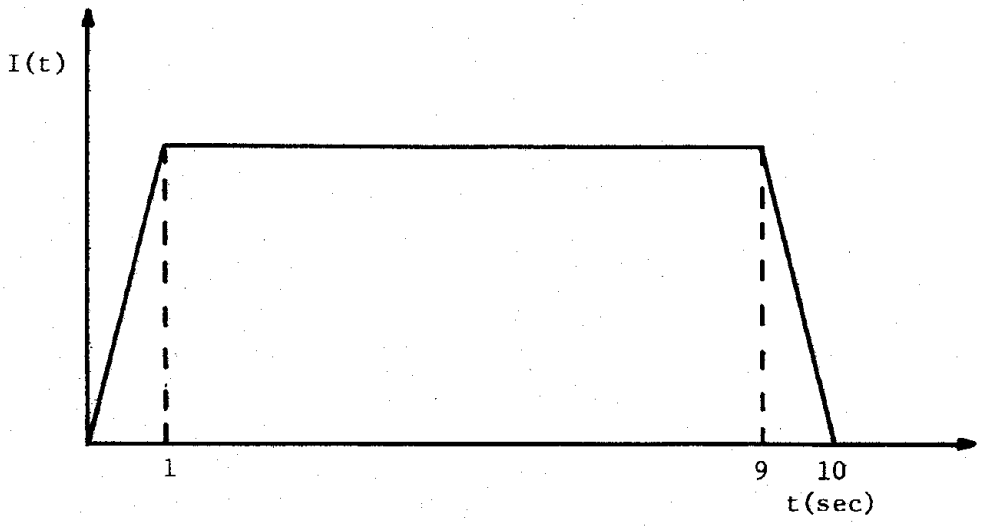

INTENSITY FUNCTION EARTHQUAKES #1, #2, #3

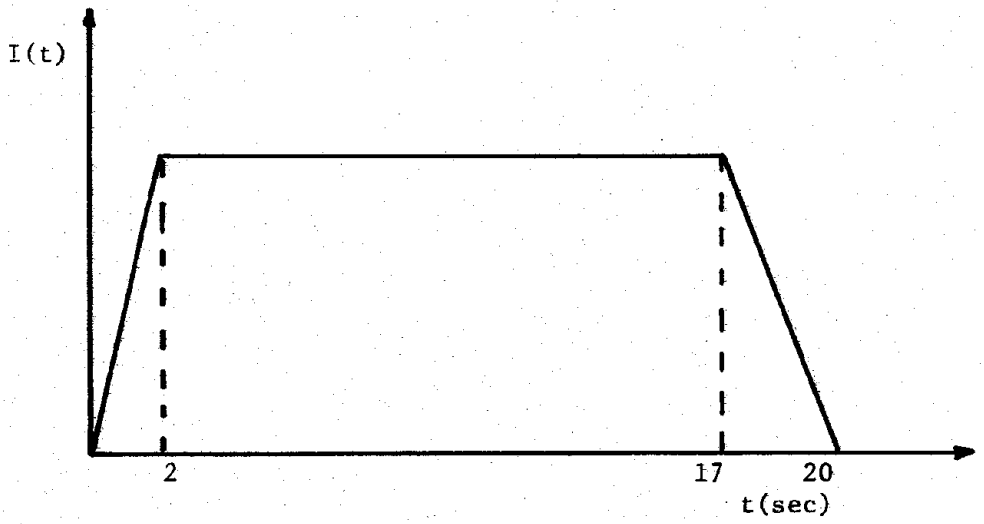

INTENSITY FUNCTION EARTHQUAKES #R1, #R2, #R3

FIGURE 3.3 - INTENSITY FUNCTIONS

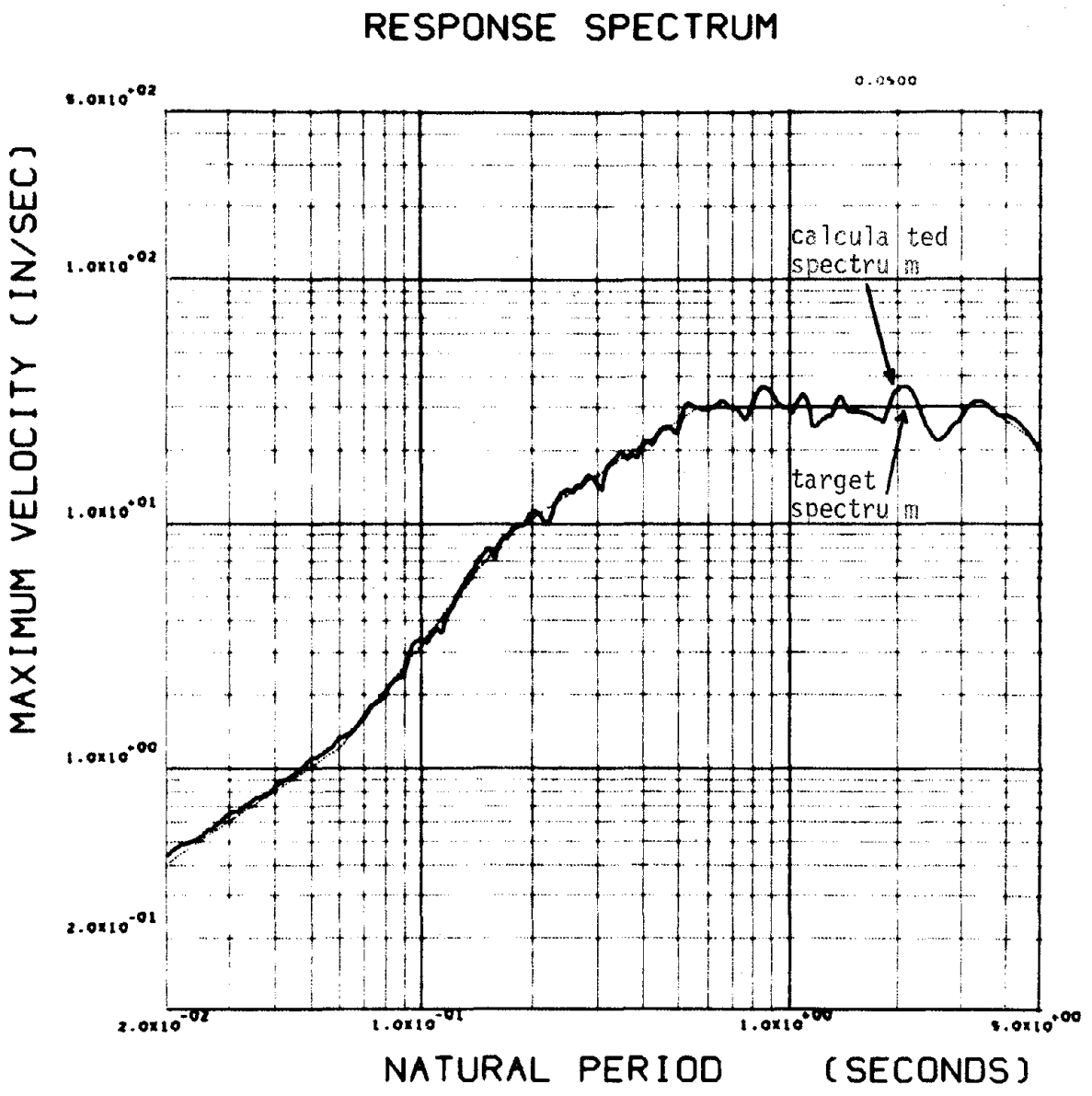

FIGURE 3.4 - CALCULATED RESPONSE SPECTRUM - EARTHQUAKE #1

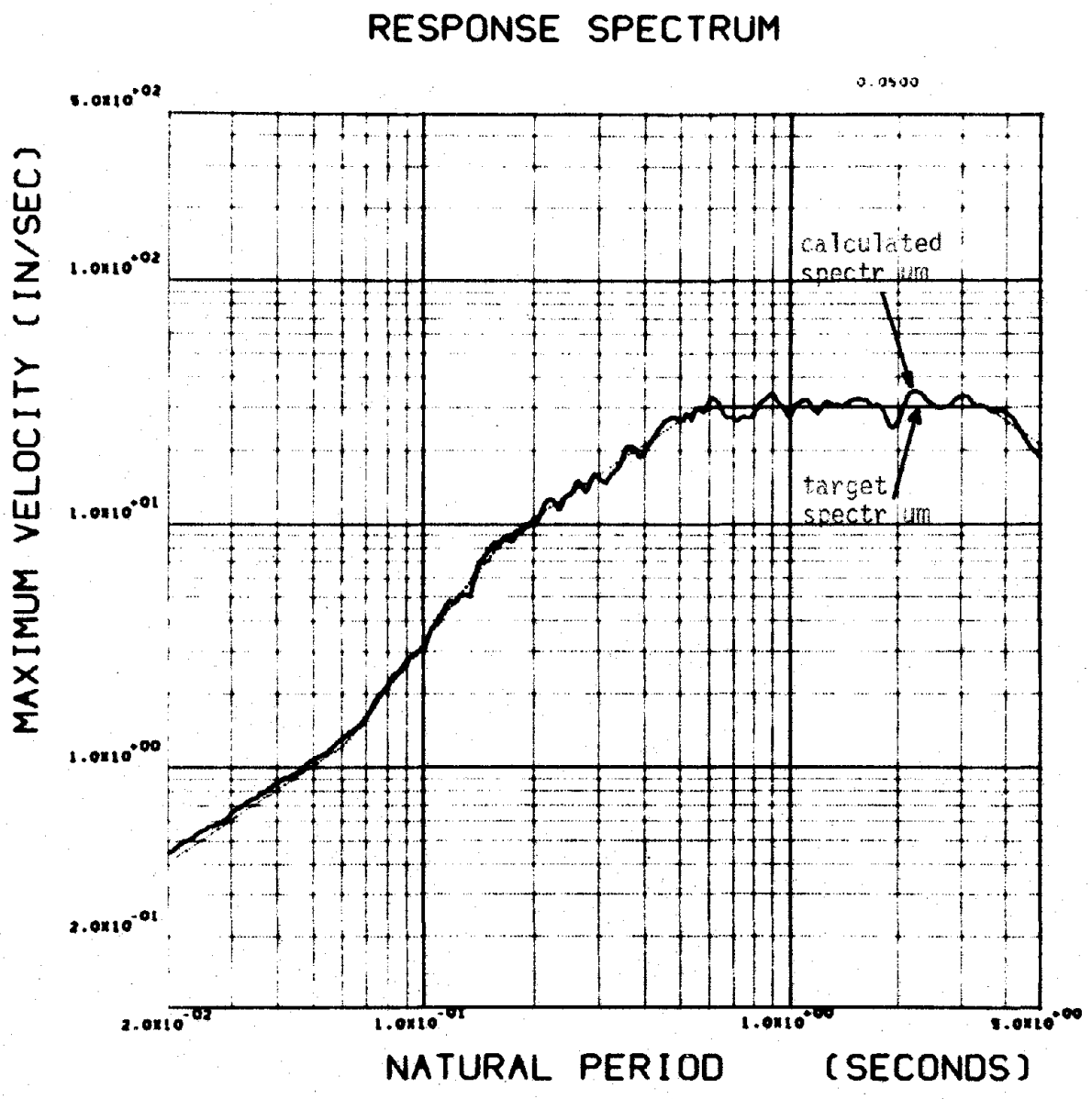

FIGURE 3.5 - CALCULATED RESPONSE SPECTRUM - EARTHQUAKE #2

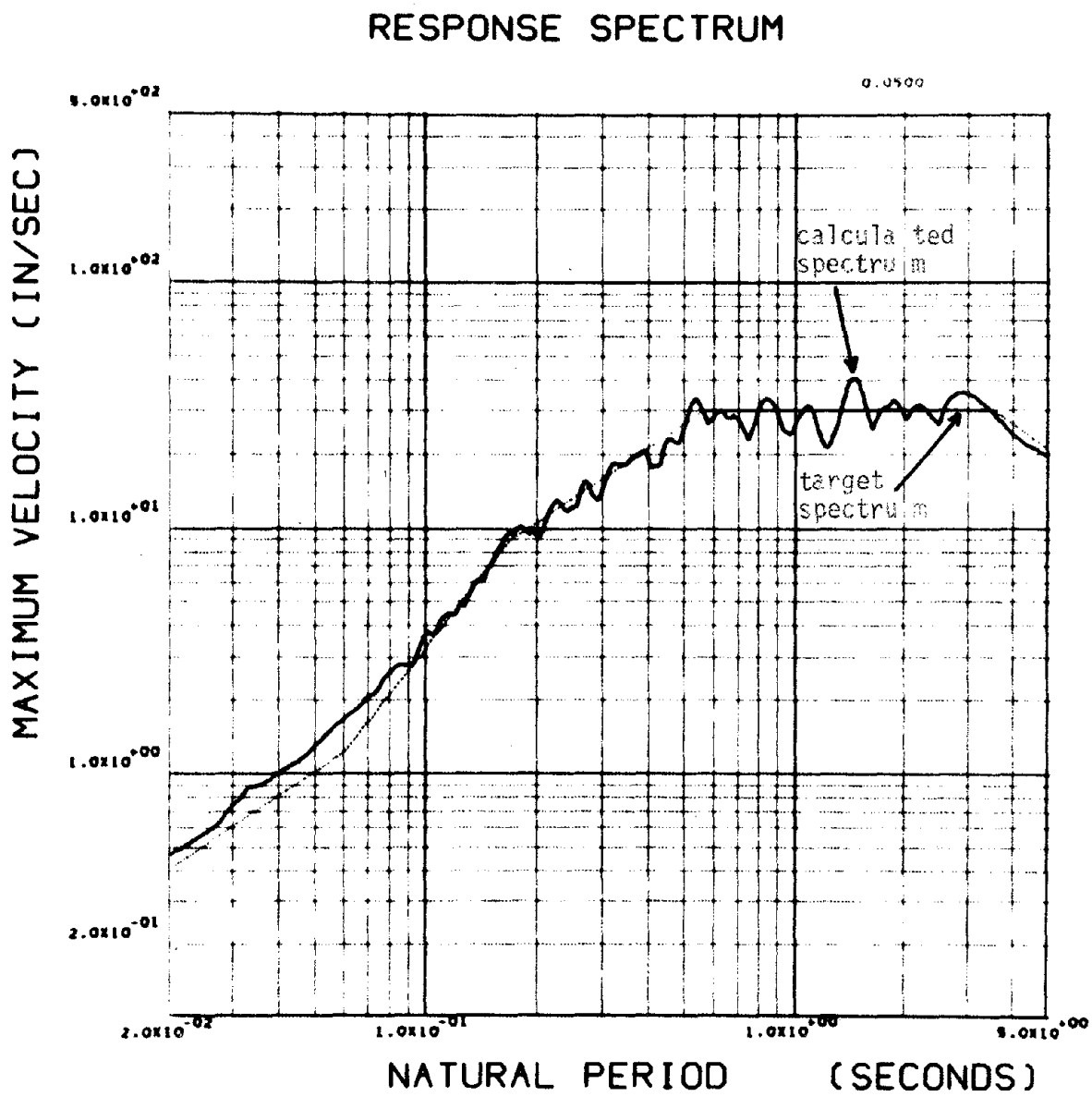

FIGURE 3.6 - CALCULATED RESPONSE SPECTRUM - EARTHQUAKE #3

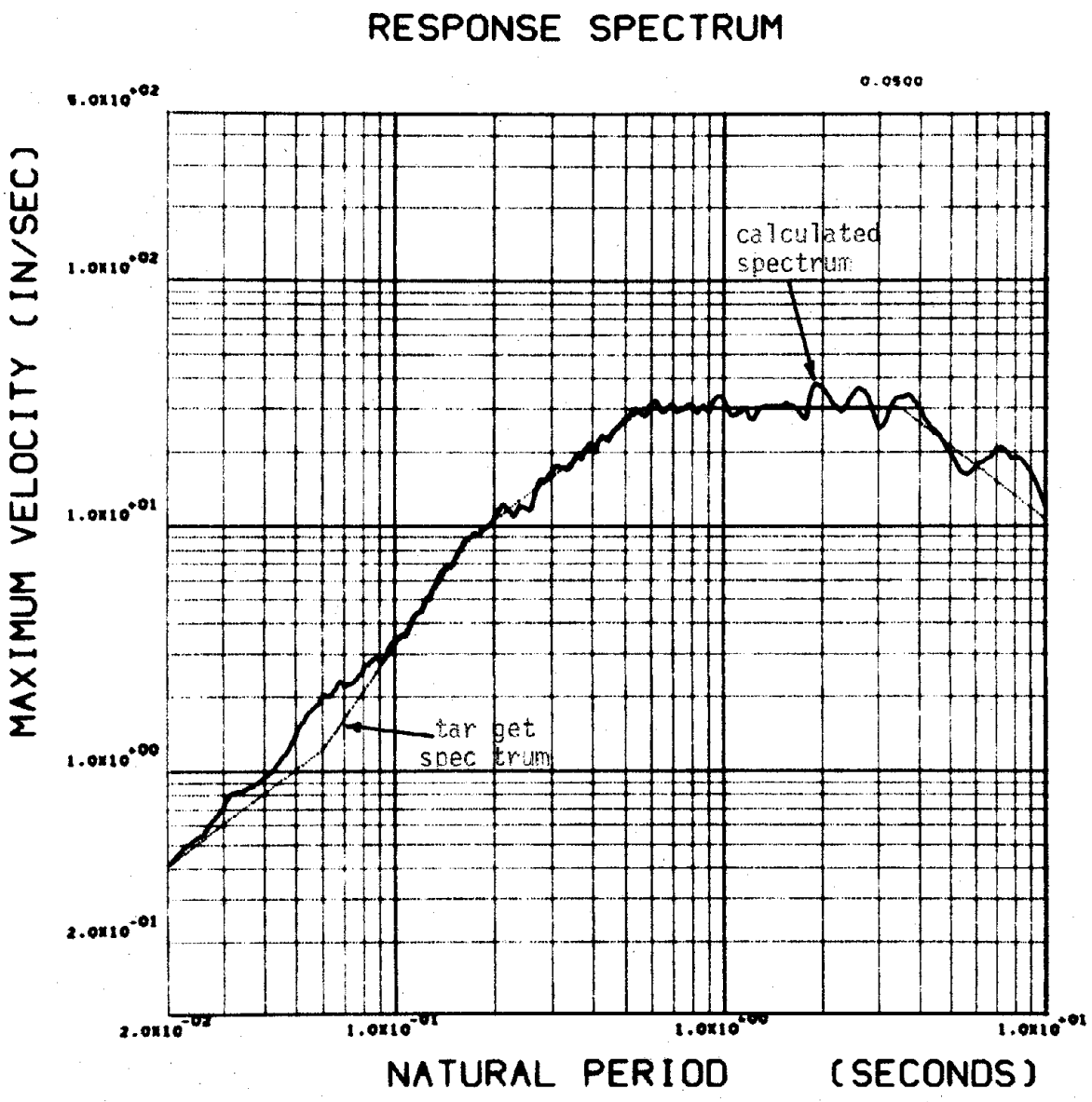

FIGURE 3.7 - CALCULATED RESPONSE SPECTRUM - EARTHQUAKE #R1

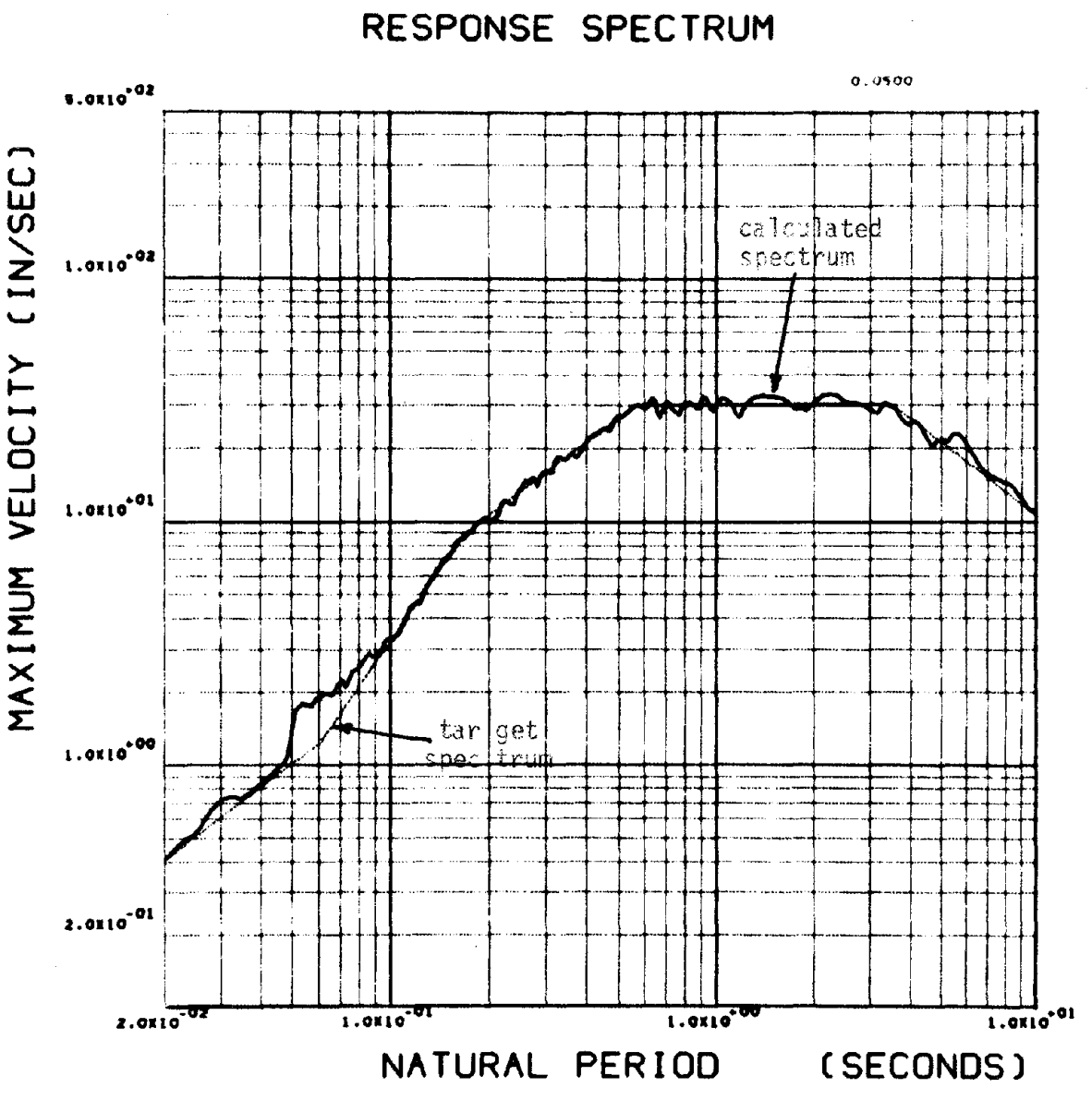

FIGURE 3.8 - CALCULATED RESPONSE SPECTRUM - EARTHQUAKE #R2

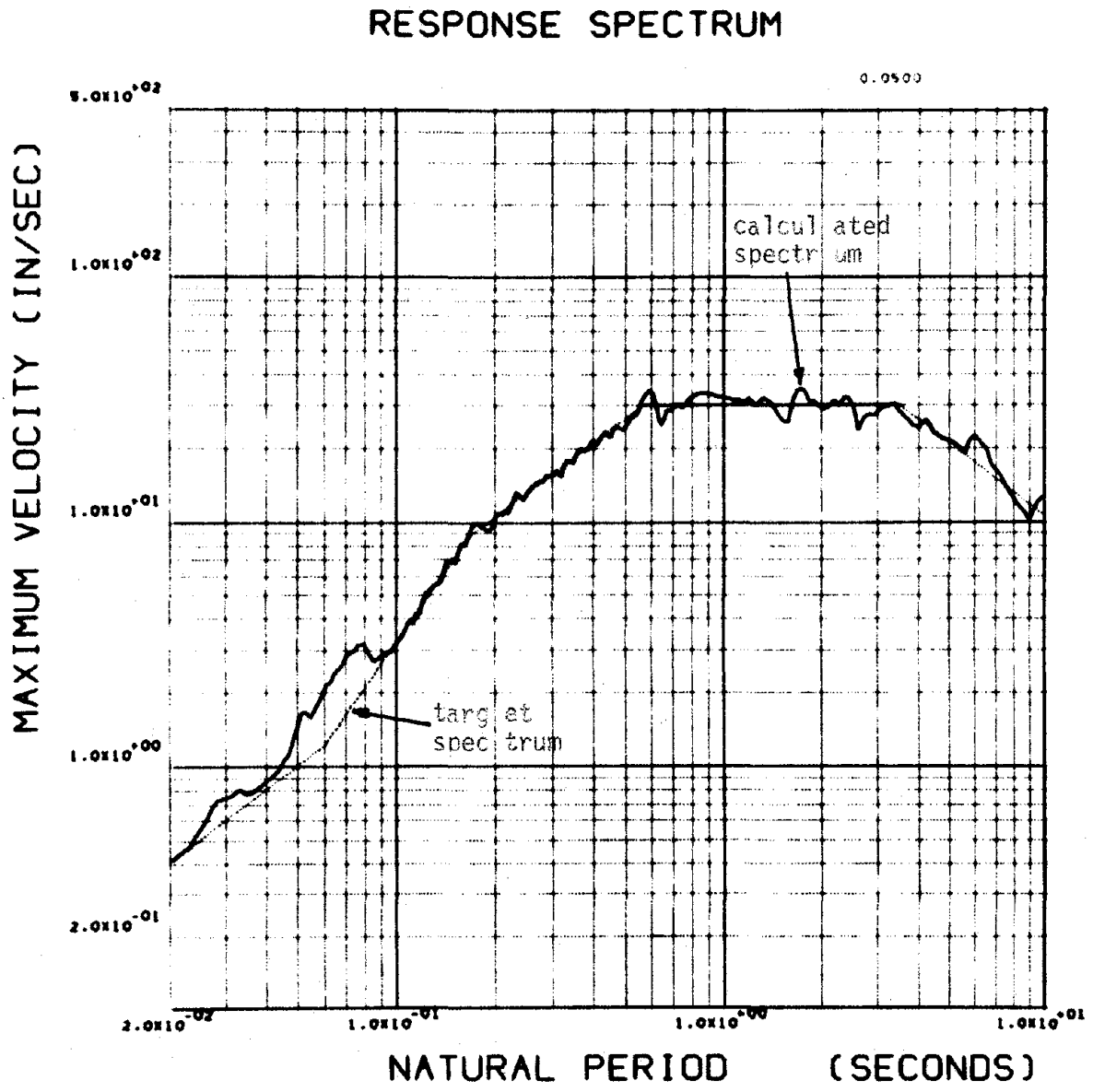

FIGURE 3.9 - CALCULATED RESPONSE SPECTRUM - EARTHQUAKE #R3

3.3 MEASUREMENT OF INELASTIC RESPONSE

Because the inelastic design procedure detailed in Chapter 2 is intended to provide some control over the distribution and level of inelastic response, the criteria used to measure inelastic behavior is of great importance. In the past, researchers (8, 26) desiring to determine the level of local member inelastic behavior have defined local ductility as:

$$\mu = \frac{\theta_{max}}{\theta_y}$$

$$\theta_y = \frac{M_p L}{6EI}$$

where L = member length

E = elastic modulus

I = cross-section moment of inertia

M_p = plastic moment capacity.

θ_y as defined above is the rotation at which incipient yielding occurs in a member which is subjected to antisymmetric bending moments. θ_{max} represents maximum total end rotation, elastic rotation plus plastic rotation. The major drawback in defining local ductility in this manner is that θ_y tends to lose significance in the presence of gravity loads because such loads destroy the antisymmetric flexural behavior which could be expected to occur under pure lateral loads with no vertical loads included in the analysis.

Because of the shortcomings encountered when measuring local ductility in terms of rotation, local ductility is defined in this report

in terms of end moments as suggested by Anderson and Bertero (2):

$$\mu = \frac{M_{el}}{M_p} = 1 + \frac{M - M_p}{pM_p} \qquad (3.1)$$

where M = member end moment

M_p = plastic moment capacity

M_{el} = moment in fictitious elastic member having same end rotation as actual member

p = ratio of second stiffness to initial member stiffness.

The relationship between the parameters used in equations (3.1) is shown in figure 3.10. It is apparent that $M_{el}/M_p = \theta_{max}/\theta_y$; however, it is not necessary to compute θ_y to determine moment ductility. The value of M_p used in calculating column ductility changes with each step of the time integration analysis. As indicated in figure 3.10, column plastic moment capacity is determined from an interaction diagram based on the axial load, P_{EQ+GR}, which changes with time and includes both gravity and seismic axial loads. Thus, the above definition of ductility reflects increases in inelastic behavior due to large axial loads which reduce column capacity.

3.4 OTHER RESPONSE PARAMETERS REPORTED FROM INELASTIC ANALYSIS

In addition to local member ductilities, the program FRIEDA also reports several other response parameters. In Chapter 4, maximum story displacements, interstory displacements, story shear forces, and story overturning moments are reported. Although this report is mainly con-

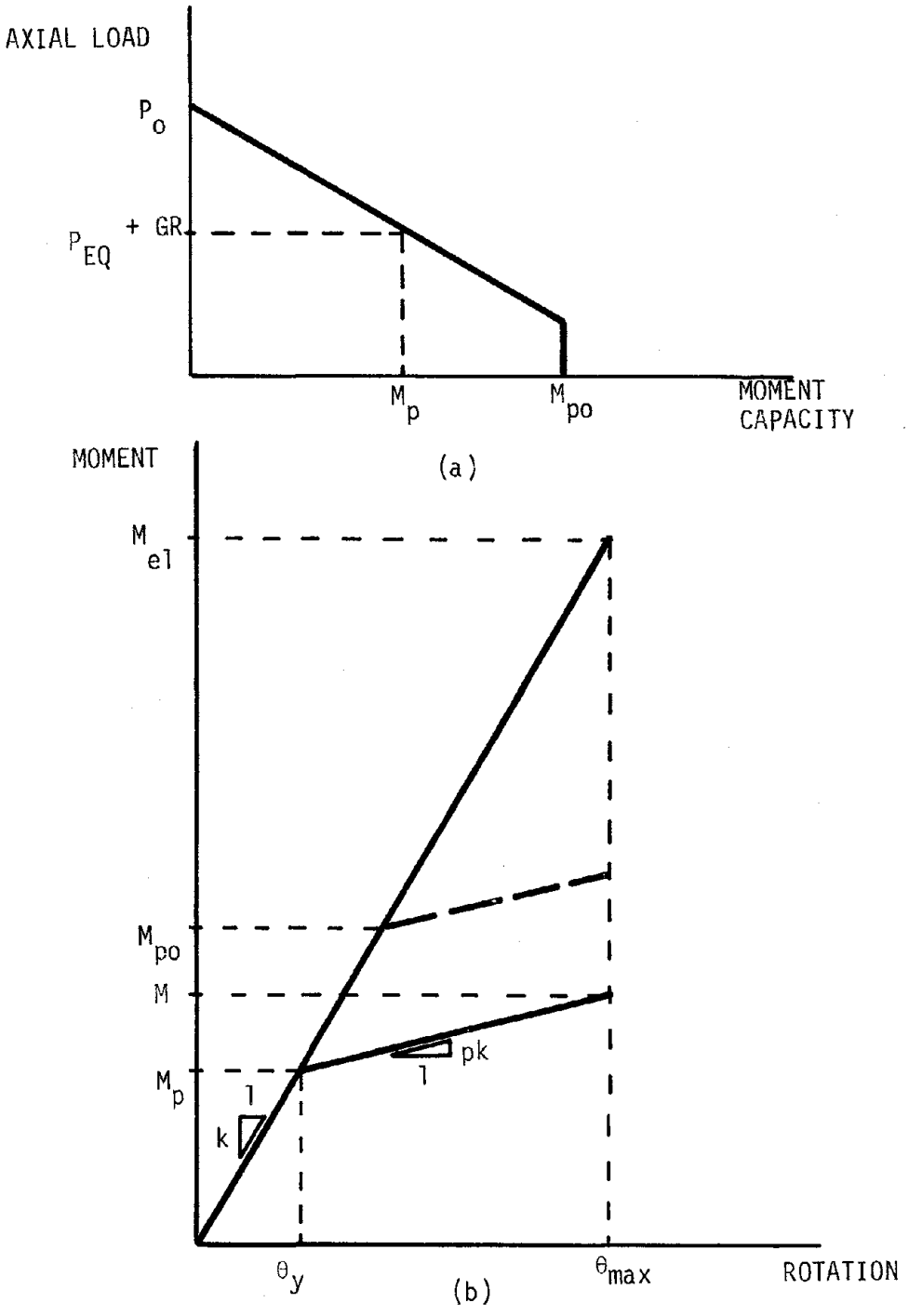

FIGURE 3.10 - DETERMINATION OF MOMENT DUCTILITY

cerned with control of local ductility values, the above parameters can be useful in attempting to understand inelastic response of structures to seismic motions.

CHAPTER 4 - RESULTS OF INELASTIC ANALYSIS

In this Chapter the results of the inelastic time integration analyses performed with the program FRIEDA are presented and discussed. The research was largely based upon analysis of the 10-story frame, as the expense of inelastic time integration analysis of multi-degree of freedom systems prohibited extensive analysis of all three frames.

Throughout this Chapter maximum local column ductility, defined as the maximum ductility occurring at any column end section in a given story, is plotted versus height. Maximum local girder ductility, similarly defined as the maximum ductility occurring at any girder end section in a given story level, has also been plotted versus height. All ductility values presented in this Chapter are moment ductilities which were calculated as detailed in Section 3.3. In most instances maximum ductility is shown separately for exterior and interior columns, while only one plot of girder maximum ductility is presented because in general there was no significant difference in the ductility requirements of exterior and interior girders.

The P-Δ effect was included only in the analyses presented in Section 4.3. Shear forces, girder axial deformations, and column buckling were not included in any of the analyses. All analyses of the 10-story and 16-story frames unless otherwise noted were performed with artificial earthquake #R2, which was described in Section 3.2. All analyses of the 4-story frame, unless otherwise noted, were performed with artificial earthquake #2. Only horizontal components of earthquake motion parallel to the plane of the frame were considered.

4.1 UNFACTORED DESIGNS

The results of analysis of the unfactored design of the 4-, 10-, and 16-story frames are presented in this Section. All three frames were designed to achieve maximum local ductilities of 4, using the procedure presented in Chapter 2. No factors either to increase member strength or design loads were included. The original unfactored member strengths are shown in tables 2.1 to 2.3 in Chapter 2.

4.1.1 10-Story Frame

Plots of maximum local ductilities determined from analysis of the 10-story frame are shown in figure 4.1. It is apparent that local ductilities exceeded the design level throughout the structure with the exception of girders located above the fourth floor. In these members the $wl^2/8$ strength requirement limited the amount of inelastic behavior which occurred. There was little uniformity in the distribution of maximum inelastic behavior over the height of the frame. The large ductility values occurring at the bottom of first floor columns were due to the assumption of a rigid connection between column base and foundation. Maximum exterior column ductility other than at the structure base was 11.9. Maximum interior column ductility was 11.0. Maximum ductility requirements in the girders was 7.1.

Figure 4.2a shows the average of the maximum ductilities occurring at all column end sections in a given story plotted versus height. Figure 4.2b is a similar graph illustrating average values of girder ductilities. Column average ductilities exceeded the design value at all levels with the exception of the top story. The effect of the $wl^2/8$

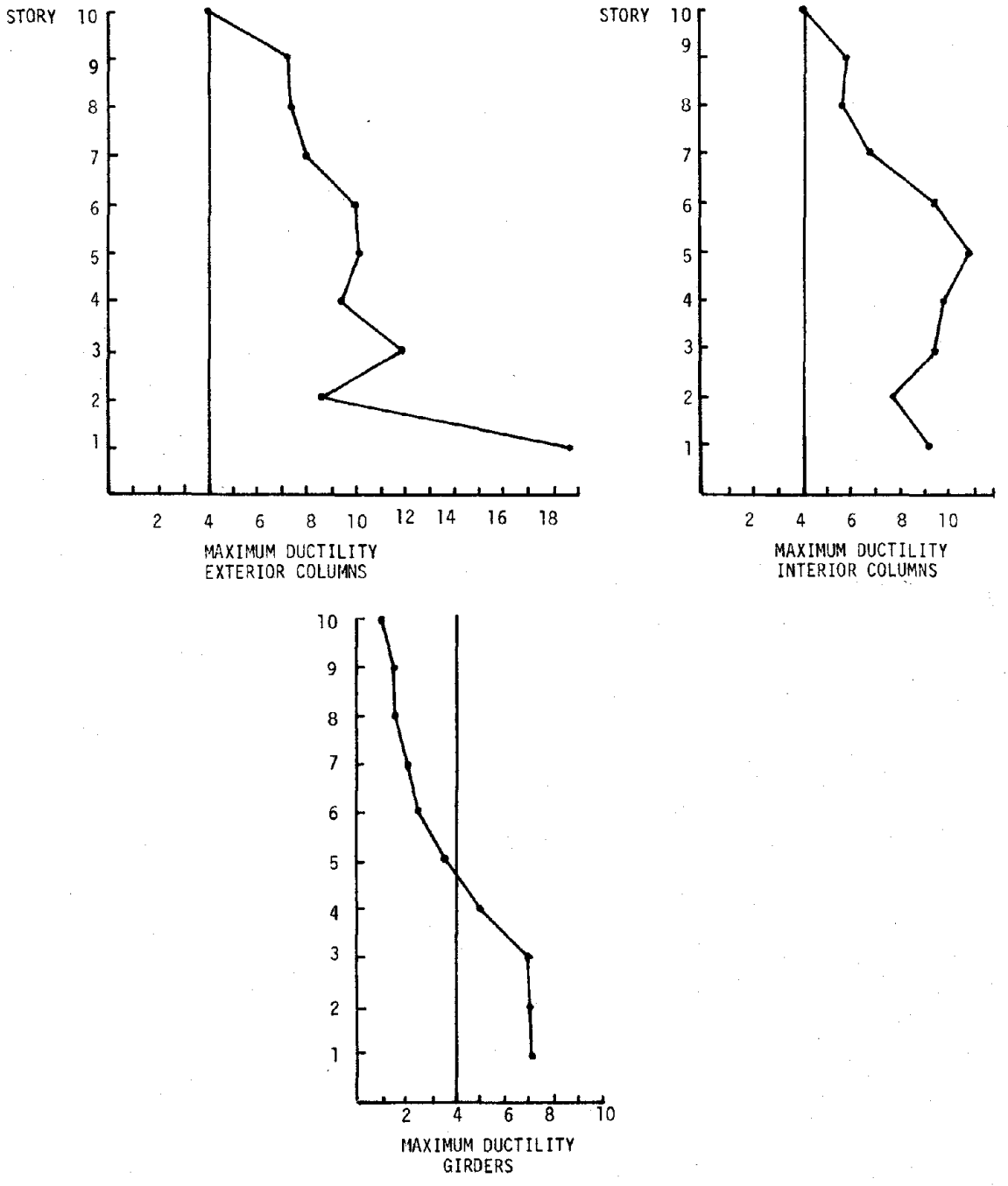

FIGURE 4.1 - MAXIMUM DUCTILITY 10-STORY FRAME - UNFACTORED DESIGN

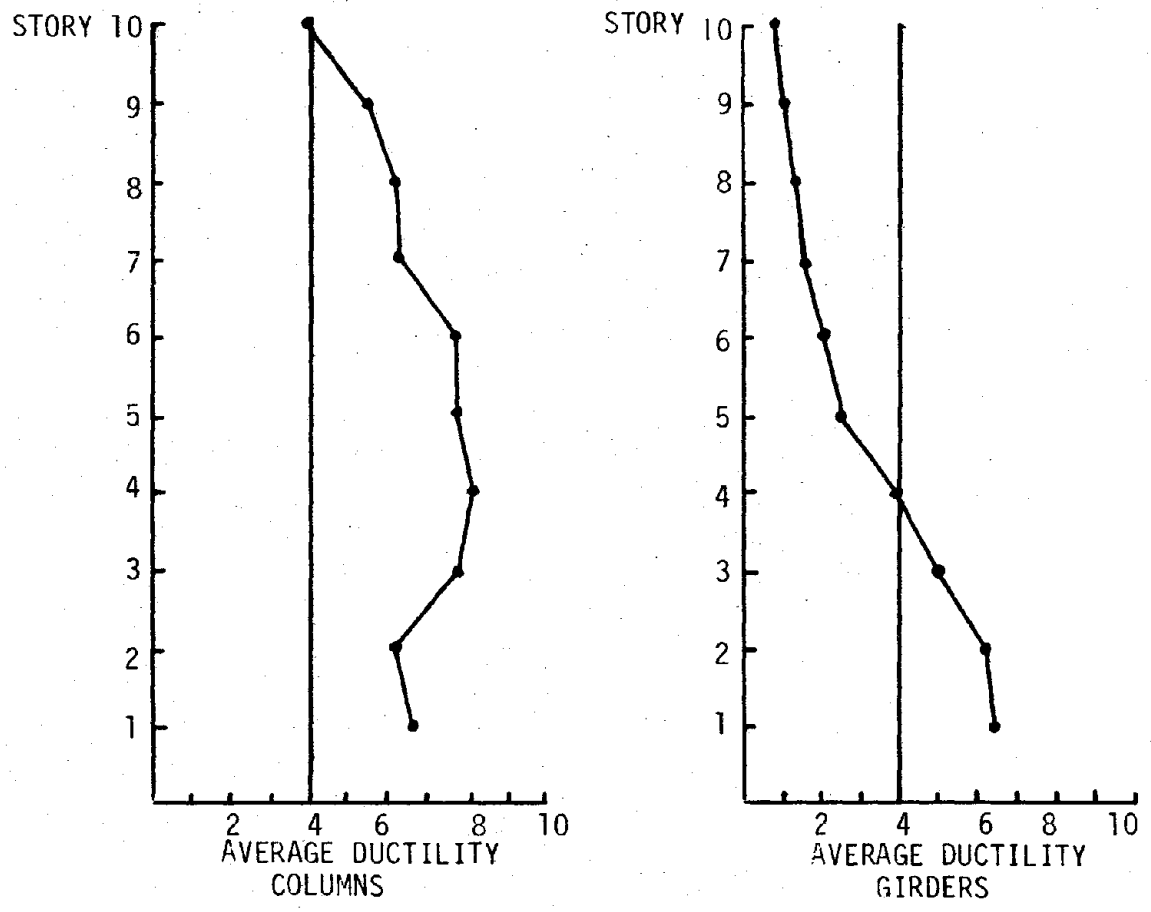

(a) (b)

FIGURE 4.2 - AVERAGE DUCTILITY - 10-STORY FRAME - UNFACTORED DESIGN

strength requirement used in determining girder resistance is again apparent in the average girder ductility values. All girder averages at floors above the third floor are substantially less than the design ductility. The average ductilities are presented only as an item of interest, as the stated goal of this research was control of local maximum ductilities rather than control of average levels of inelastic behavior. It was felt that even if average ductility levels could be controlled, unacceptable levels of local inelastic behavior might still exist at some critical locations in the structure.

Figures 4.3 to 4.5 are plots of maximum relative displacement, maximum interstory displacement, maximum interstory shear, maximum story overturning moment, and maximum column axial forces. The corresponding values based on a modal analysis using an inelastic response spectrum (labeled SRSS) are also shown for comparison. (The factored forces and displacements shown were determined from an analysis in which member strength was increased to improve response and are discussed in Section 4.2). The increase in story shear and overturning moment was due to inclusion of post yield strain hardening in the time integration analysis. The axial forces labeled "SRSS + GRAV" were determined by summing seismic axial forces from the modal analysis and gravity load axial forces resulting from static analysis. The axial forces given by the above sum closely matched the maximum axial loads calculated by FRIEDA. Maximum relative displacement values determined in the modal analysis were given by the inelastic acceleration or yield displacement spectrum, thus the values were multiplied by the

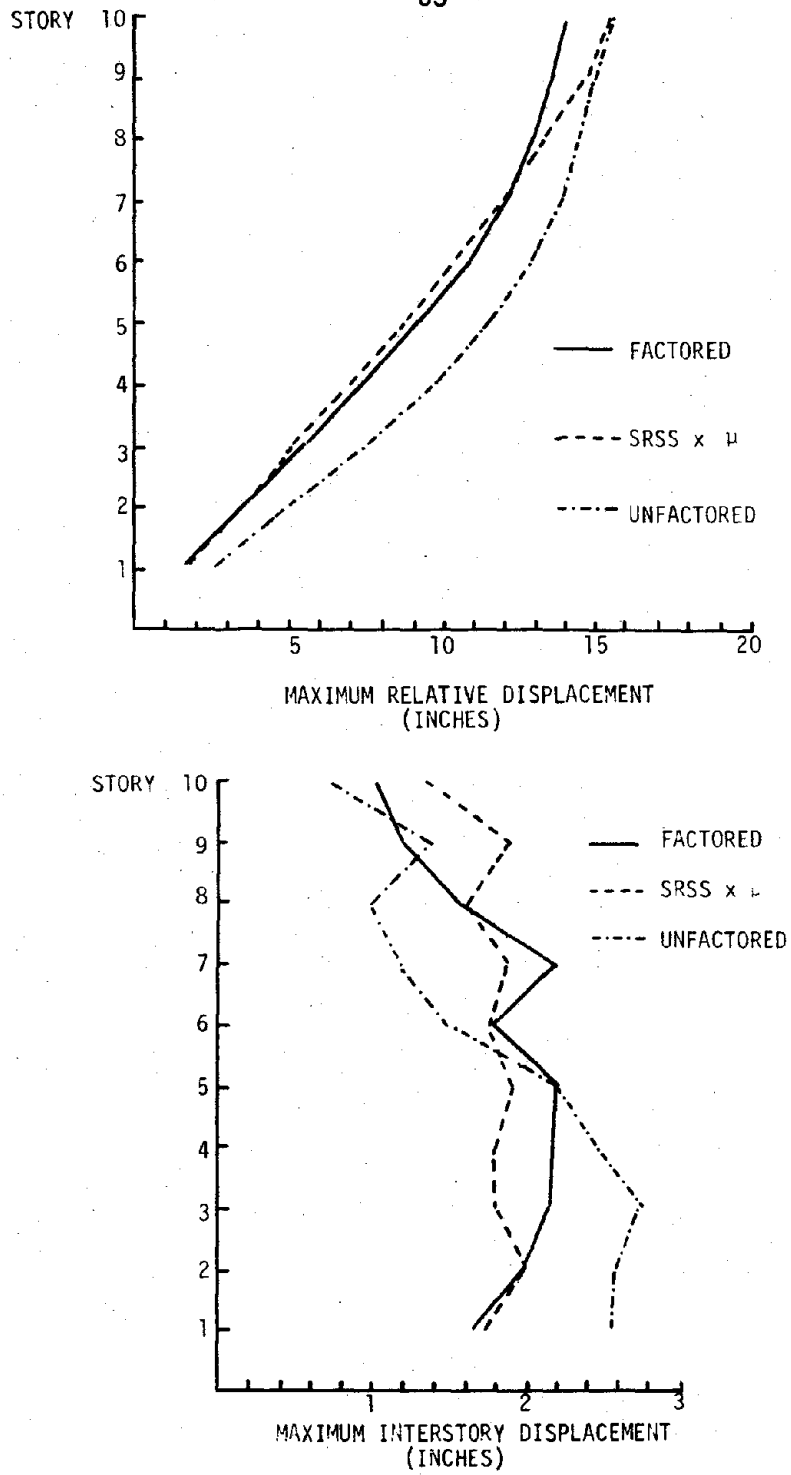

FIGURE 4.3 - MAXIMUM RELATIVE DISPLACEMENT AND MAXIMUM INTERSTORY DISPLACEMENT - 10-STORY FRAME - UNFACTORED DESIGN, FACTORED DESIGN, SRSS

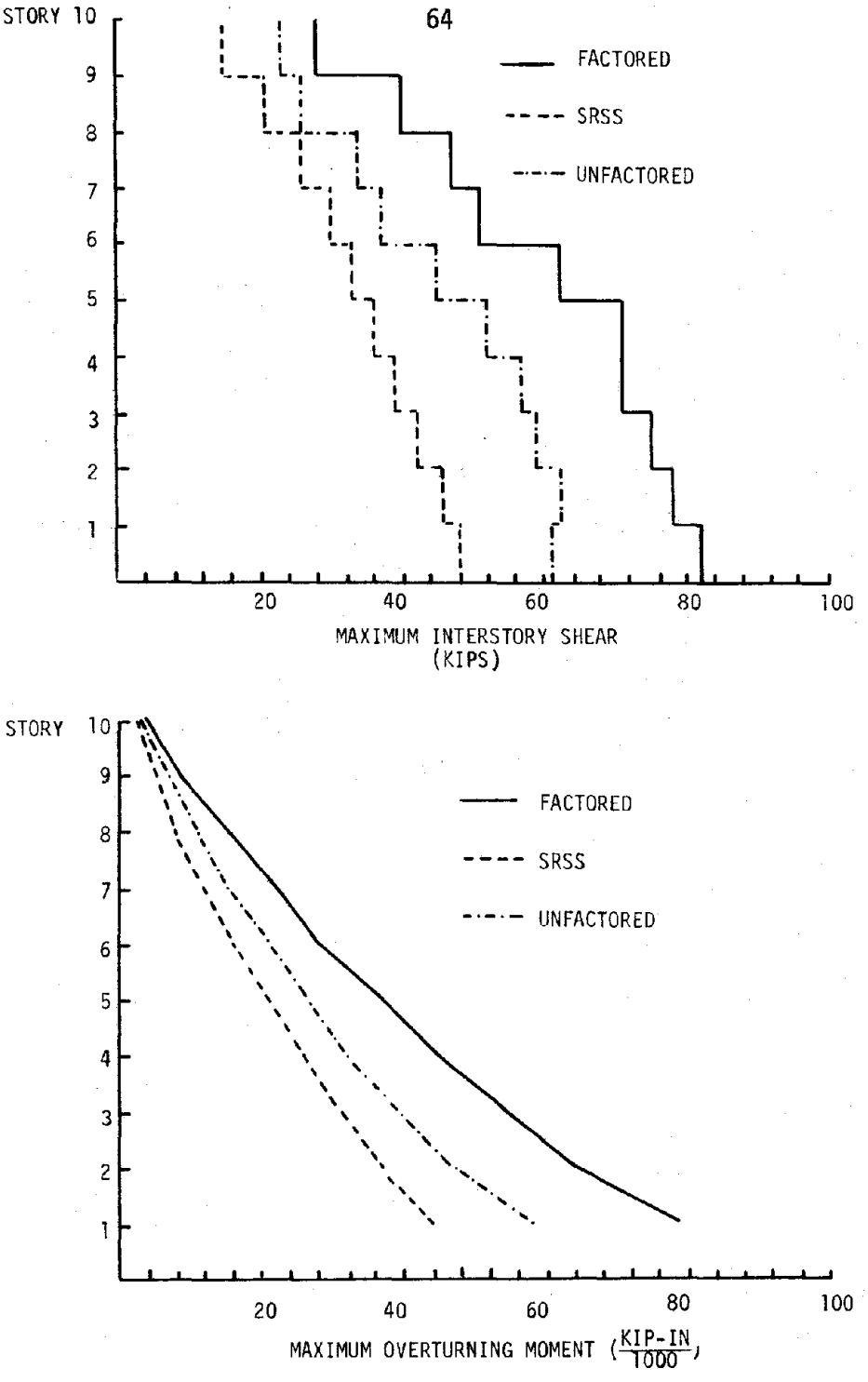

FIGURE 4.4 - MAXIMUM STORY SHEAR AND MAXIMUM STORY OVERTURNING MOMENT - 10-STORY FRAME - UNFACTORED DESIGN, FACTORED DESIGN, SRSS

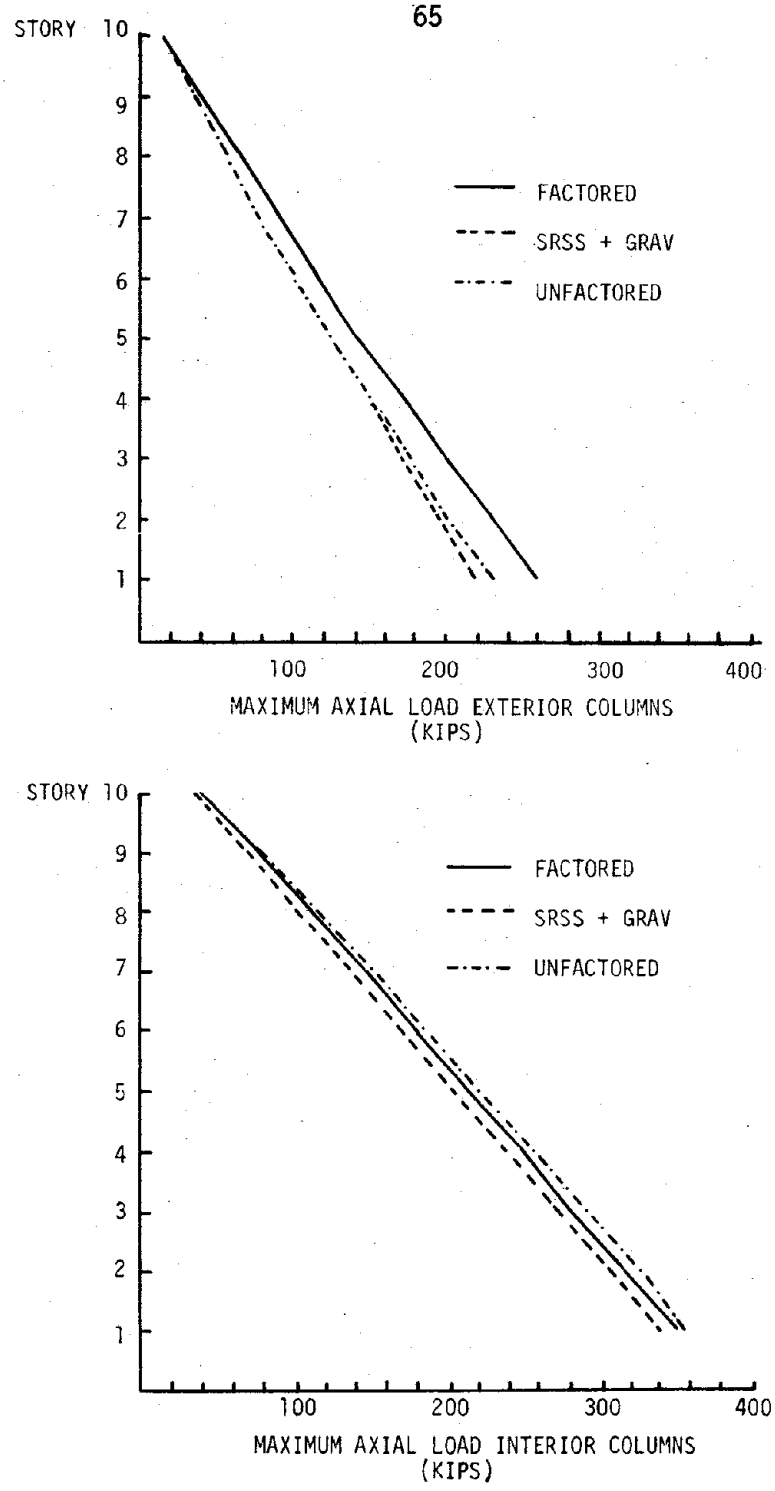

FIGURE 4.5 - MAXIMUM AXIAL FORCES - 10-STORY FRAME - UNFACTORED DESIGN, FACTORED DESIGN, SRSS

ductility factor, $\mu = 4$, for comparison with results determined from FRIEDA. The maximum relative displacements determined by FRIEDA exceeded those determined by modal analysis. Modal analysis underestimated interstory displacement in lower stories and overestimated interstory displacement in upper stories.

4.1.2 4-Story Frame

Figures 4.6 and 4.7 show the results of analysis of the unfactored design of the 4-story frame. Plots of maximum column ductility again indicate that maximum inelastic behavior exceeded the desired level of inelastic behavior. The response of the exterior columns was characterized by extremely large moment ductilities, particularly in the second and third stories, where the maximum local ductility was 12.2. The interior column ductilities were somewhat less; however, the maximum interior column ductility of 7.4 still exceeded the design ductility requirement by a substantial amount. The amount of inelastic behavior occurring in the girders was considerably less than the amount which occurred in the columns. The maximum exterior girder ductility was 1.7; the maximum interior girder ductility was 2.9. The influence of the $wl^2/8$ strength requirement and the difference in span lengths is apparent in the response of both columns and girders. The resistance of all exterior girders, which were 20 feet in length, was determined according to gravity load strength requirements. The resistance of the interior girders, which were 15 feet in length, was governed by seismic end moments in the first two stories of the frame. This differ-

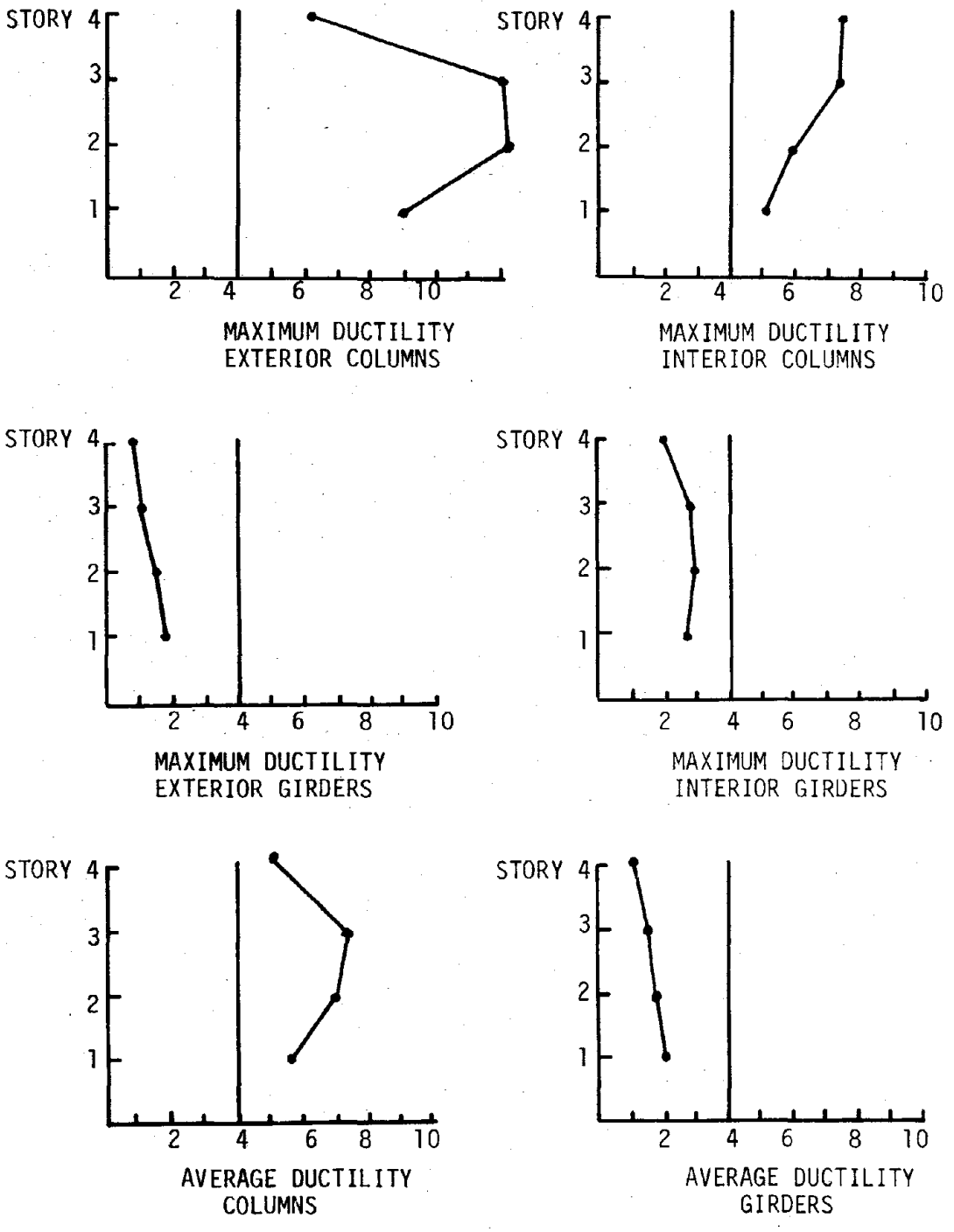

FIGURE 4.6 - MAXIMUM DUCTILITY AND AVERAGE DUCTILITY -
4-STORY FRAME - UNFACTORED DESIGN

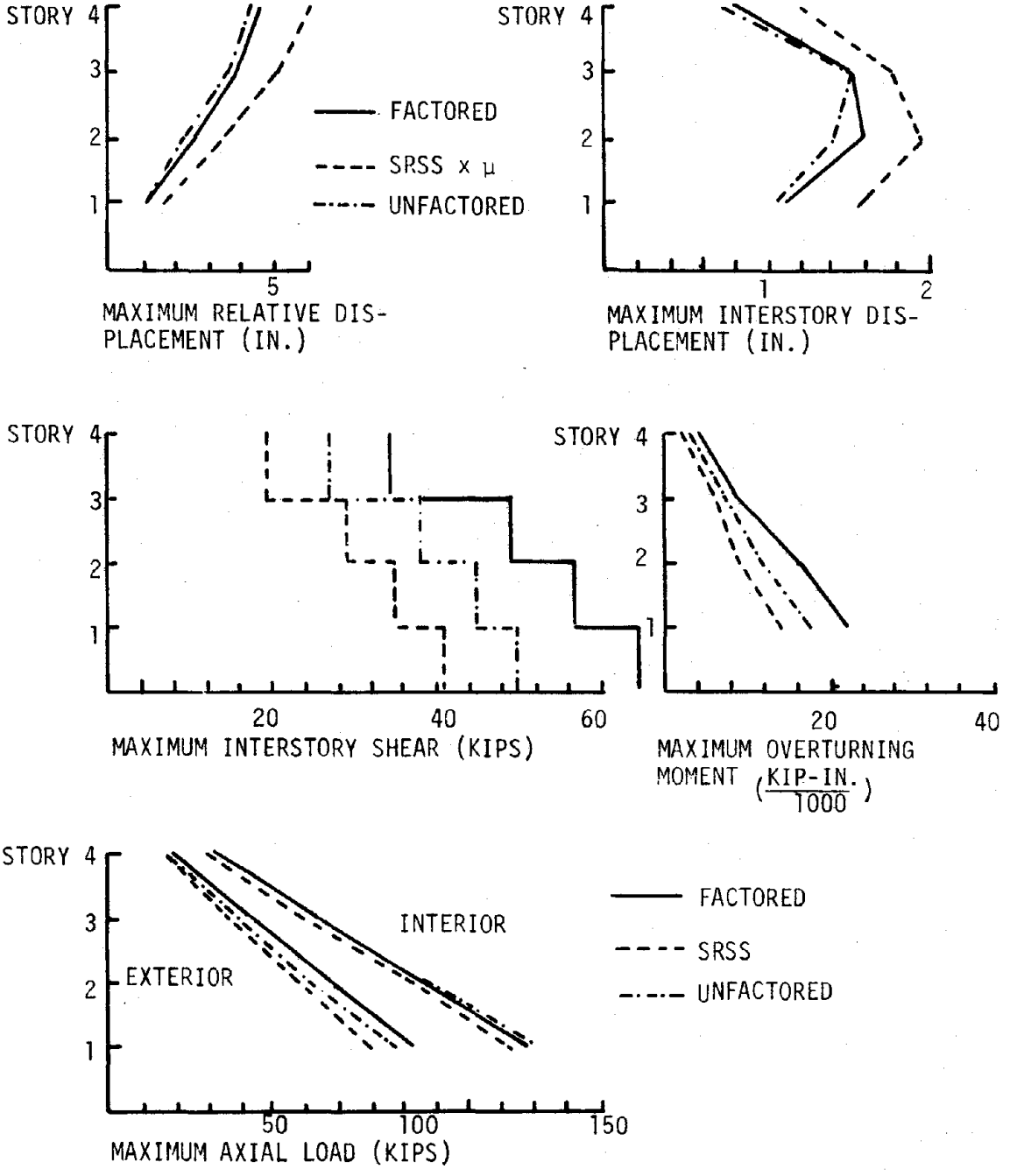

FIGURE 4.7 - MAXIMUM RELATIVE DISPLACEMENT, MAXIMUM INTERSTORY DISPLACEMENT, MAXIMUM STORY SHEAR, MAXIMUM OVERTURNING MOMENT, MAXIMUM AXIAL FORCE - 4-STORY FRAME, UNFACTORED DESIGN, FACTORED DESIGN, SRSS.

ence in girder length resulted in a difference in gravity load strength requirements and in substantially less inelastic behavior in exterior girders than in interior girders. Ductility in all girders was below the design level. The characteristics of girder inelastic response resulted in greater amounts of yielding in exterior columns than in interior columns due to the superior seismic strength of exterior girders when compared to interior girders.

The plots of the story averages of local maximum ductility shown in figure 4.6 again show the importance of gravity forces in influencing inelastic response. Column average ductilities exceeded the design ductility, but by an amount significantly less than the amount by which the maximum ductility exceeded the design level. The girder averages, as expected, were a great deal less than the design ductility.

Maximum frame displacements and forces plotted against height are shown in figure 4.7. The corresponding modal analysis values are also shown. (The forces and displacements corresponding to the factored design which are shown in figure 4.7 are discussed in Section 4.2.2). A comparison of modal analysis shear forces and overturning moments with the time integration values of the same parameters reveals the same relationship found in the analysis of the 10-story frame. However, the maximum relative and interstory displacements predicted by modal analysis of the 4-story frame, unlike those predicted by modal analysis of the 10-story frame, exceeded the values determined by FRIEDA. The modal analysis underestimated the column axial forces calculated by FRIEDA.

4.1.3 16-Story Frame

An attempt was made to analyze an unfactored design of the 16-story frame. However, 3.4 seconds after response began, the axial load in an exterior column of the first story exceeded the column axial strength which was determined by the expression $P_y = M_p/6$ (see Section 2.4). This axial load "failure" caused an immediate halt in the running of FRIEDA.

4.1.4 Conclusion

It is apparent that designing a 4-story or a 10-story frame according to the procedures of Chapter 2 does not limit local maximum ductility to the design level, or promote a uniform distribution of inelastic behavior over height. This conclusion is in agreement with the findings of both Luyties (15) and Haviland (12). It is also apparent that column axial strength can be a crucial factor in the response of tall frames to seismic loading as the axial forces necessary to resist overturning become increasingly more significant.

4.2 USE OF STRENGTH FACTORS TO CONTROL DUCTILITY

The results of Section 4.1 indicate that it is necessary to modify member strengths determined by modal analysis if local maximum ductilities are to be limited to the design level. In this section the process by which strength factors were determined and used to increase member capacity and thus improve inelastic response is presented. The strength factors were determined empirically by trial and error, as detailed below.

The member capacities determined in the unfactored designs (Section 4.1) were multiplied by the strength factors to determine new increased member resistances. The use of strength factors in the design of the 10-story frame was studied extensively, and an attempt was made to apply the results of the examination of the 10-story frame to the 4-story and 16-story frames.

4.2.1 10-Story Frame

Figures 4.8 to 4.11 show maximum ductility versus height resulting from the application of the set of strength factors shown on the right to the column and girder strengths listed in table 2.2. These figures should be compared with figure 4.1, which shows ductility resulting from the unfactored design. Exterior and interior column strength factors were chosen independently; the same strength factor was applied to all girders in any single story.

In keeping with the feeling that strength factors should be varied as little as possible over frame height, the first set of factors applied to the columns were uniform over height except for increases at the base of the frame to provide some compensation for the assumption of a rigid base connection. Exterior and interior column resistances along with girder resistances in the first three stories were increased by a factor of 1.2. A factor of 1.1 was applied to girder strength in the fourth floor, and a factor of 1.0, indicating no increase in member capacity, was applied to girders in floors above the fourth story. Girder strength above the fourth floor was not increased because

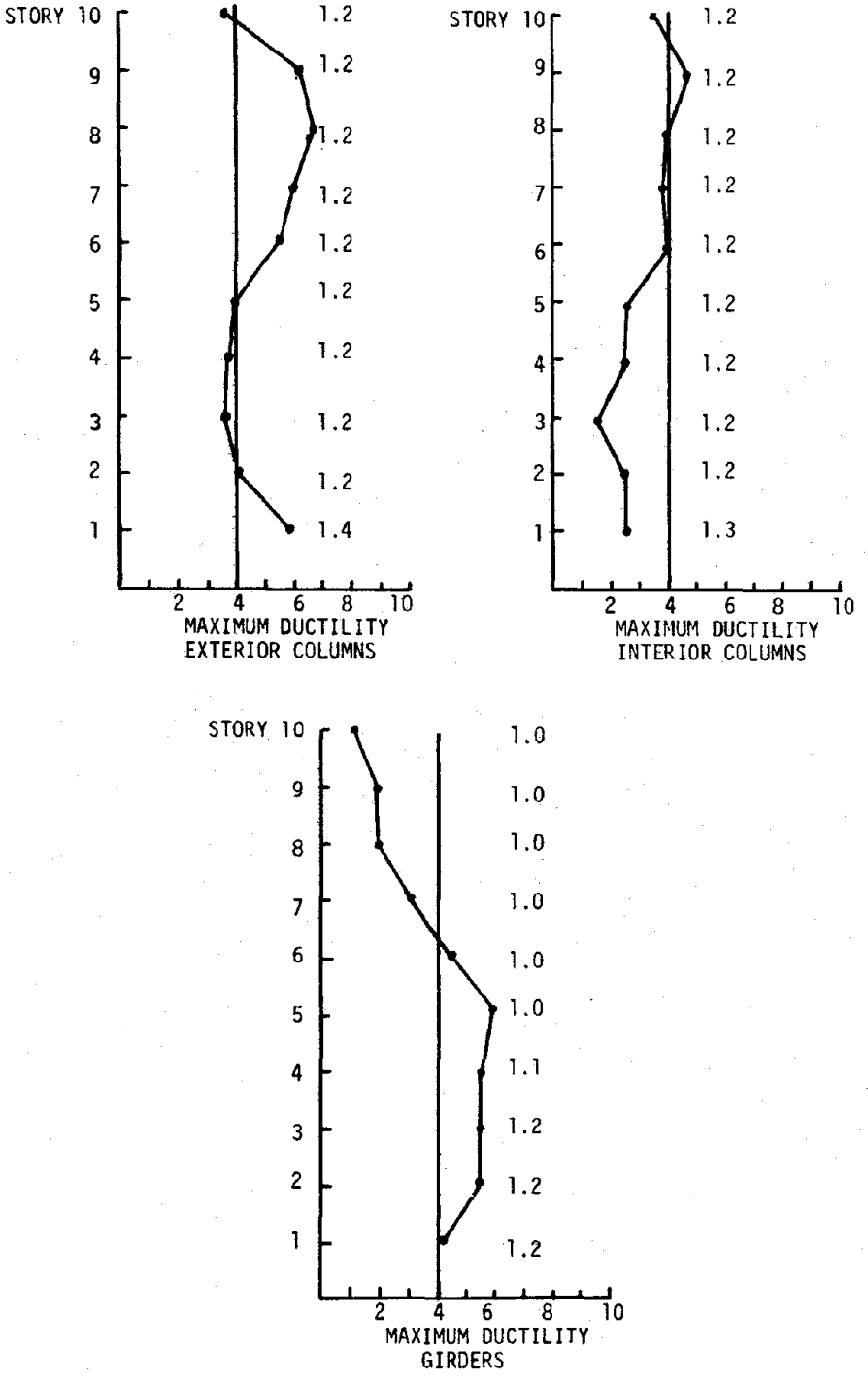

FIGURE 4.8 - MAXIMUM DUCTILITY - 10-STORY FRAME - FIRST SET OF STRENGTH FACTORS

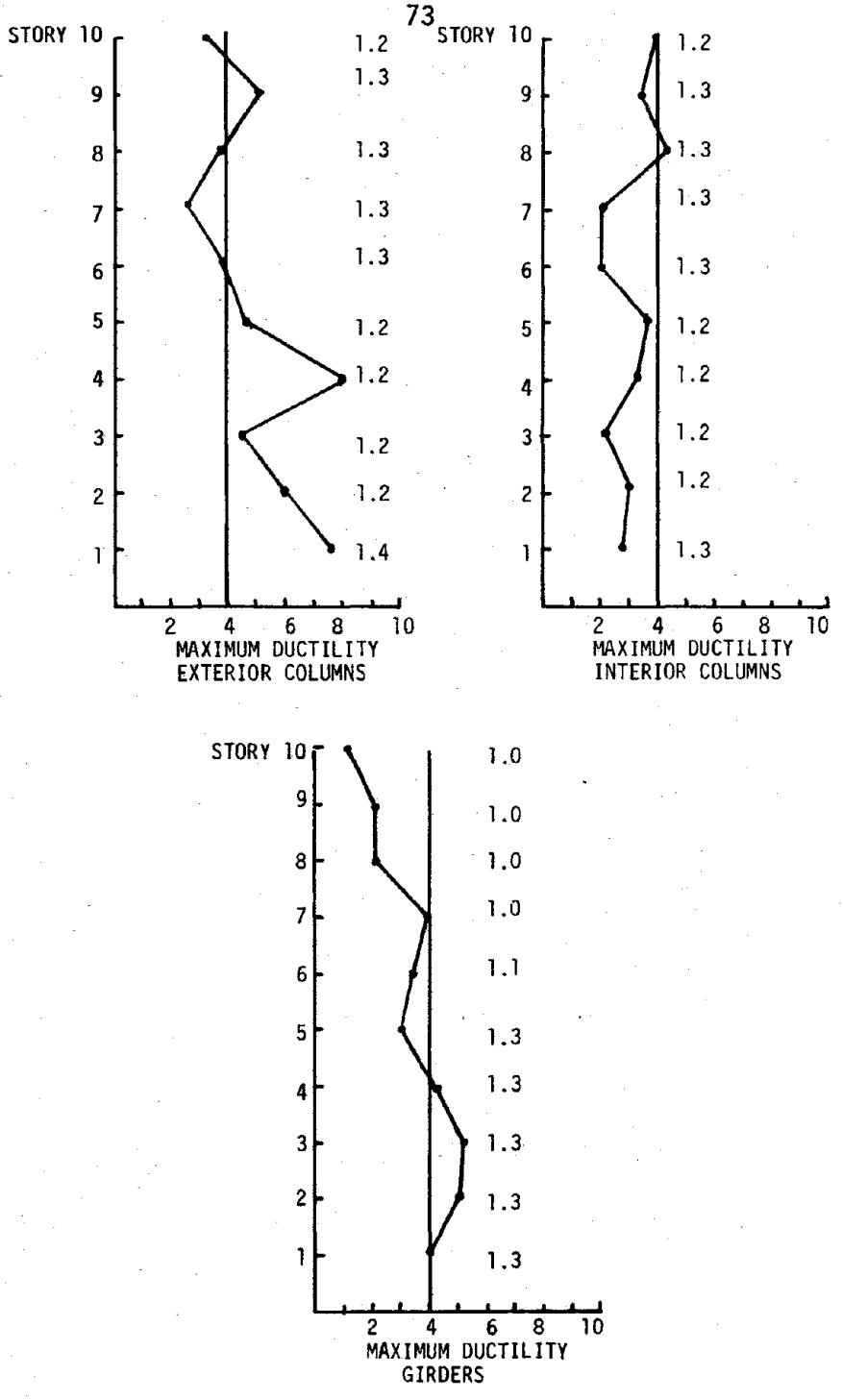

FIGURE 4.9 - MAXIMUM DUCTILITY - 10-STORY FRAME - SECOND SET OF STRENGTH FACTORS

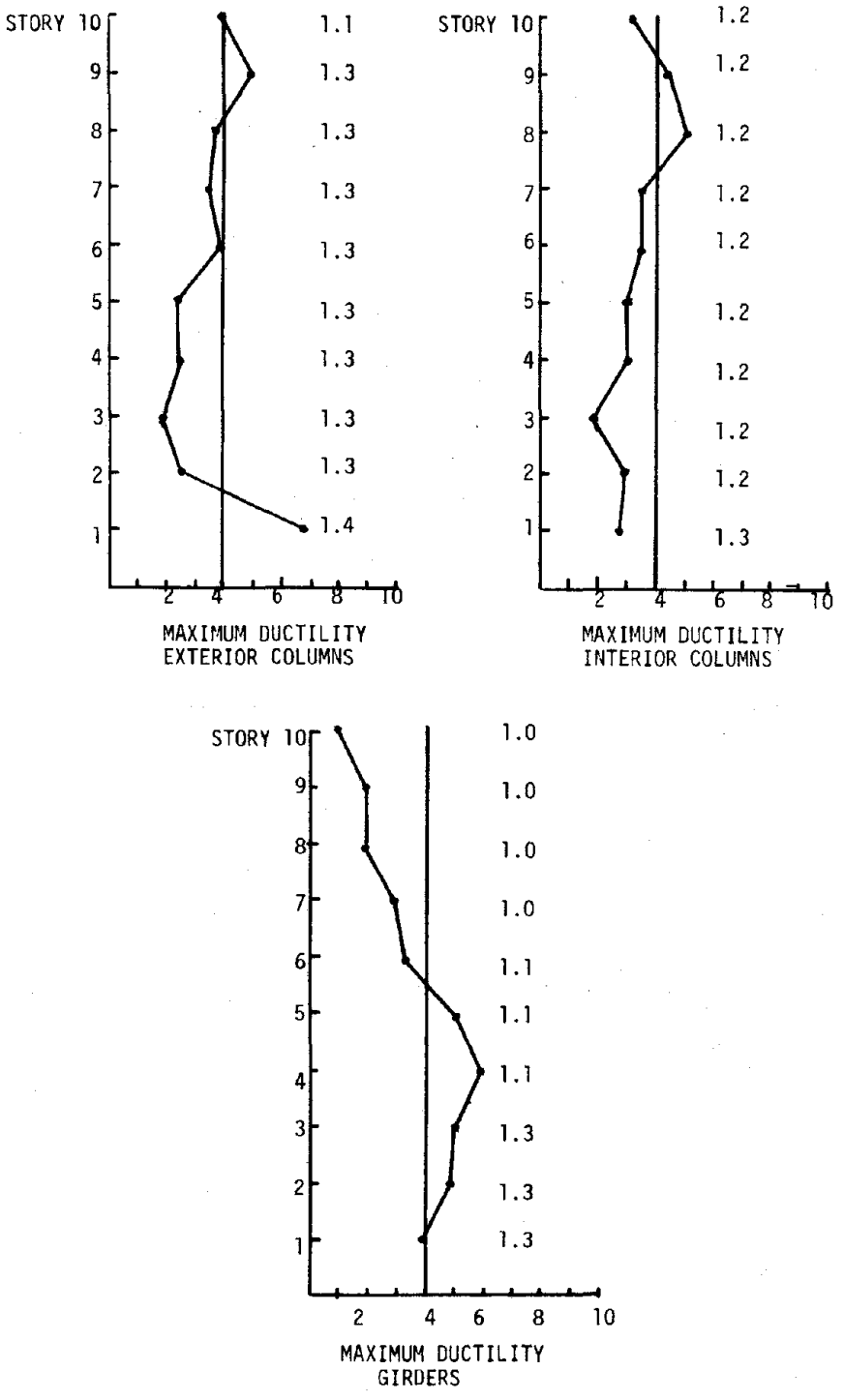

FIGURE 4.10 - MAXIMUM DUCTILITY - 10-STORY FRAME - THIRD SET OF STRENGTH FACTORS

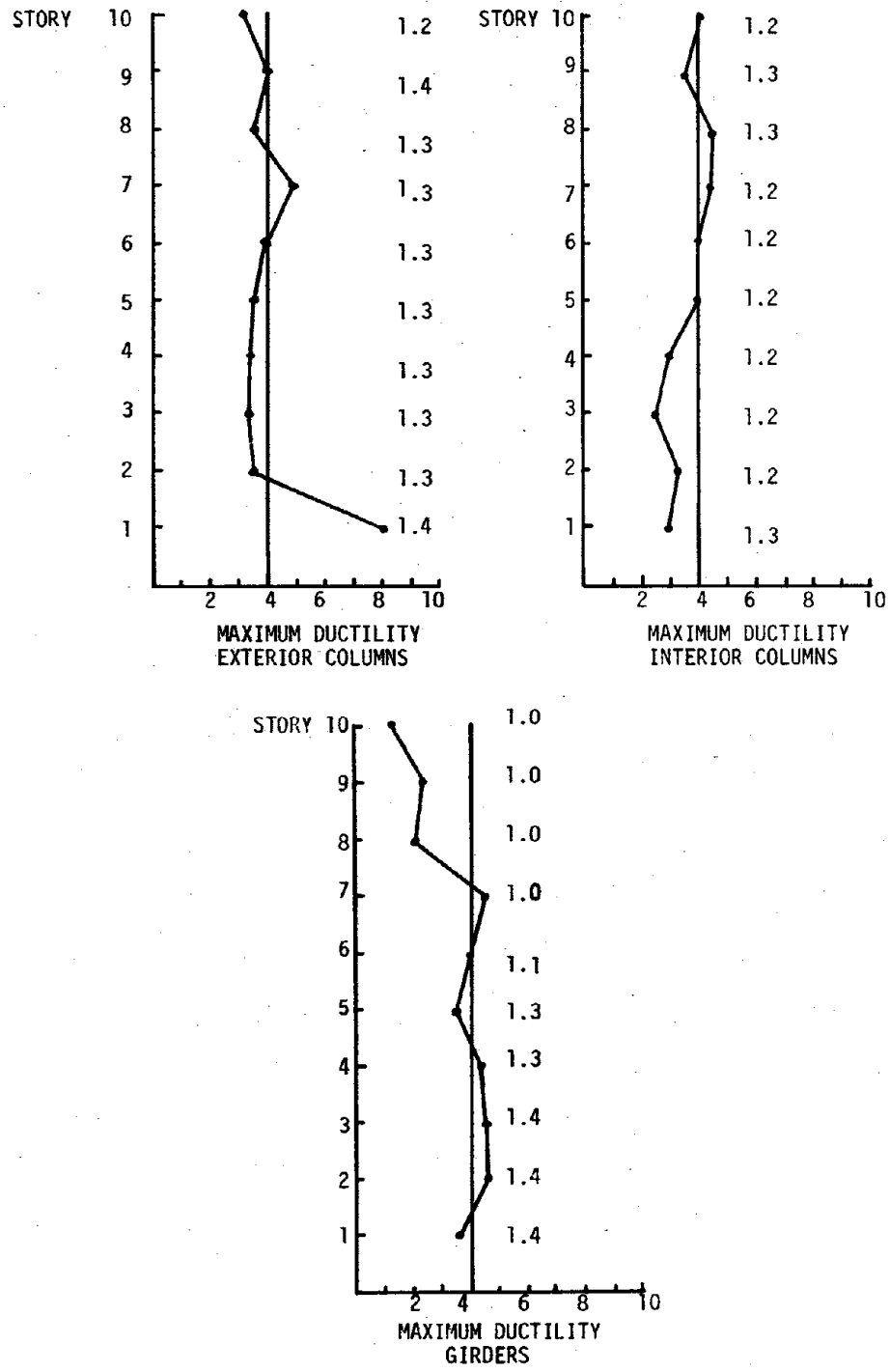

FIGURE 4.11 - MAXIMUM DUCTILITY - 10-STORY FRAME - FINAL SET OF STRENGTH FACTORS

response determined for the unfactored design indicated that above that level application of the $wl^2/8$ strength requirement resulted in girders which were overdesigned seismically. The ductility requirements of exterior columns after applying the first set of strength factors form the reversed S-shape shown in figure 4.8. Exterior column ductility in the lower stories was uniformly limited to the design level indicated by the vertical straight line passing through $\mu = 4$. In the upper stories exterior column maximum ductilities exceeded the design ductility, reaching a maximum of 6.8 in the eighth floor. The interior column ductilities like those of the exterior columns showed a marked increase in the upper stories when compared to lower story ductility values. However, the upper story ductilities in interior columns were limited to the design level (the only exception was a ductility of 4.7 in the ninth floor), and lower story ductilities were in some instances substantially less than the design ductility. Girder ductility in the lower stories was uniformly distributed over height, but was not limited to the design level. Above the sixth floor, girder response was as expected controlled by gravity load strength requirements, resulting in local ductility maxima less than the design ductility. It is interesting to compare the pattern of ductility requirements corresponding to girders and columns. Where the girder ductility demand was high, the column demand remained at or below the design level. Where girder maximum ductilities were necessarily influenced by vertical load strength requirements, column ductilities increased, and in the case of exterior columns, exceeded the design level.

After noting the inelastic behavior resulting from the first set of spectral factors, a second set of strength factors was chosen which showed an increase in upper story exterior and interior column strength factors from 1.2 to 1.3, and an increase in lower story girder strength factors from 1.2 to 1.3. Lower story column strength factors remained unchanged. The results of applying the second set of strength factors to initial member capacity is shown in figure 4.9. Despite the increase in strength, girder ductility requirements were reduced very little in the first three stories. The increase in girder strength from the first set of factors to the second set was greater in the fourth and fifth floors (from 1.0 and 1.1 to 1.3) than the increase in strength in the first three floors (from 1.2 to 1.3). Thus the decrease in maximum ductility at the fourth and fifth floors was also more significant. The lower story exterior columns, particularly those located in the fourth story, exhibited significant increases in maximum ductility requirements, apparently as a result of the increase in girder strength. A slight increase in lower story interior column ductility demand also occurred. Exterior column ductility demand was reduced above the fifth floor, reflecting the increase in upper story column resistances. The interior columns showed a substantial reduction in inelastic behavior in the sixth and seventh stories, but an increase in ductility occurred at the eighth floor in spite of an increase in member strength.

The second set of strength factors in general resulted in poor control of ductility in the lower level exterior columns. In addition, the variation in ductility demand from one story to the next showed a substantial increase over the variation in ductility resulting from

implementation of the first set of strength factors. Thus in choosing a third set of strength factors a decision was made to return to applying nearly uniform column strength factors. However, in this case, the exterior column strength factors were increased to 1.3. The factor applied to interior columns was returned to 1.2. Noting the adverse effect on column ductility of increased girder capacity, girder resistance in the fourth and fifth floors was reduced in the hope of reducing exterior column ductility demand. The results plotted in figure 4.10 indicate that choosing uniform column strength factors does improve uniformity of ductility distribution. Column inelastic behavior was well controlled except in the eighth and ninth floors. The decreased inelastic behavior in lower story column ductility again occurs in stories in which girder inelastic behavior is excessive.

In choosing a fourth and final set of strength factors, the only improvements made in the third set of factors was an increase in lower story girder factors from 1.3 to 1.4 and from 1.1 to 1.3. Column strength was increased only in the eighth and ninth floors. Figure 4.11 shows that the final set of strength factors applied to initial member capacities very nearly achieved uniformly distributed local maximum ductilities limited to the design ductility levels. Exterior column ductility exceeded the design ductility only in the seventh story where ductility equaled 4.9, while interior column ductility exceeded the design level twice, with ductilities of 4.4 and 4.5 occurring in the seventh and eighth floors. The girder ductility level exceeded the design level slightly in four floors, with a maximum ductility of 4.5 occurring in the second floor.

The factors which were determined above correspond to an increase in member capacity over the resistances which were determined according to the inelastic design procedure detailed in Chapter 2. It is perhaps of greater interest to the engineer to know what increase in seismic design forces obtained from the modal analysis is necessary to achieve the desired inelastic behavior. Table 4.1 lists the final set of strength factors together with the "spectral" factors which one would have to apply to the design seismic moments, determined by modal analysis, to achieve design forces which would result in the computation of the member capacities which were determined by applying the final strength factors. The spectral factors give some indication of the amount by which the modal analysis underestimates the inelastic behavior calculated by time integration analysis. The column spectral factors were backfigured from the strength factors according to the following expression:

$$(STF)(M_p) = (SPF)\left[\frac{M_{EQ}}{1.18}\right] + (SPF)(6P_{EQ}) + 6\,P_{GR}$$

$$SPF = \frac{(STF)(M_p) - 6P_{GR}}{M_{EQ}/1.18 + 6P_{EQ}} \qquad (4.1)$$

where SPF = spectral factor

STF = strength factor

M_p = original unfactored plastic moment capacity

M_{EQ} = seismic moment from modal analysis

P_{GR} = gravity load axial force from static analysis.

P_{EQ} = seismic axial force from modal analysis

TABLE 4.1 - FINAL STRENGTH FACTORS AND SPECTRAL FACTORS - 10-STORY FRAME

STORY	STRENGTH FACTOR	SPECTRAL FACTOR	STORY	STRENGTH FACTOR	SPECTRAL FACTOR
	EXTERIOR COLUMNS			INTERIOR COLUMNS	
1	1.4	1.8	1	1.3	1.8
2	1.3	1.7	2	1.2	1.6
3	1.3	1.6	3	1.2	1.6
4	1.3	1.6	4	1.2	1.5
5	1.3	1.6	5	1.2	1.5
6	1.3	1.6	6	1.2	1.5
7	1.3	1.6	7	1.2	1.5
8	1.3	1.8	8	1.3	1.6
9	1.4	1.7	9	1.3	1.6
10	1.2	2.3	10	1.2	1.3
	EXTERIOR GIRDERS			INTERIOR GIRDERS	
1	1.4	1.4	1	1.4	1.4
2	1.4	1.4	2	1.4	1.4
3	1.4	1.4	3	1.4	1.4
4	1.3	1.5	4	1.3	1.5
5	1.3	1.6	5	1.3	1.6
6	1.1	1.5	6	1.1	1.4
7	1.0	1.0	7	1.0	1.0
8	1.0	1.0	8	1.0	1.0
9	1.0	1.0	9	1.0	1.0
10	1.0	1.0	10	1.0	1.0

Girder spectral factors were obtained as follows:

$$SPF = \frac{(STF)(M_p)}{M_{EQ}} \qquad (4.2)$$

In some instances M_p was determined according to gravity load strength requirements, yet strength factors were still necessary to achieve desired inelastic behavior indicating that in fact seismic end moments dictated member response. In these instances spectral factors were calculated based on the modal analysis spectral forces even though these forces were not used as design forces in the initial design. At locations where initial design was based on gravity moments and no increase in resistance was necessary to control inelastic response, a spectral factor of 1.0 was assumed indicating that the estimate of inelastic behavior given by modal analysis, whether good or bad, had no bearing on response due to the superior influence of gravity forces.

The calculated column spectral factors are larger than the column strength factors and vary more with height. The last observation is particularly true in the upper stories of the frame where apparently the modal analysis greatly underestimated maximum column seismic forces. Girder spectral and strength factors are identical in the first three floors where initial design was controlled by spectral forces. In floors four through six the original unfactored design was based on the $wl^2/8$ requirement; thus the calculated spectral factors are somewhat larger than the strength factors.

Figures 4.3 to 4.5 show forces and displacements versus height resulting from analysis of the 10-story frame with final strength factors

applied. The results of the modal analysis (labeled SRSS) and the results of the unfactored design are also shown. The relative displacements predicted by the modal analysis when multiplied by the ductility factor closely match the maximum displacement calculated from the factored design. Interstory displacement corresponding to the factored design also is closer to the displacement predicted by modal analysis than is interstory displacement corresponding to the unfactored design. Interstory shear, story overturning moment, and exterior column axial forces all showed an increase over the unfactored design results. Only interior column axial loads decreased.

4.2.2 4-Story and 16-Story Frames

An initial set of strength factors for the 4-story frame was chosen based on the results of the factored 10-story frame design and the unfactored 4-story frame design. The resulting ductility distribution is shown in figure 4.12. (Compare with figure 4.6, showing results of unfactored design). No factors were applied to the girders because it was felt that response in these members would be limited by vertical load strength requirements. The results indicate that interior girder ductility exceeded design ductility because column strength was increased without a corresponding increase in interior girder strength. Again it should be pointed out that the interior girders of the 4-story frame were shorter than the exterior girders; consequently moments due to vertical loads were less significant in interior girders. The exterior column ductilities were close to the design ductility; however, interior column ductility in the lower

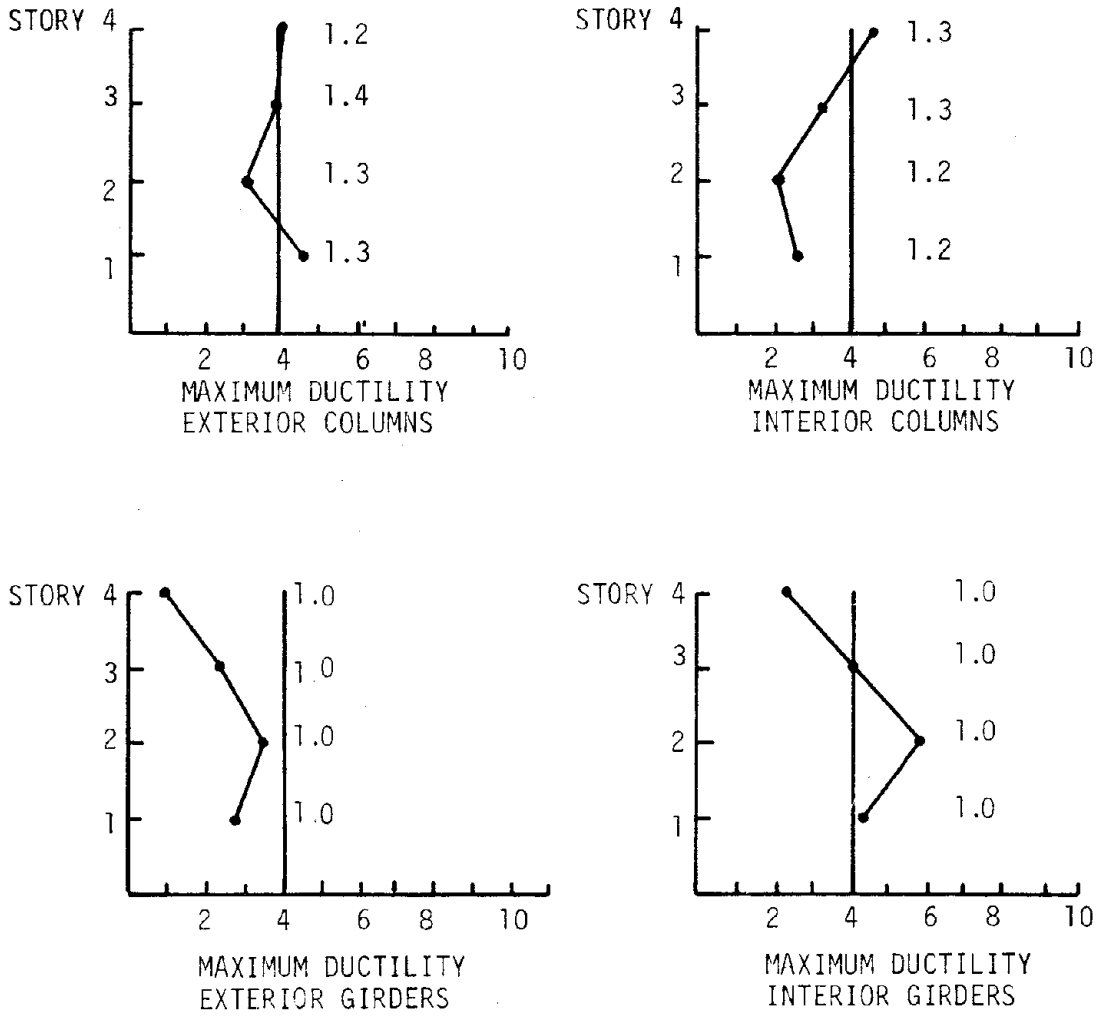

FIGURE 4.12 - MAXIMUM DUCTILITY - 4-STORY FRAME - INITIAL SET OF STRENGTH FACTORS

stories indicated that these members were overdesigned.

The changes indicated in figure 4.13 were made in the initial set of strength factors. The result was improved behavior in both girders and columns. Maximum ductility at all levels in all members was less than the design ductility, and except in locations where response was controlled by gravity forces, ductility distribution was reasonably uniform over height.

The forces and displacements from analysis of factored and unfactored designs, together with the modal analysis results, are shown in figure 4.7. In general the factored and unfactored displacements shown are very similar. Including strength factors in design, however, resulted in an increase in interstory shears, in story overturning moments, and in exterior column axial loads. Interior column axial loads calculated for the factored design match those calculated for the unfactored design very closely.

The spectral factors backfigured from the 4-story frame strength factors according to equations (4.1) and (4.2) are listed in table 4.2. The spectral factors as expected are somewhat larger than the strength factors and are generally in the range of the spectral factors determined for the 10-story frame. The spectral factors of all exterior girders are 1.0, indicating that seismic moments did not control the level of inelastic response.

The initial strength factors selected for the 16-story frame were based solely on the strength factors selected for the 10-story frame. The resulting ductility distribution shown in figure 4.14 was generally

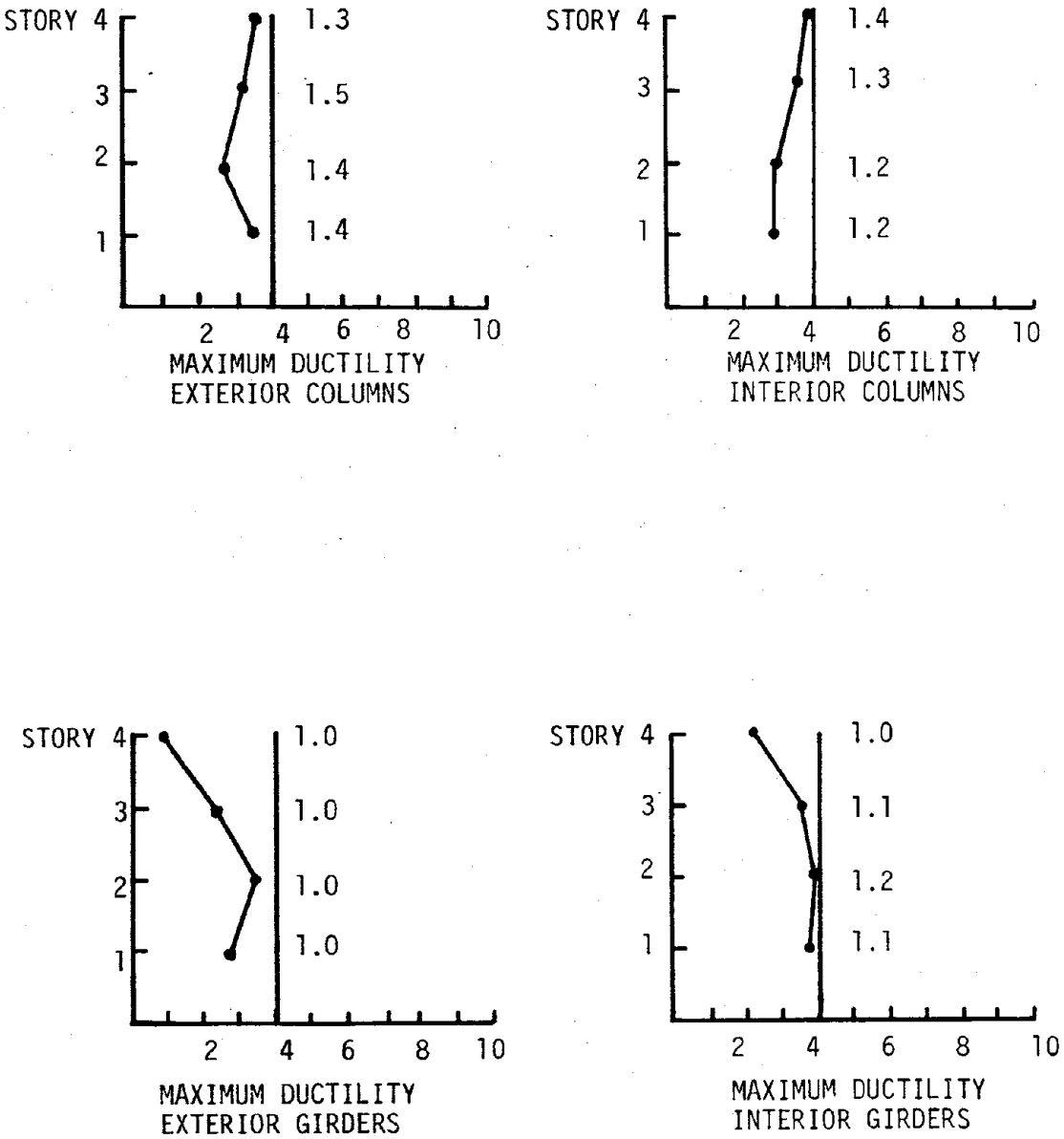

FIGURE 4.13 - MAXIMUM DUCTILITY - 4-STORY FRAME - FINAL SET OF STRENGTH FACTORS

TABLE 4.2 - FINAL STRENGTH FACTORS AND SPECTRAL FACTORS - 4-STORY FRAME

STORY	STRENGTH FACTOR	SPECTRAL FACTOR	STORY	STRENGTH FACTOR	SPECTRAL FACTOR
	EXTERIOR COLUMNS			INTERIOR COLUMNS	
1	1.4	1.7	1	1.2	1.4
2	1.4	1.7	2	1.2	1.4
3	1.5	1.8	3	1.3	1.5
4	1.3	2.5	4	1.4	1.6
	EXTERIOR GIRDERS			INTERIOR GIRDERS	
1	1.0	1.0	1	1.1	1.1
2	1.0	1.0	2	1.2	1.2
3	1.0	1.0	3	1.1	1.4
4	1.0	1.0	4	1.0	1.0

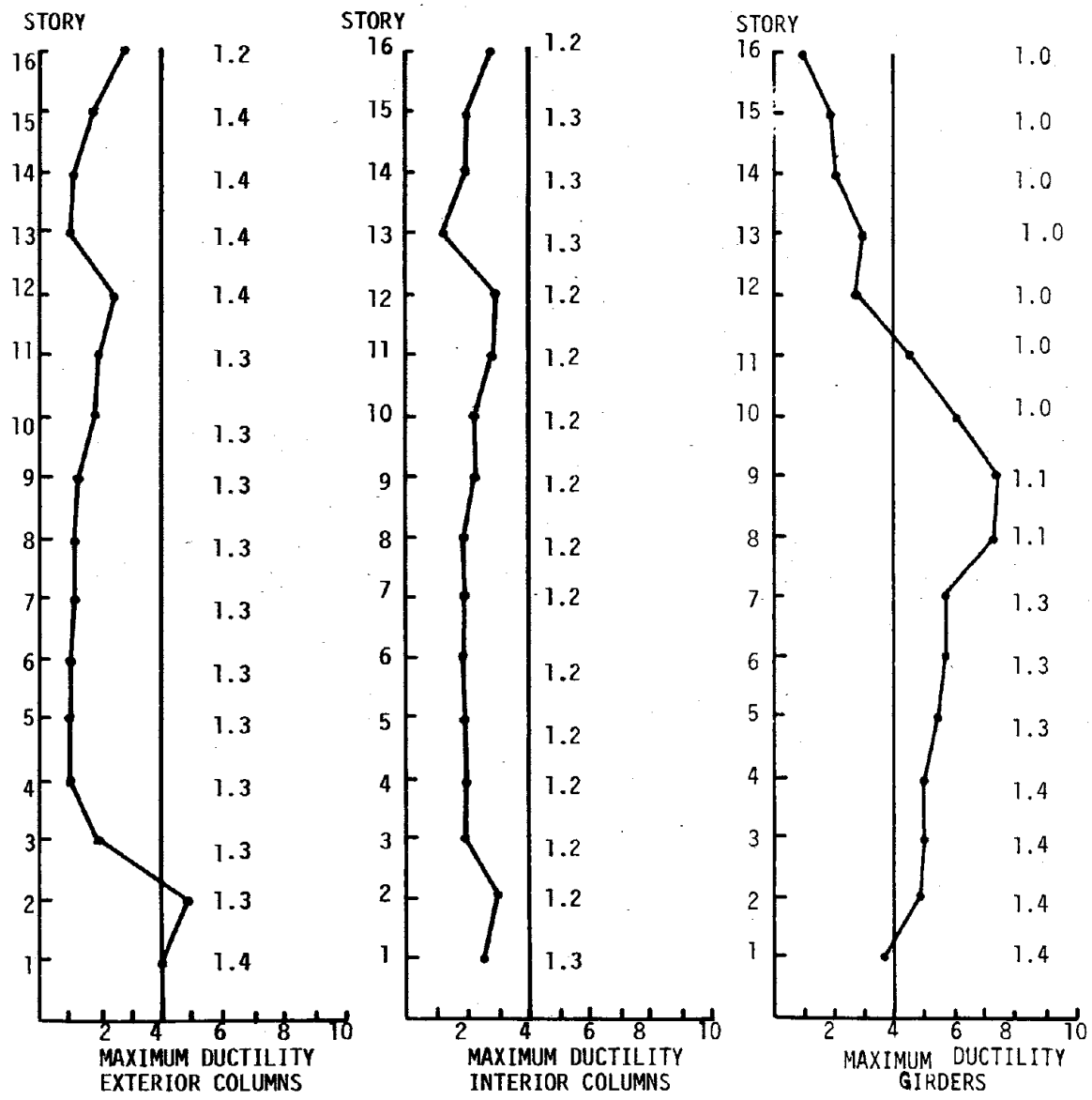

FIGURE 4.14 - MAXIMUM DUCTILITY - 16-STORY FRAME - INITIAL SET OF STRENGTH FACTORS

good, although it is apparent that the lower story columns were somewhat overdesigned and the lower story girders were somewhat underdesigned. A second set of strength factors in which exterior column factors were reduced from 1.3 to 1.2 and interior column factors from 1.2 to 1.1, and an increase was made in all girder factors below the tenth floor to 1.4. This set of strength factors resulted in an axial load failure similar to the failure which occurred when an attempt was made to analyze the unfactored design of the 16-story frame.

In keeping with the findings of the analysis of the 10-story frame, a final attempt was made to improve inelastic behavior in both columns and girders by increasing the resistance in the girders. Column resistance was reduced only in the uppermost floors in an attempt to make a relatively minor adjustment in ductility level. The results of increasing girder strength are shown in figure 4.15. Uniformity of ductility in the exterior columns and the level of ductility in the lower story girders might have been further improved; however, the expense involved in analyzing the 16-story frame limited the number of sets of strength factors which were applied. Nevertheless the final set of strength factors shown in figure 4.15 result in reasonable maximum ductility values. Column ductility was less than the design level, and although girder ductility exceeds the design level slightly, the uniformity of ductility distribution was good. The relationship between modal analysis forces and displacements and time integration analysis forces and displacements shown in figures 4.16 to 4.19 was similar to that shown for the 4- and 10-story frames.

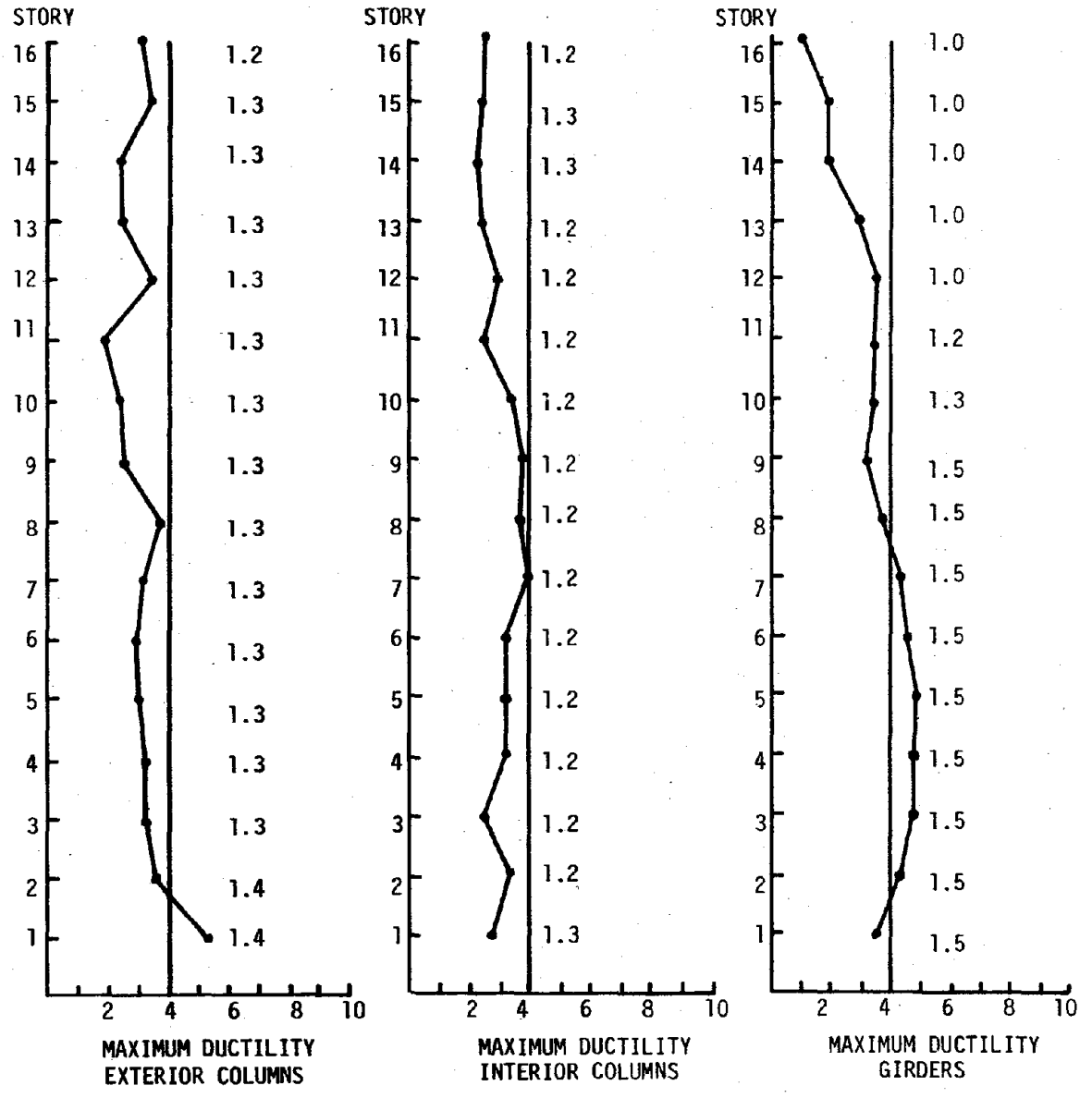

FIGURE 4.15 - MAXIMUM DUCTILITY - 16-STORY FRAME -
FINAL SET OF STRENGTH FACTORS

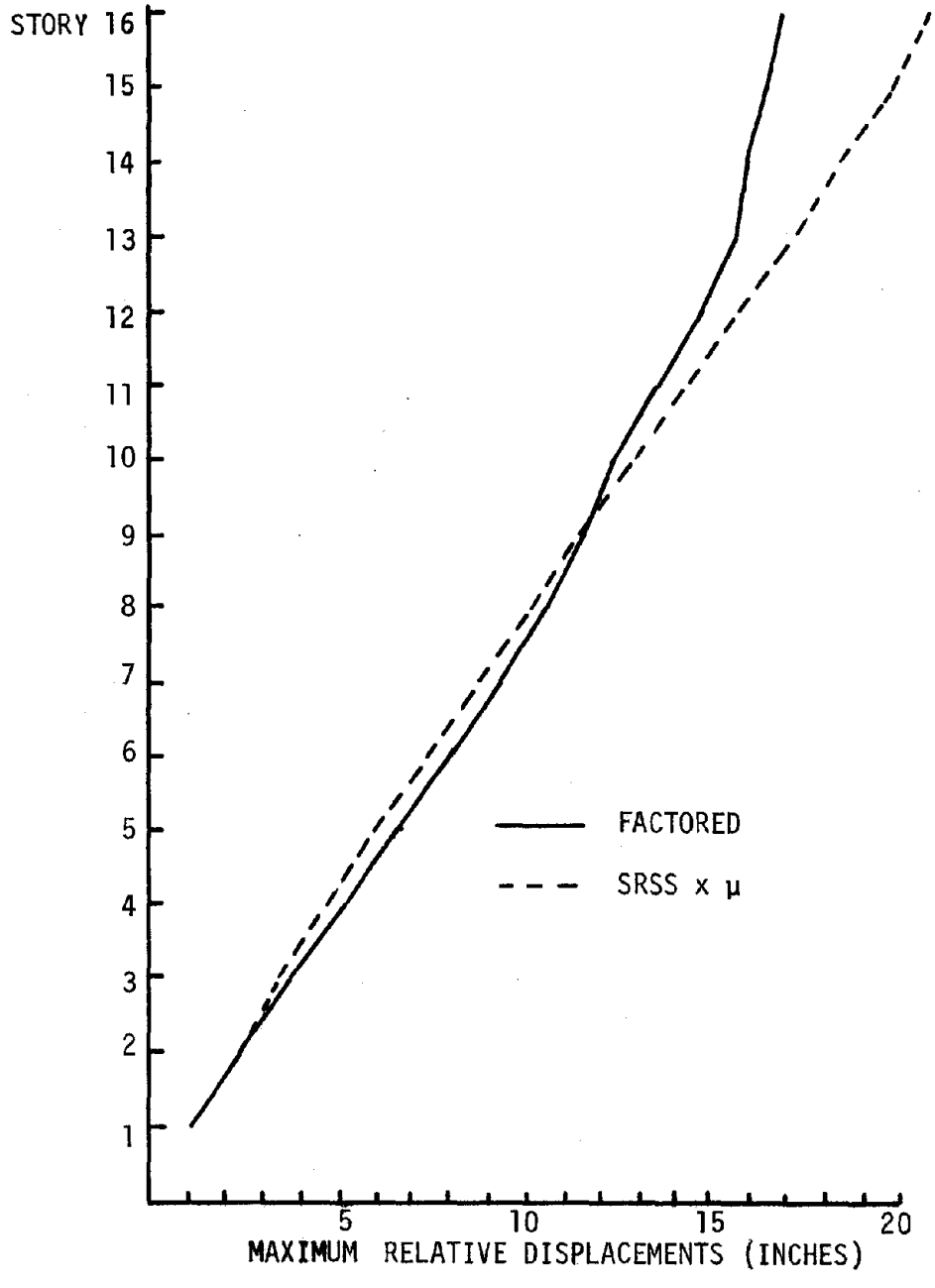

FIGURE 4.16 - MAXIMUM RELATIVE DISPLACEMENT - 16-STORY FRAME - FACTORED DESIGN AND SRSS

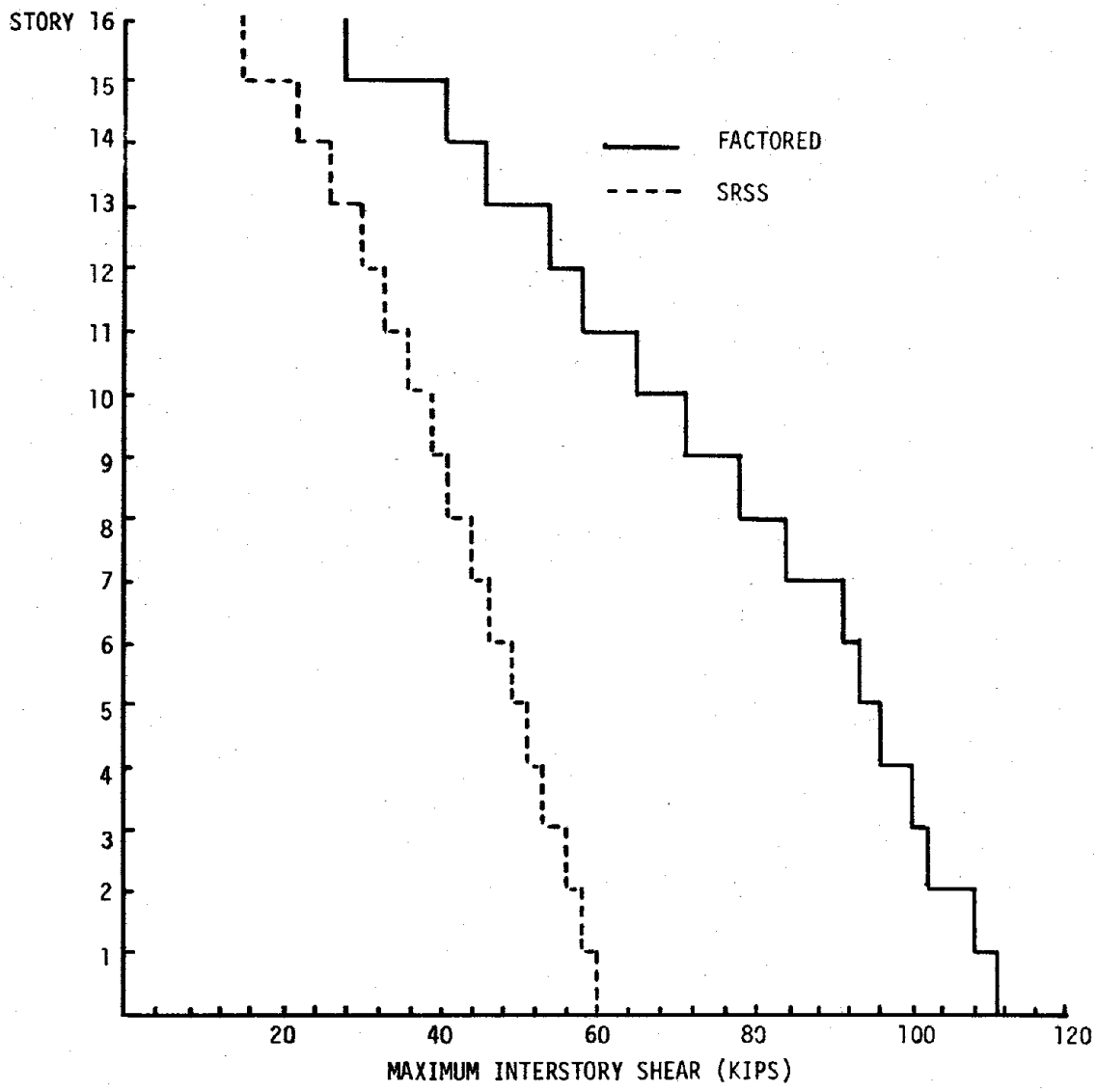

FIGURE 4.17 - MAXIMUM INTERSTORY SHEAR - 16-STORY FRAME - FACTORED DESIGN AND SRSS

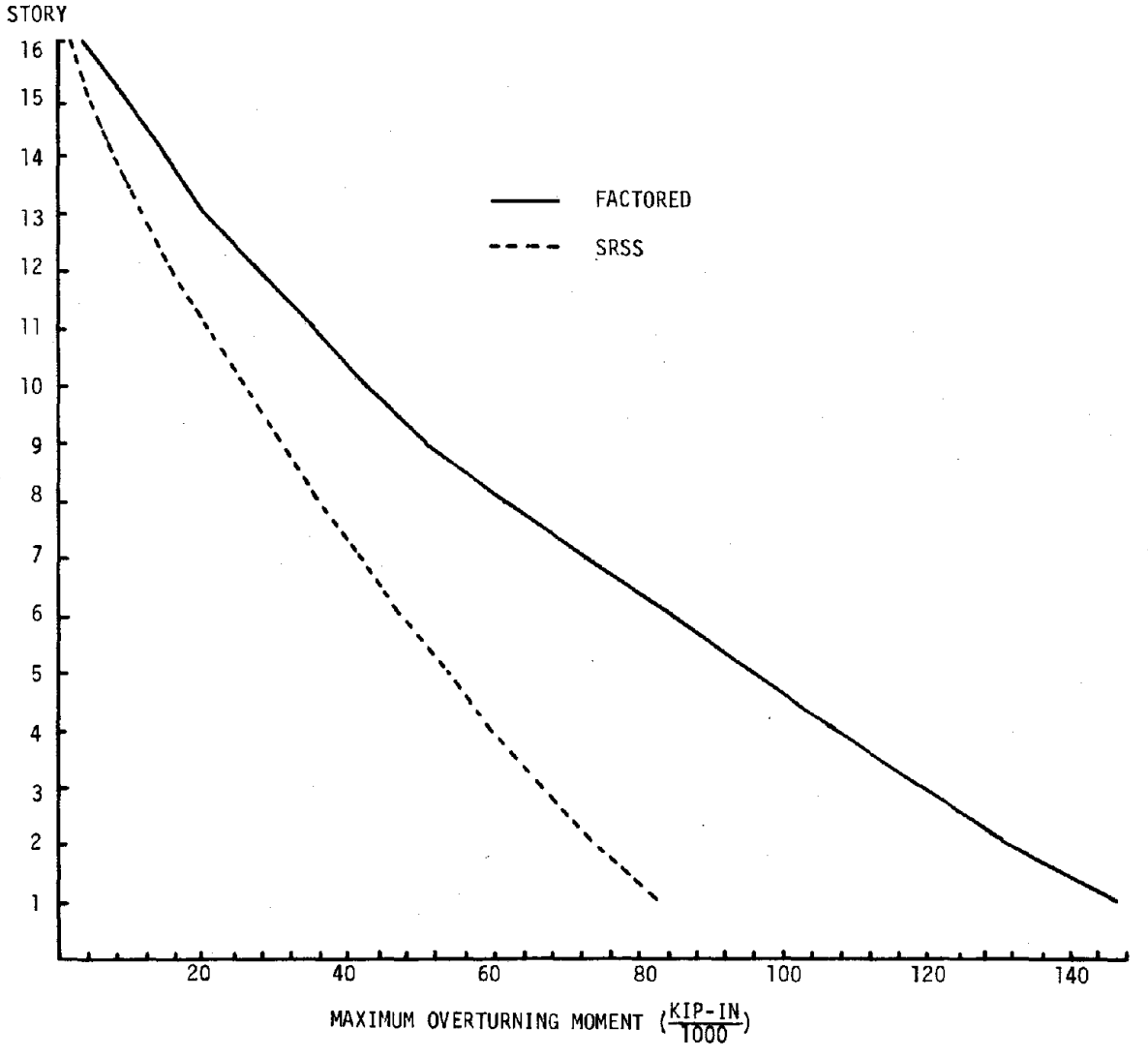

FIGURE 4.18 - MAXIMUM OVERTURNING MOMENT - 16-STORY FRAME - FACTORED DESIGN AND SRSS

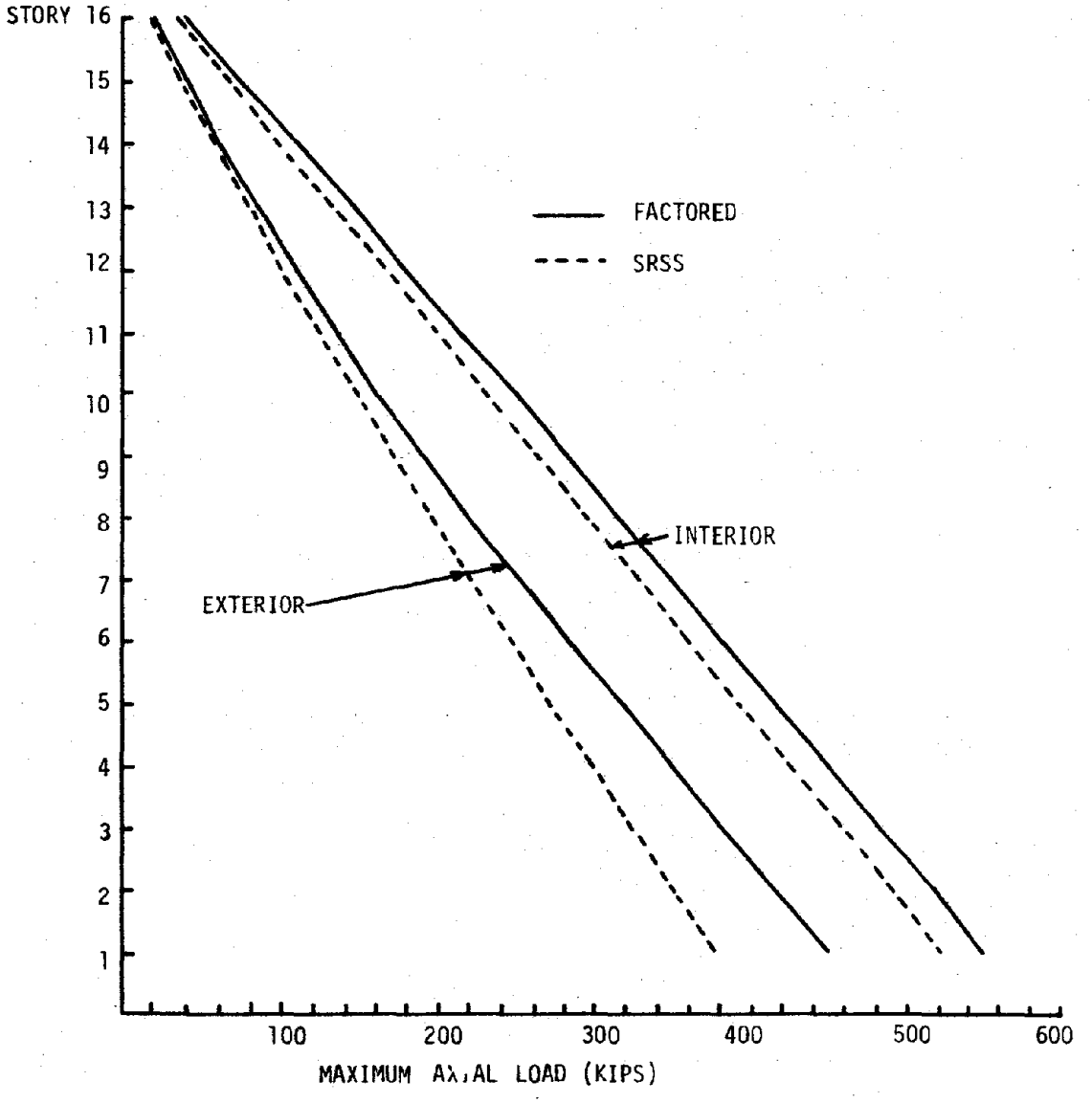

FIGURE 4.19 - MAXIMUM COLUMN AXIAL FORCES - 16-STORY FRAME - FACTORED DESIGN AND SRSS

Spectral factors for the 16-story frame backfigured from the strength factors are listed in table 4.3. The same pattern observed in the 10-story frame spectral factors is evident in the list of 16-story frame spectral factors. The 16-story frame factors, however, tend to be larger at some locations than the corresponding spectral factors at similar locations in the 10-story frame.

4.2.3 Conclusions

The results presented in this Section were determined from limited study of three frames subjected to a single artificial earthquake motion. Thus the following conclusions should be viewed with some caution:

1) It is possible to satisfactorily control the level and distribution of maximum local ductility values by applying strength factors to the unfactored member capacities computed according to the design procedure detailed in Chapter 2. Uniformity of inelastic behavior over height is best obtained by applying column strength factors which are nearly uniform in magnitude over height with slight increases in magnitude in the first story and in the first two to three stories below the roof level. Exterior column strength factors should generally be greater than interior column strength factors; the factors used most often in this study were 1.3 and 1.2 for exterior and interior columns respectively. Girder strength factors should be uniform in lower stories, must be gradually decreased in middle stories, and should be equal to 1.0 in the upper stories. This pattern reflects the increased effect of loads due to gravity forces on necessary girder resistance in the upper stories of the frames which were studied.

TABLE 4.3 - FINAL STRENGTH FACTORS AND SPECTRAL FACTORS - 16-STORY FRAME

STORY	STRENGTH FACTOR	SPECTRAL FACTOR	STORY	STRENGTH FACTOR	SPECTRAL FACTOR
	EXTERIOR COLUMNS			INTERIOR COLUMNS	
1	1.4	1.8	1	1.3	1.9
2	1.4	1.9	2	1.2	1.7
3	1.3	1.7	3	1.2	1.7
4	1.3	1.7	4	1.2	1.6
5	1.3	1.7	5	1.2	1.6
6	1.3	1.7	6	1.2	1.6
7	1.3	1.7	7	1.2	1.6
8	1.3	1.7	8	1.2	1.6
9	1.3	1.7	9	1.2	1.5
10	1.3	1.7	10	1.2	1.5
11	1.3	1.7	11	1.2	1.5
12	1.3	1.7	12	1.2	1.5
13	1.3	1.6	13	1.2	1.4
14	1.3	1.9	14	1.3	1.6
15	1.3	1.5	15	1.3	1.6
16	1.2	2.3	16	1.2	1.3
	EXTERIOR GIRDERS			INTERIOR GIRDERS	
1	1.5	1.5	1	1.5	1.5
2	1.5	1.5	2	1.5	1.5
3	1.5	1.5	3	1.5	1.5
4	1.5	1.5	4	1.5	1.5
5	1.5	1.5	5	1.5	1.5
6	1.5	1.5	6	1.5	1.5
7	1.5	1.5	7	1.5	1.5
8	1.5	1.5	8	1.5	1.5
9	1.5	1.6	9	1.5	1.5
10	1.3	1.6	10	1.3	1.4
11	1.2	1.5	11	1.2	1.3
12	1.0	1.0	12	1.0	1.0
13	1.0	1.0	13	1.0	1.0
14	1.0	1.0	14	1.0	1.0
15	1.0	1.0	15	1.0	1.0
16	1.0	1.0	16	1.0	1.0

2) Spectral factors backfigured from strength factors indicate that spectral design forces used to compute member resistances according to the procedure presented in Chapter 2 must be increased generally by a factor of from 1.5 to 1.7 and by as much as 2.3 times to achieve a satisfactory level and distribution of inelastic behavior.

3) The magnitude of local maximum ductility values in exterior columns is more sensitive to changes in strength in the member and in nearby members than girders and interior columns.

4) Attempts to improve the level and distribution of inelastic behavior should be based upon strengthening or weakening girders and interior columns as necessary and on strengthening exterior columns. Decreasing the strength of exterior columns should be done with caution, as such measures can result in axial loads which exceed available axial strength.

4.3 ANALYSIS AND DESIGN INCLUDING THE P-Δ EFFECT

In this section the P-Δ effect, which was not included in the analyses presented in other sections of this Chapter, is considered both in analysis and in design. The program FRIEDA is capable of approximating the P-Δ effect in analysis by assuming that fictitious lateral loads, PΔ/H, exist at the ends of axially loaded columns. P is the column axial force, Δ is the difference in lateral displacement of the column ends or the interstory displacement, and H is the column height. (See figure 4.20). The fictitious lateral forces are proportional to Δ and their effect is included in the column stiffness matrix by subtracting P/H from the appropriate term in the stiffness matrix.

Figure 4.21 illustrates the effects on maximum ductility distribution of approximating the P-Δ effect in analysis of the 10-story frame

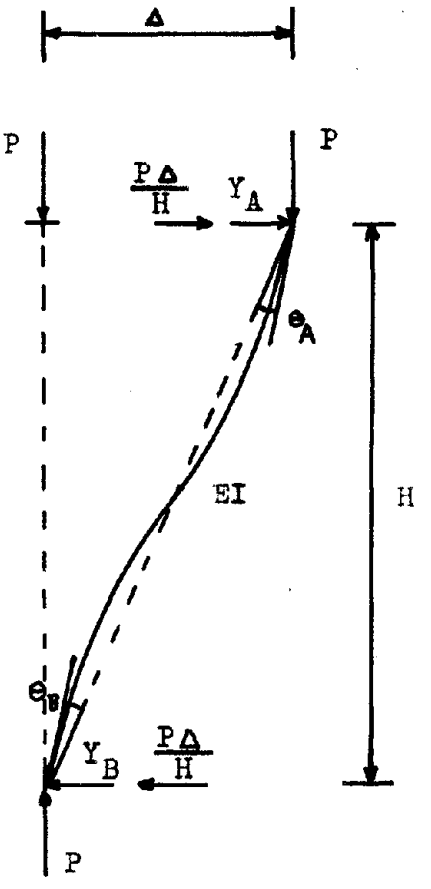

$$Y_A = \frac{12EI}{H^3}\Delta + \frac{6EI}{H^2}\theta_A + \frac{6EI}{H^2}\theta_B - \frac{P\Delta}{H}$$

$$Y_B = -\frac{12EI}{H^3}\Delta - \frac{6EI}{H^2}\theta_A - \frac{6EI}{H^2}\theta_B - \frac{P\Delta}{H}$$

E = elastic modulus I = moment of inertia

FIGURE 4.20 - APPROXIMATION OF THE P-Δ EFFECT BY THE PROGRAM FRIEDA

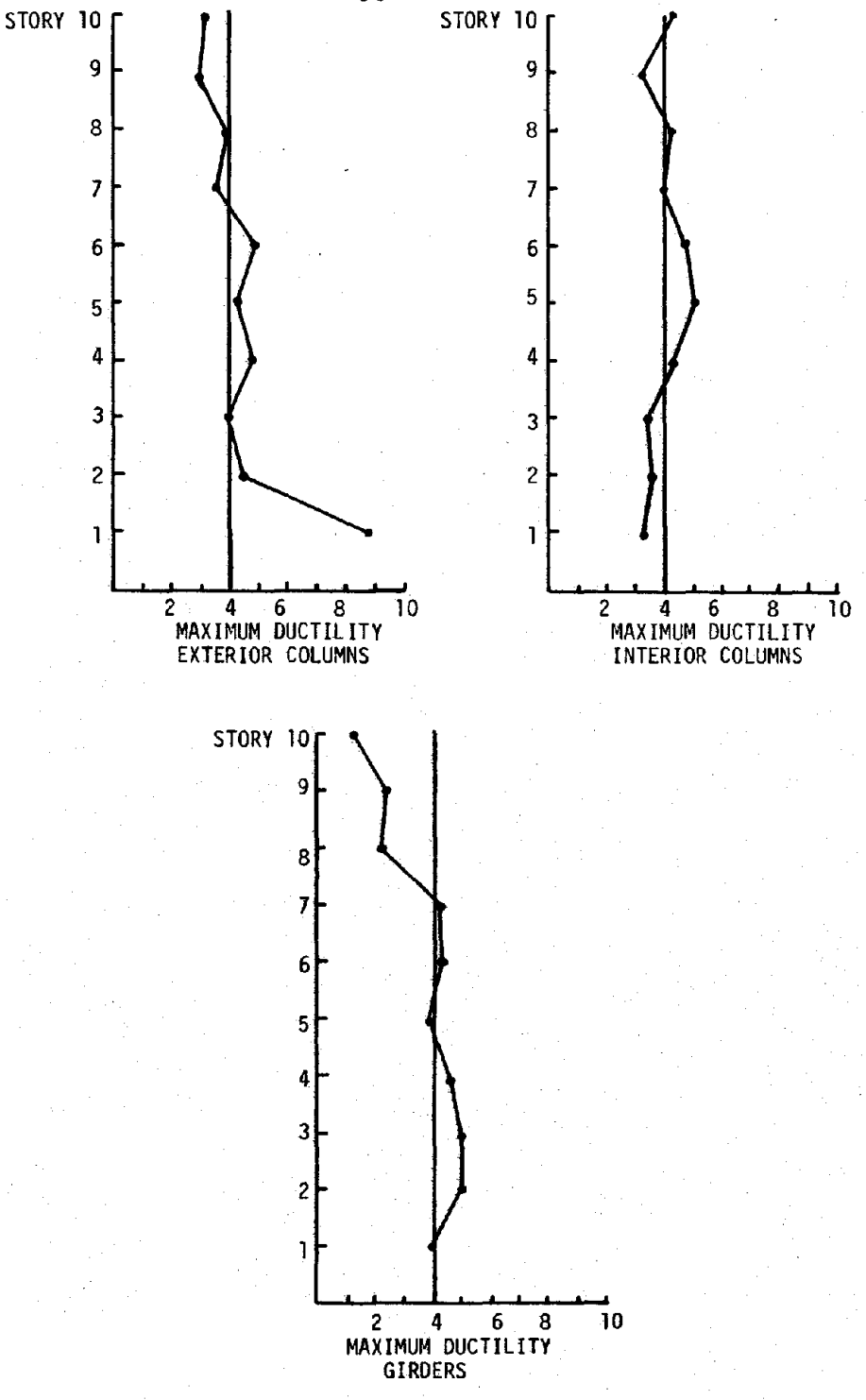

FIGURE 4.21 - MAXIMUM DUCTILITY - 10-STORY FRAME - P-Δ EFFECT INCLUDED IN ANALYSIS ONLY

with the final strength factors determined in Section 4.2.1 applied to member capacity (compare with figure 4.11). The P-Δ effect generally resulted in a slight increase in the amount of local inelastic behavior which occurred. The maximum ductilities required in exterior columns and in the girders in particular exceeded the design level in most stories. As might be expected, the P-Δ effect was more noticeable in lower and middle stories than in upper stories. Nevertheless, general uniformity of ductility distribution was maintained, and no extremely large increases in maximum ductility occurred.

An effort was made to include the P-Δ effect in the process of determining member strength. The basic aspects of the method used to determine the necessary increase in resistance are outlined below:

1) Calculate the SRSS value of interstory displacement from modal analysis using an inelastic design spectrum.

2) Calculate fictitious story shear PΔ/H for each story, where
   P = weight of frame and gravity load above story in question,
   Δ = interstory displacement determined in step 1), and
   H = story height.

3) Calculate lateral story forces resulting from shear forces determined in step 2) and perform a static analysis to determine end moments and column axial forces due to P-Δ lateral loads.

4) Determine necessary additional moment capacity.

   a) columns: $M_{add} = M_{p-\Delta}/1.18 + 6P_{p-\Delta}$

   b) girders: $M_{add} = M_{p-\Delta}$

c) no increase in the strength of girders in which $wl^2/8$ controls response.

M_{add} = necessary additional capacity

$M_{p-\Delta}$ = average P-Δ end moment

$P_{p-\Delta}$ = P-Δ axial load.

5) Add the capacities determined in step 4) to the factored strength of each member.

The above procedure was used in redesigning the 10-story frame to resist P-Δ effects. The shear forces determined from modal analysis, the story forces applied in the static analysis of P-Δ forces, the additional moment capacity and the increased member resistances are all listed in table 4.4. It should be noted that inclusion of the P-Δ effect results in additional girder end moments which are nearly antisymmetric. Such moments do not increase the internal moment at midspan and, strictly speaking, the strength of girders designed to satisfy the $wl^2/8$ strength requirement should not need additional capacity for resistance of P-Δ effects. However, the strength factors calculated in Section 4.2.1, along with the ductility distribution shown in figure 4.11, indicate that in fact many of the girders originally designed for $wl^2/8$ actually should have been proportioned for seismic end forces. The capacity of such members was increased for P-Δ effects. The inelastic response of the girders in the eighth, ninth, and tenth floors clearly indicated that these members were overdesigned with respect to seismic end moments and therefore no increase in capacity was made to resist additional end moments due to the P-Δ effect.

TABLE 4.4 - SHEAR FORCES, STORY FORCES, ADDITIONAL MOMENT CAPACITY
NEW MEMBER CAPACITY - 10-STORY FRAME - P-Δ DESIGN

Story	Interstory Shear (kips)	Story Force (kips)	Additional Moment Capacity (K-in)	New Member Capacity (K-in)	Additional Moment Capacity (K-in)	New Member Capacity (K-in)
			EXTERIOR COLUMNS		INTERIOR COLUMNS	
1	9.613	-2.755	211	3036	230	4328
2	12.368	2.271	188	2314	253	3549
3	10.097	1.285	155	2089	203	3153
4	8.812	0.794	125	1812	182	2846
5	8.018	1.829	111	1593	162	2500
6	6.189	0.987	83	1346	126	2140
7	5.202	1.825	58	1038	114	1861
8	3.377	0.741	35.5	835.9	75	1599
9	2.636	1.710	36.7	737.8	47	1066
10	.926	0.926	8.5	520.3	20.6	599.7
			EXTERIOR GIRDERS		INTERIOR GIRDERS	
1			246	1692	239	1650
2			260	1694	258	1678
3			233	1644	232	1643
4			196	1506	197	1507
5			169	1479	170	1480
6			135	1244	145	1254
7			96	1104	118	1126
8			0	1008*	0	1008*
9			0	1008*	0	1008*
10			0	986.4*	0	986.4*

* No change in strength - midspan gravity moment controls design.

The ductility distribution resulting from the P-Δ design is compared with the ductility distribution resulting from including the P-Δ effect in analysis only in figure 4.22. It is apparent that the redesign of the 10-story frame resulted in excellent control of increased yielding due to the P-Δ effect. At almost all story levels in both columns and girders, local maximum ductilities were reduced to a level below the design ductility. The lower story columns were slightly overdesigned, but overall uniformity of ductility distribution was good. Displacements and maximum axial loads corresponding to modal analysis, analysis in which P-Δ is included in analysis only, and analysis of the P-Δ design are shown in figures 4.23 and 4.24. It is interesting to note that although modal analysis underestimates interstory displacements, the increased moment capacities based on SRSS interstory displacements successfully controlled increased yielding due to P-Δ effects.

Although no firm conclusions should be drawn from a single example, it appears that the combinations of modal and static analyses detailed above can be used to satisfactorily include P-Δ effects in an inelastic design procedure. It is important to note that the results of including P-Δ effects only in analysis indicate that the P-Δ effect is of limited significance when compared to the effect of motion detail and the effect of other parameters over which little control can be exercised in practical situations.

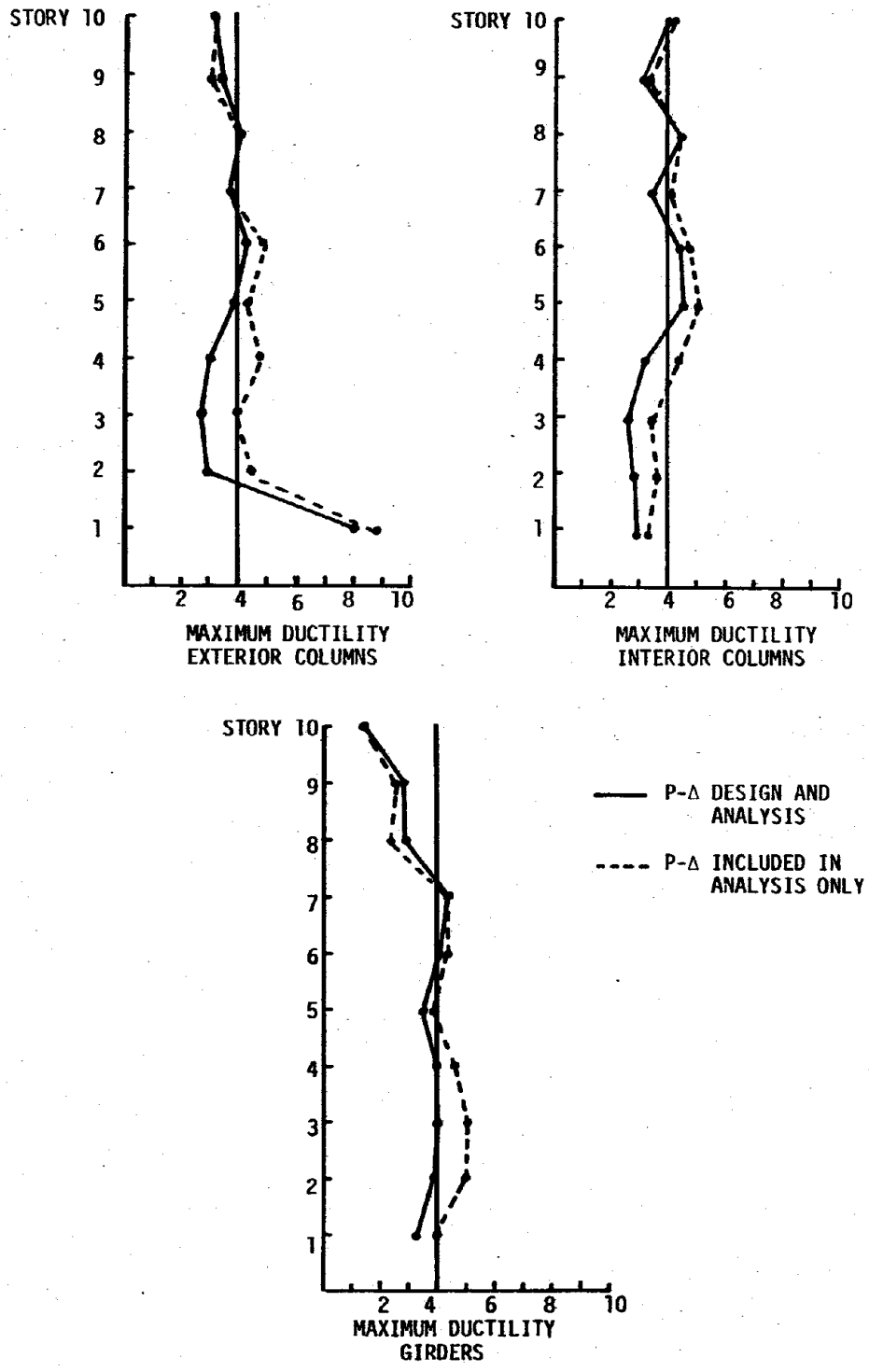

FIGURE 4.22 - MAXIMUM DUCTILITY - 10-STORY FRAME - P-Δ INCLUDED IN DESIGN AND ANALYSIS, P-Δ INCLUDED IN ANALYSIS ONLY

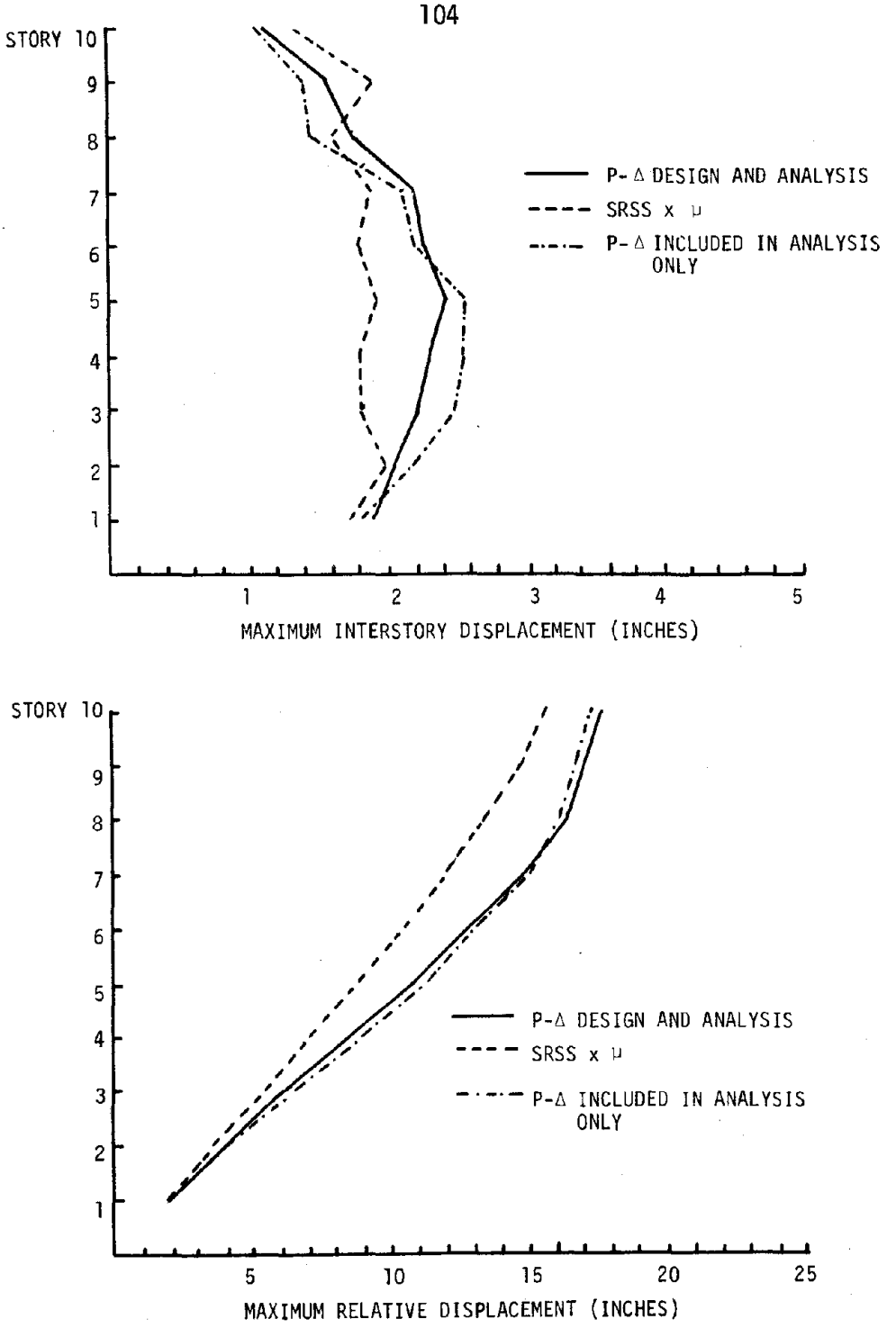

FIGURE 4.23 - MAXIMUM INTERSTORY DISPLACEMENT, MAXIMUM RELATIVE DISPLACEMENT - 10-STORY FRAME - P-Δ INCLUDED IN DESIGN AND ANALYSIS, P-Δ INCLUDED IN ANALYSIS ONLY, SRSS

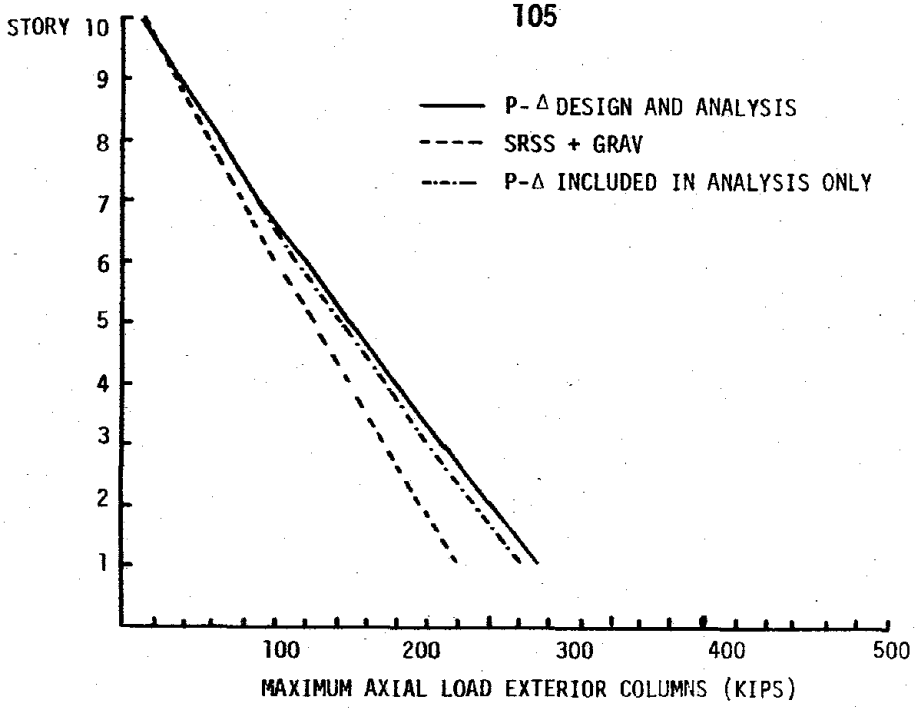

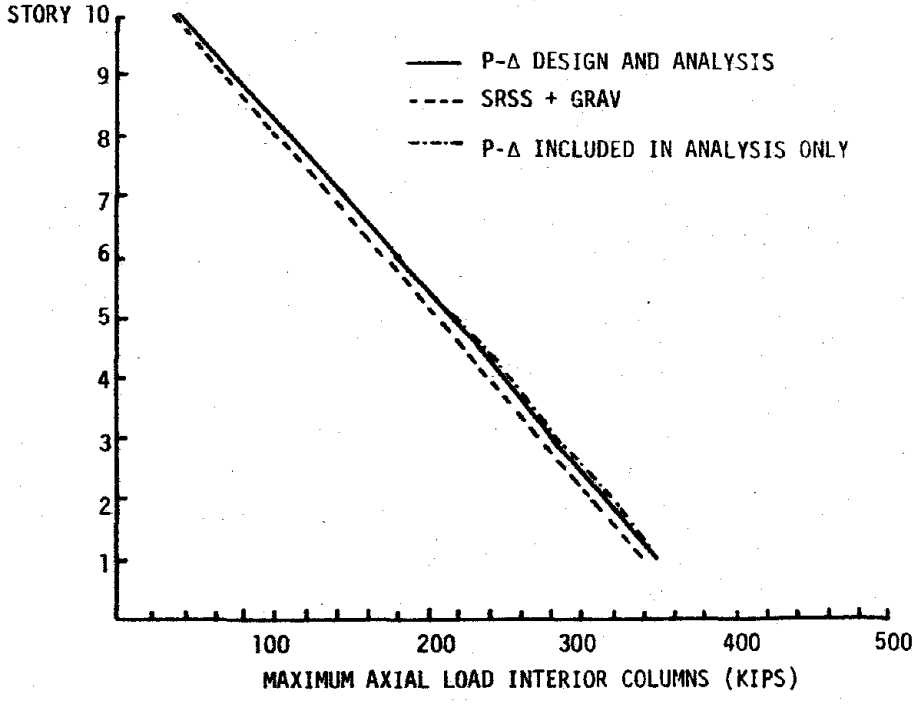

FIGURE 4.24 - MAXIMUM COLUMN AXIAL FORCES - 10-STORY FRAME - P-Δ INCLUDED IN DESIGN AND ANALYSIS, P-Δ INCLUDED IN ANALYSIS ONLY, SRSS

4.4 INFLUENCE OF DETAILS OF EARTHQUAKE MOTION, LEVEL OF DAMPING AND EARTHQUAKE INTENSITY

In this section a limited investigation of the influence of various parameters on the level and distribution of local maximum ductility is presented. The final strength factors were applied to obtain member resistances in the 10-story frame which is investigated in this section.

4.4.1 Details of Motion

It is a well-known fact that frame response is heavily dependent upon the details of individual earthquake motions. Motions having the same intensity can have vastly differing effects on the same structure. Figures 4.25 to 4.28 show the response of the 10-story frame investigated in Section 4.2.1 to artificial earthquakes #R1 and #R3, both of which have calculated spectra which closely match the target elastic response spectrum from which the design inelastic spectrum was determined. (These figures should be compared with figure 4.11, which shows ductility distribution from analyses using motion #R2.) The effect of motion details is immediately obvious. The exterior column ductilities shown in figure 4.25, which resulted from analysis using earthquake #R1, varied greatly over height but were generally less than the design ductility. Exterior column ductility distribution resulting from analysis using #R3 (figure 4.26) was more uniform over height, but generally exceeded the design level. Interior column ductilities for both motions were similar. They were characterized by ductilities substantially below the design level in the uppermost stories. Girder ductility due to #R1 was generally uni-

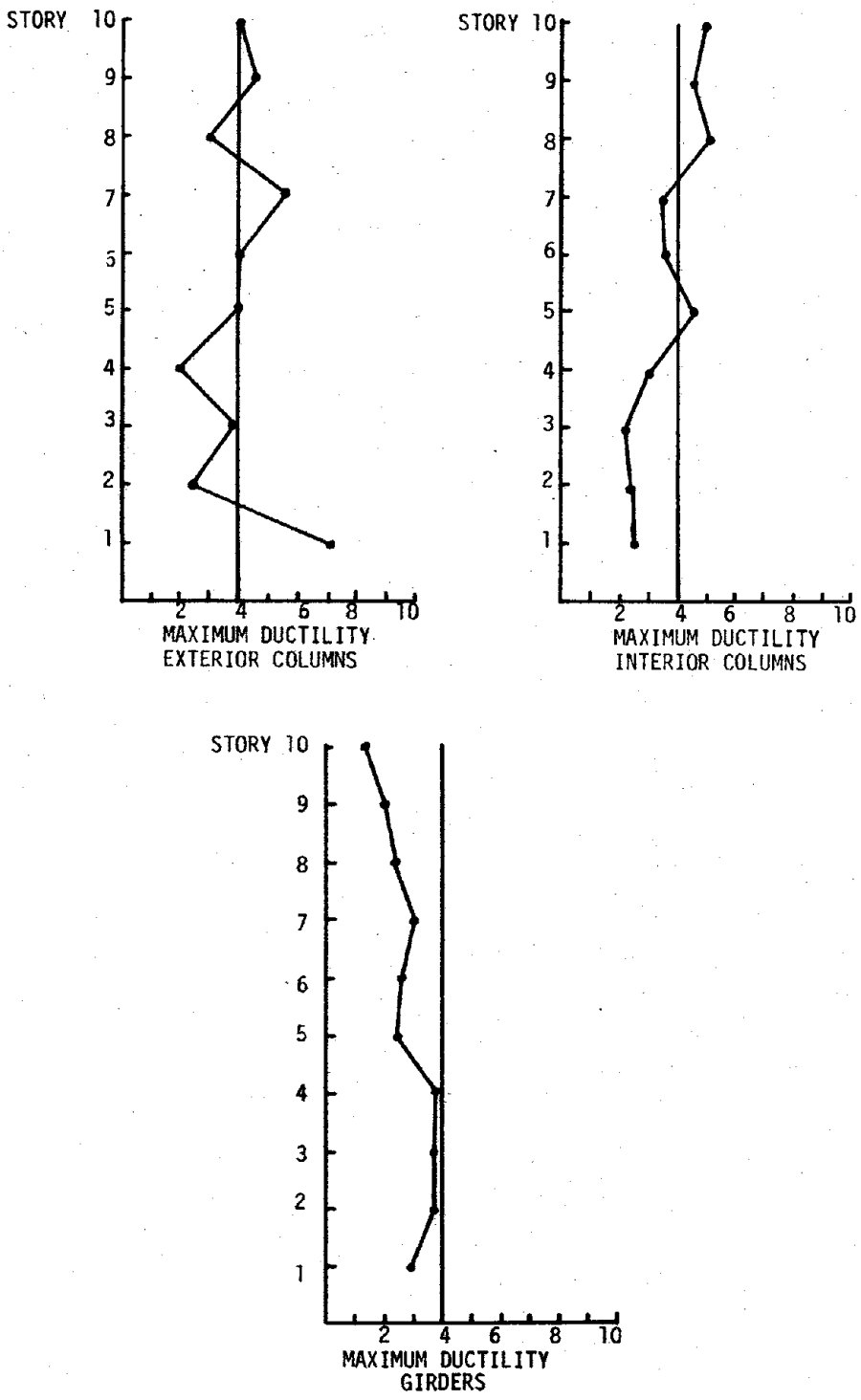

FIGURE 4.25 - MAXIMUM DUCTILITY - 10-STORY FRAME - FINAL STRENGTH FACTORS - EARTHQUAKE #R1

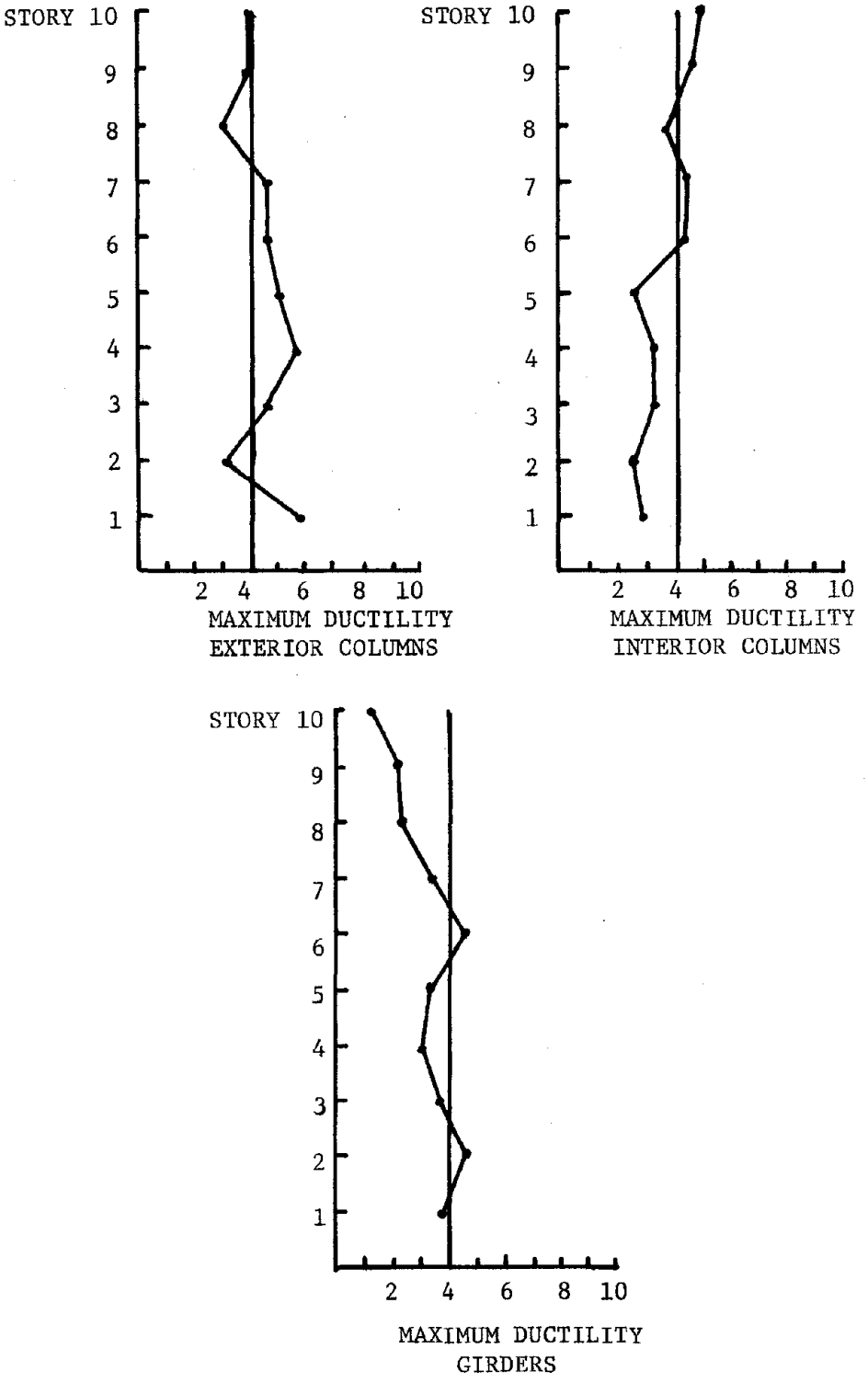

FIGURE 4.26 - MAXIMUM DUCTILITY - 10-STORY FRAME - FINAL STRENGTH FACTORS - EARTHQUAKE #R3

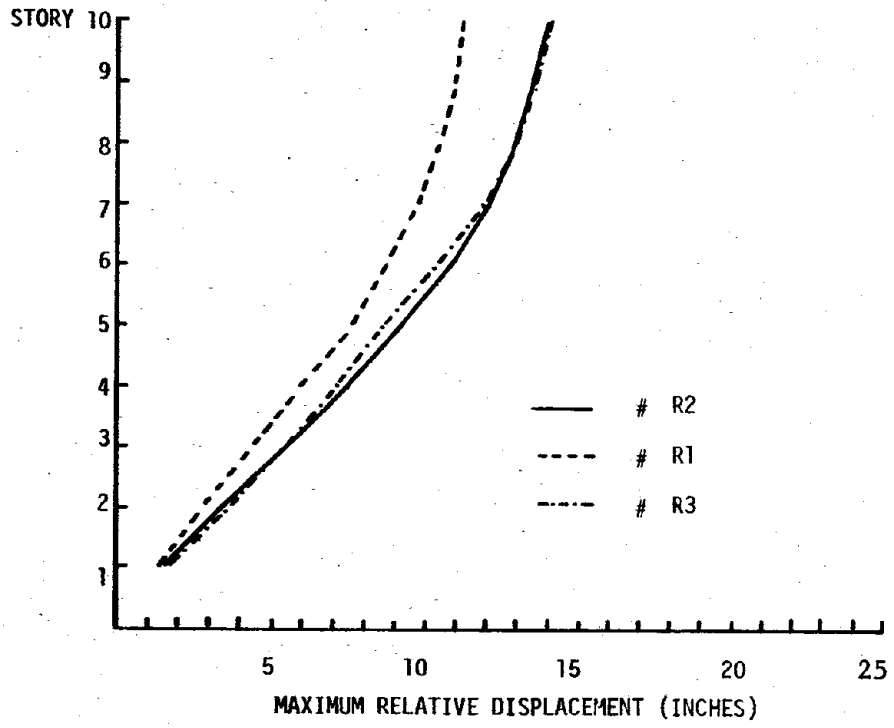

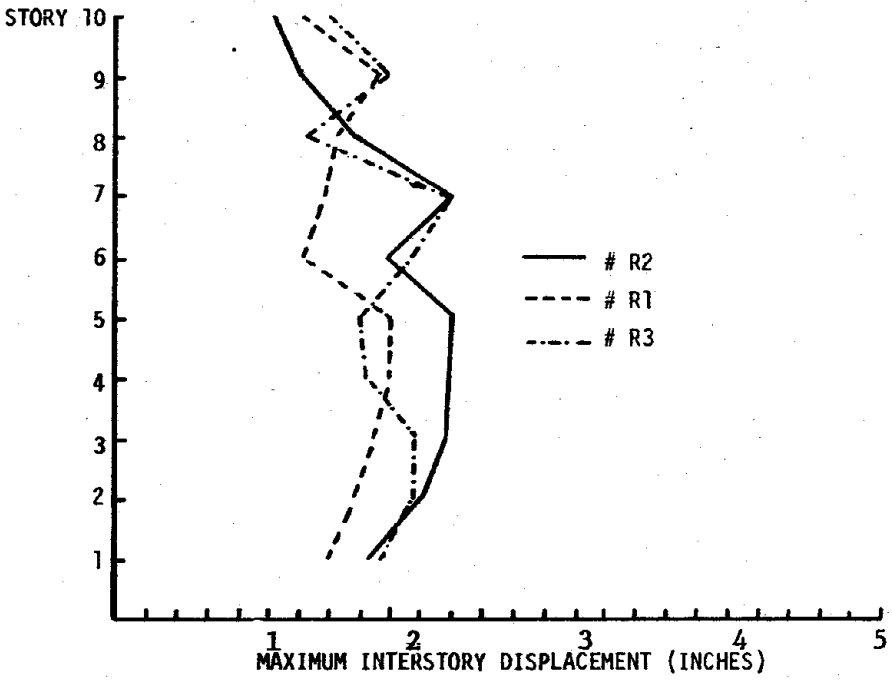

FIGURE 4.27 - MAXIMUM RELATIVE DISPLACEMENT, MAXIMUM INTERSTORY DISPLACEMENT - 10-STORY FRAME - FINAL STRENGTH FACTOR - EARTHQUAKES #R1, #R2, #R3

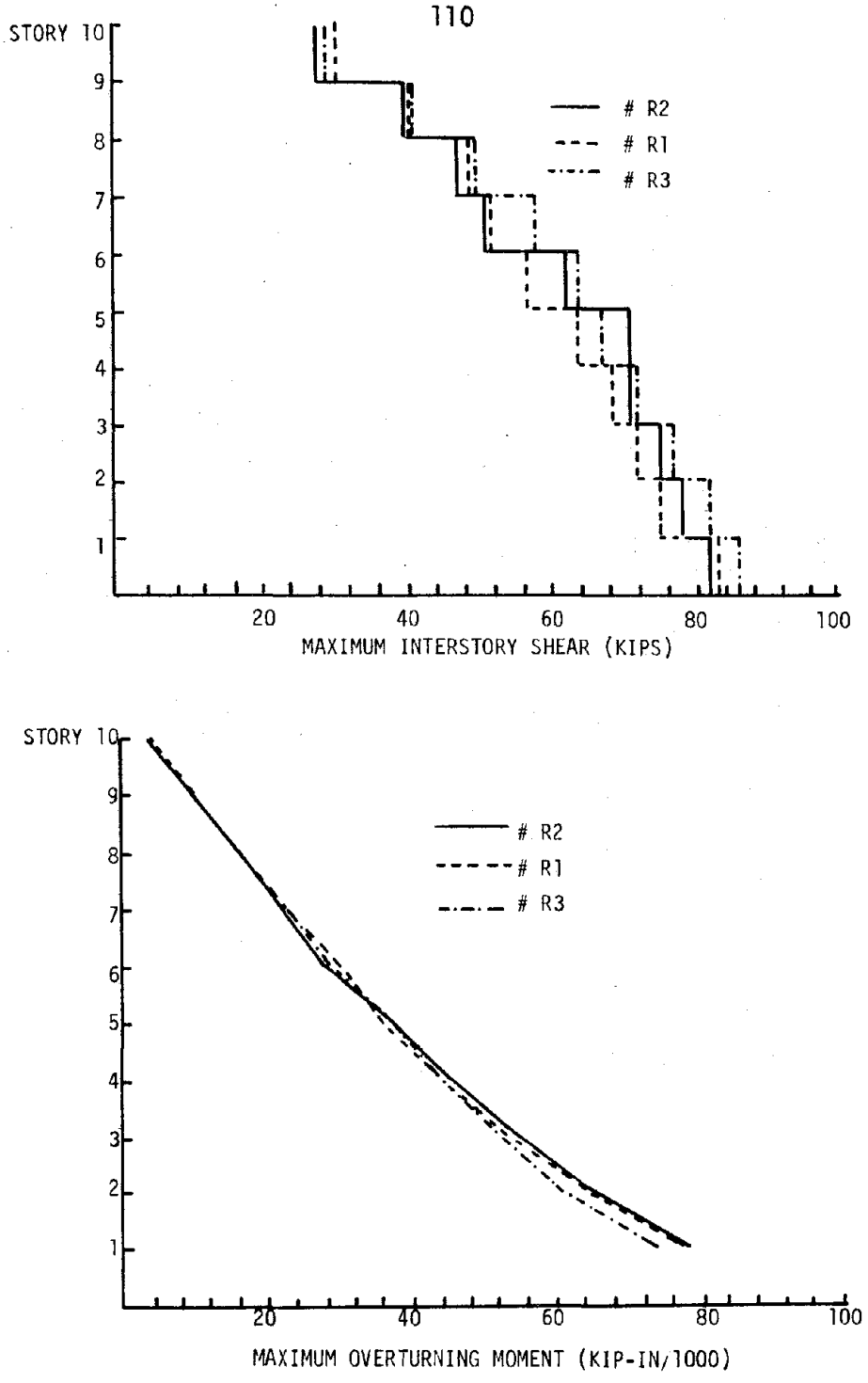

FIGURE 4.28 - MAXIMUM INTERSTORY SHEAR, MAXIMUM OVERTURNING MOMENT - 10-STORY FRAME - FINAL STRENGTH FACTORS - EARTHQUAKES #R1, #R2, #R3.

form and remained below the design ductility over the entire height of the structure. Girder ductility due to #R3 reflected the increase in exterior column ductility due to #R3 over the exterior column ductilities due to #R1 and #R2 (see figure 4.11). In floors two through six the girder ductilities and exterior column ductilities are nearly mirror images of one another.

Maximum relative displacement, shown for all three motions in figure 4.27, was very similar for motions #R2 and #R3, while displacement due to #R1 at any given story was generally one to three inches less. Interstory displacement shown in the same figures varies greatly with each motion over height. Shear forces and overturning moments in most instances were similar (figure 4.28).

4.4.2 Level of Damping

Heretofore it has been assumed in both design and analysis that damping was 5% of critical damping. It was felt that it might be of interest to determine the effect of assuming a damping level in analysis which was greater than or less than the design damping level. Figures 4.29 through 4.32 show the results of analyses in which viscous damping was assumed to be 2% and 10% of critical damping and should be compared with 4.11, showing the results of 5% assumed damping. In general, no surprising trends can be seen in these results. As expected, the level of ductility decreased with increased damping, and increased with decreased damping. Reduction of damping to 2% resulted in maximum ductil-

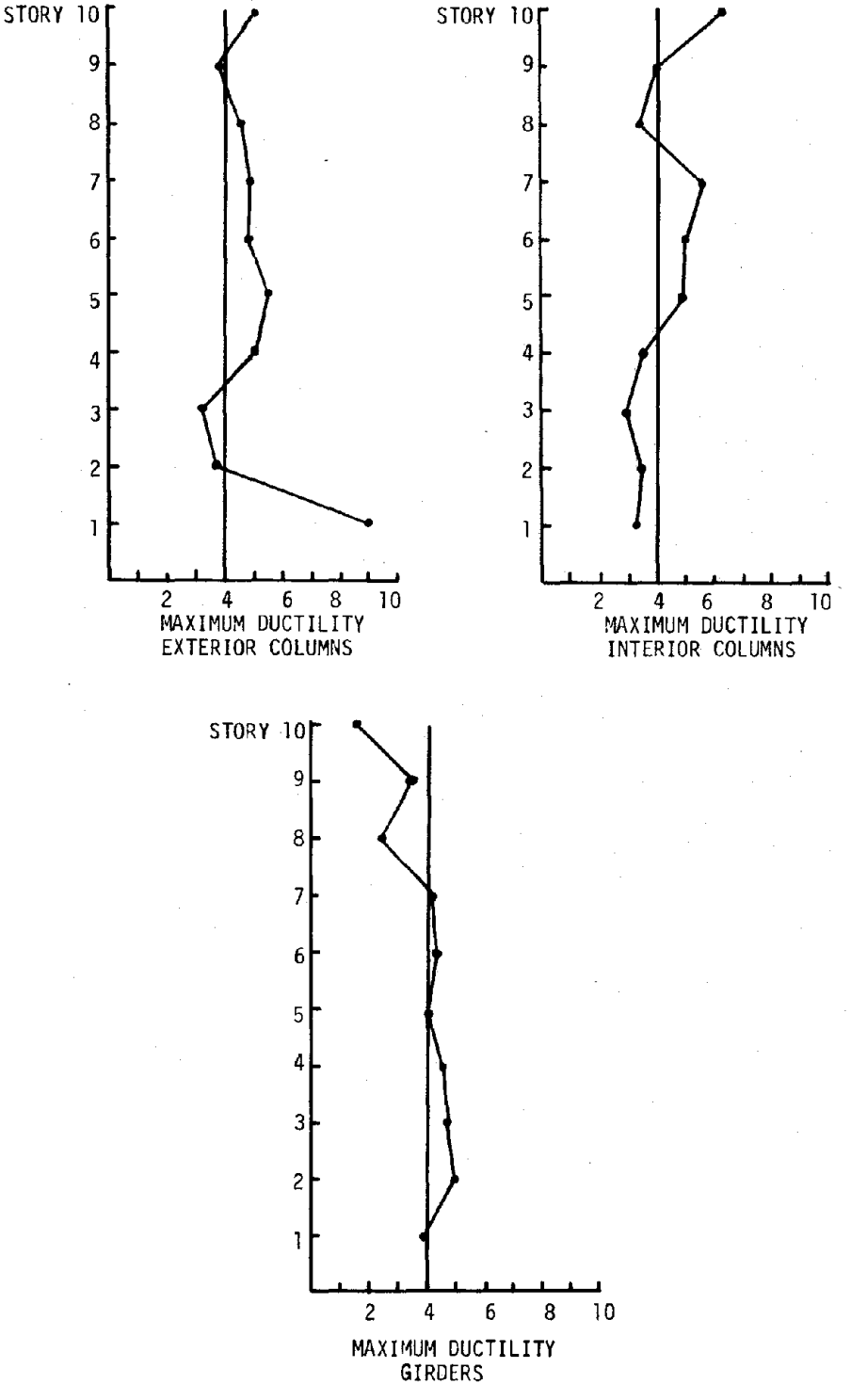

FIGURE 4.29 - MAXIMUM DUCTILITY - 10-STORY FRAME - 2% DAMPING

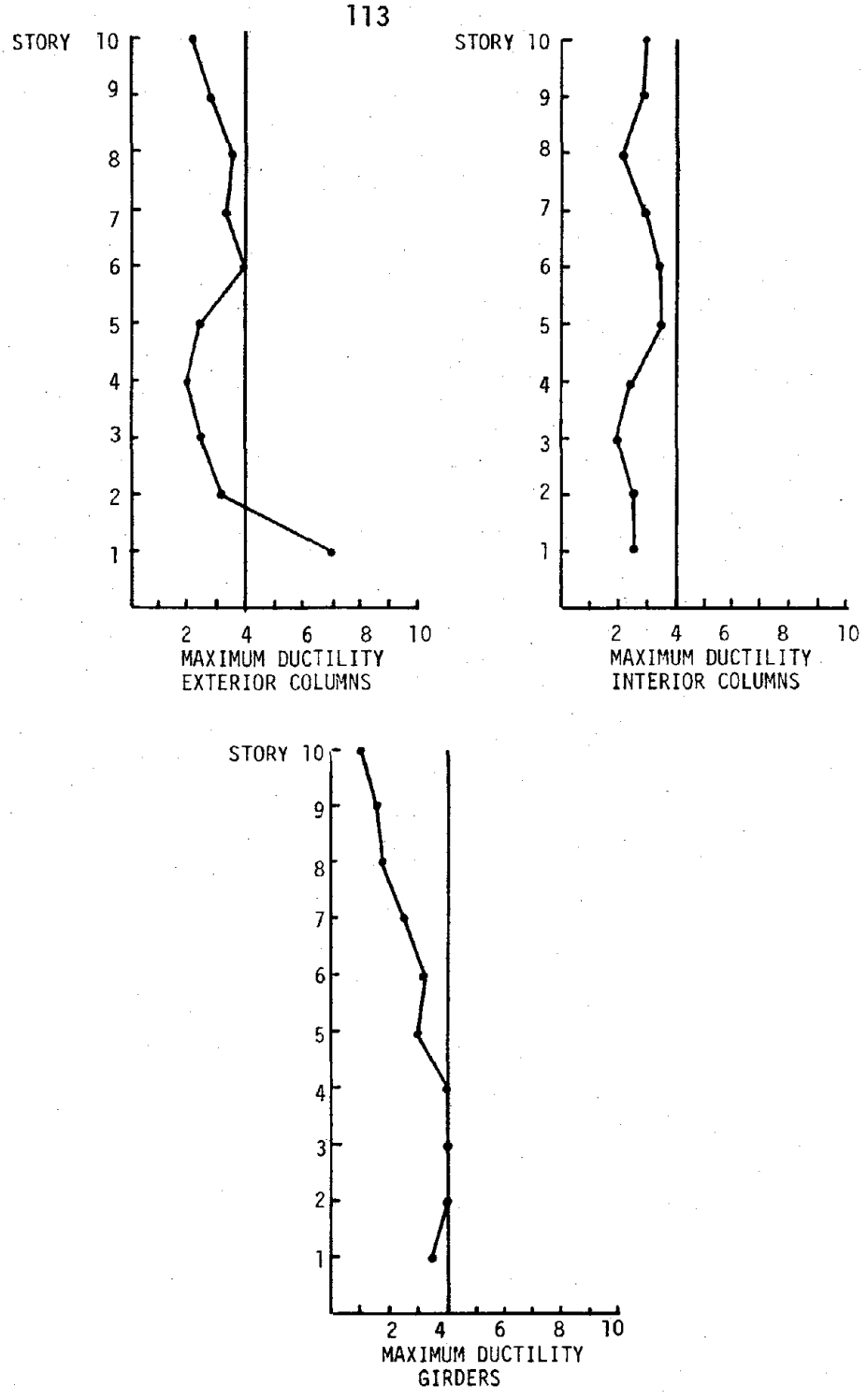

FIGURE 4.30 - MAXIMUM DUCTILITY - 10-STORY FRAME - 10% DAMPING

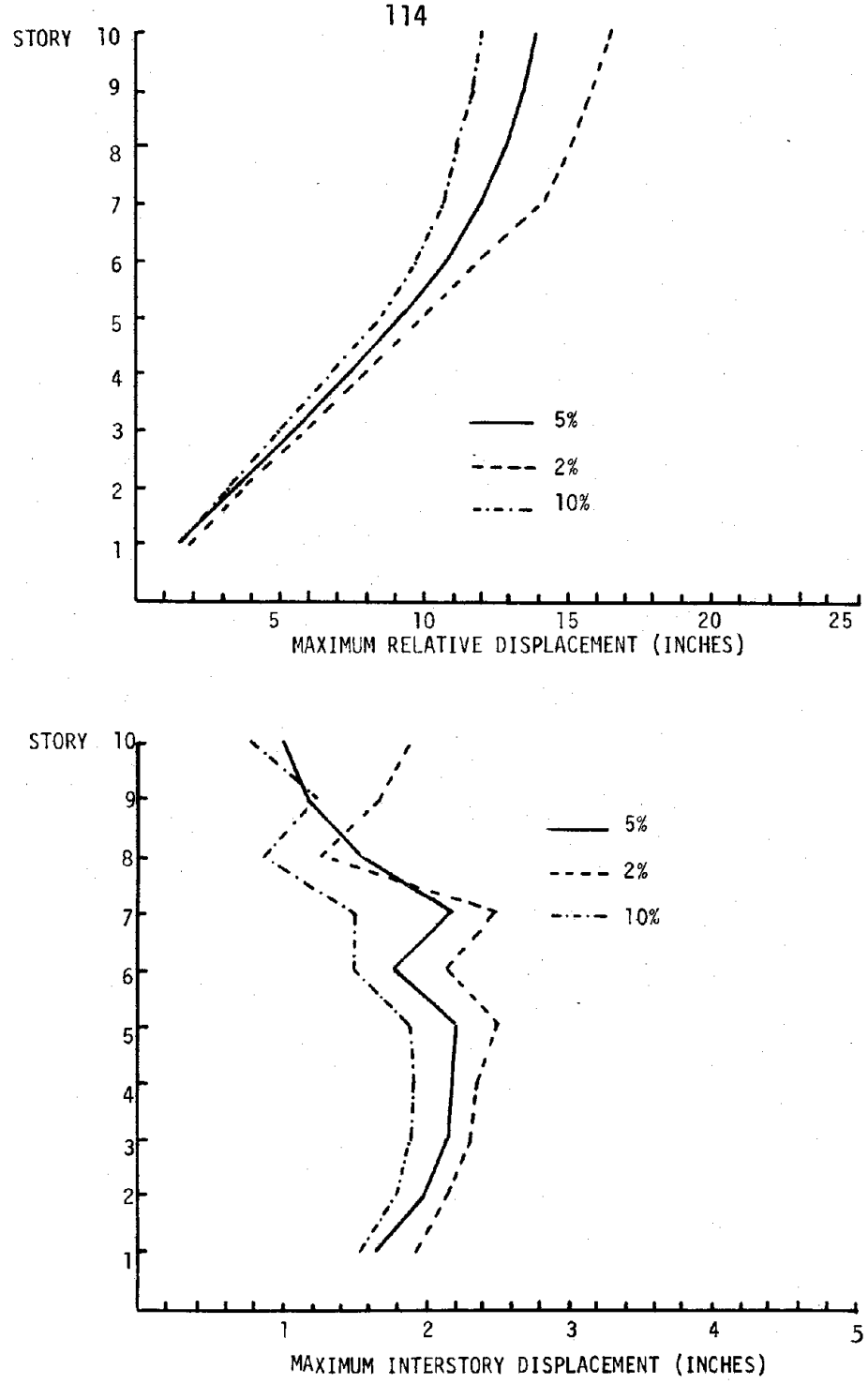

FIGURE 4.31 - MAXIMUM RELATIVE DISPLACEMENT, MAXIMUM INTERSTORY DISPLACEMENT - 10-STORY FRAME - DAMPING = 2%, 5%, 10%

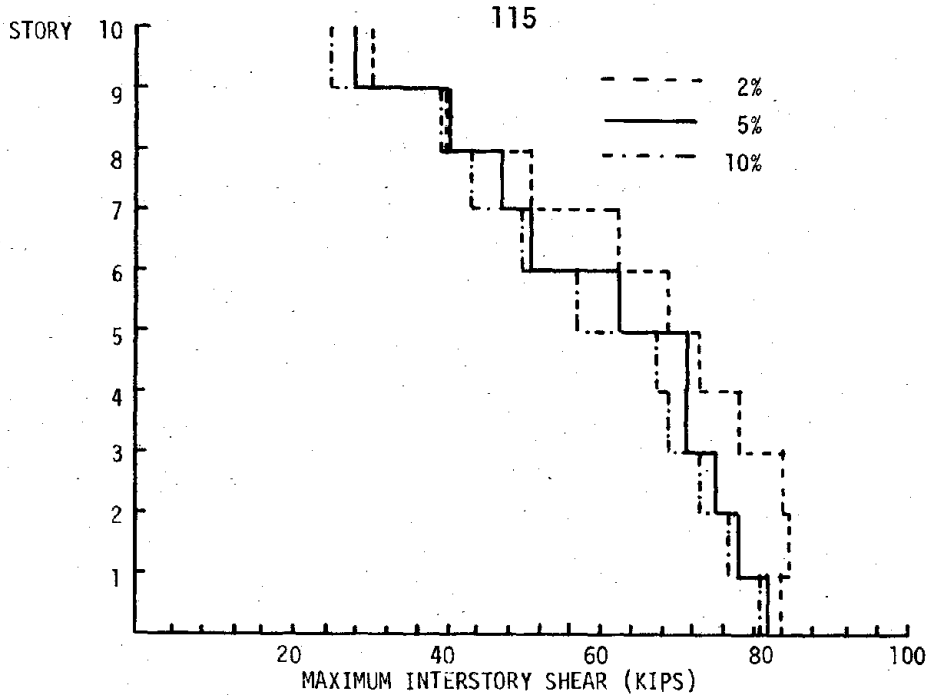

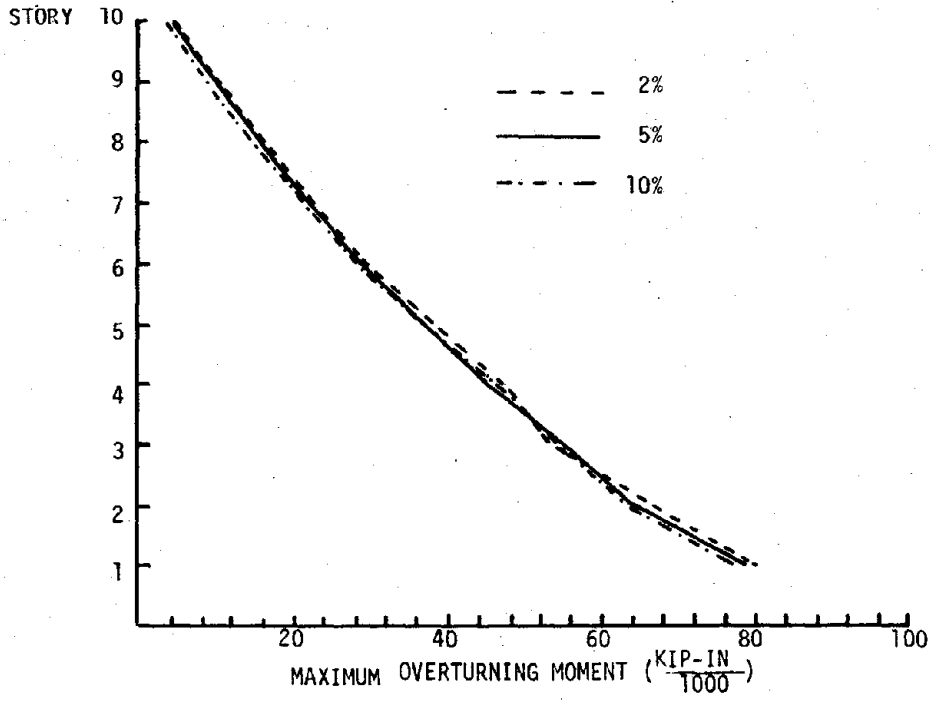

FIGURE 4.32 - MAXIMUM INTERSTORY SHEAR, MAXIMUM OVERTURNING MOMENT - 10-STORY FRAME - DAMPING = 2%, 5%, 10%

ities which exceeded the design ductility in most floors. Specifying a ductility of 10% reduced all maximum ductilities to a level below the design ductility with the single exception of the ductility at the base of the first floor exterior columns.

The displacements and forces shown in figures 4.31 and 4.32 also indicate the expected trends. Both maximum relative displacement and maximum interstory displacement increased with decreased damping. Interstory shear forces also tended to be greater when the damping assumed in analysis was only 2% of critical. There is little discernible difference in the overturning moments plotted in figure 4.32.

Figure 4.33 shows the elastic spectra, based on the original motion parameters presented in Section 2.2 (maximum displacement = 11.88 in., maximum velocity = 15.84 in./sec., max. acceleration = .33 g), corresponding to 2% damping and 10% damping. Also shown is the original inelastic design spectrum determined for 5% damping and a maximum ductility of 4. If these spectra are examined in the region of the fundamental period of the 10-story frame (T_1 = 2.322 sec.) and the elastic spectral ordinates are divided by the corresponding pseudo-velocity value taken from the inelastic spectrum, it becomes apparent that the same frame would have resulted from a design for 2% damping and a ductility of 5.90, or a design for 10% damping and a ductility of 2.74. (Note that the final strength factors determined in Section 4.2 have also been included in the equivalent designs). The maximum ductilities plotted in figure 4.30 indicate that designing for 10% damping and a ductility of 2.74 produces local ductilities which compare to the design ductility much as the

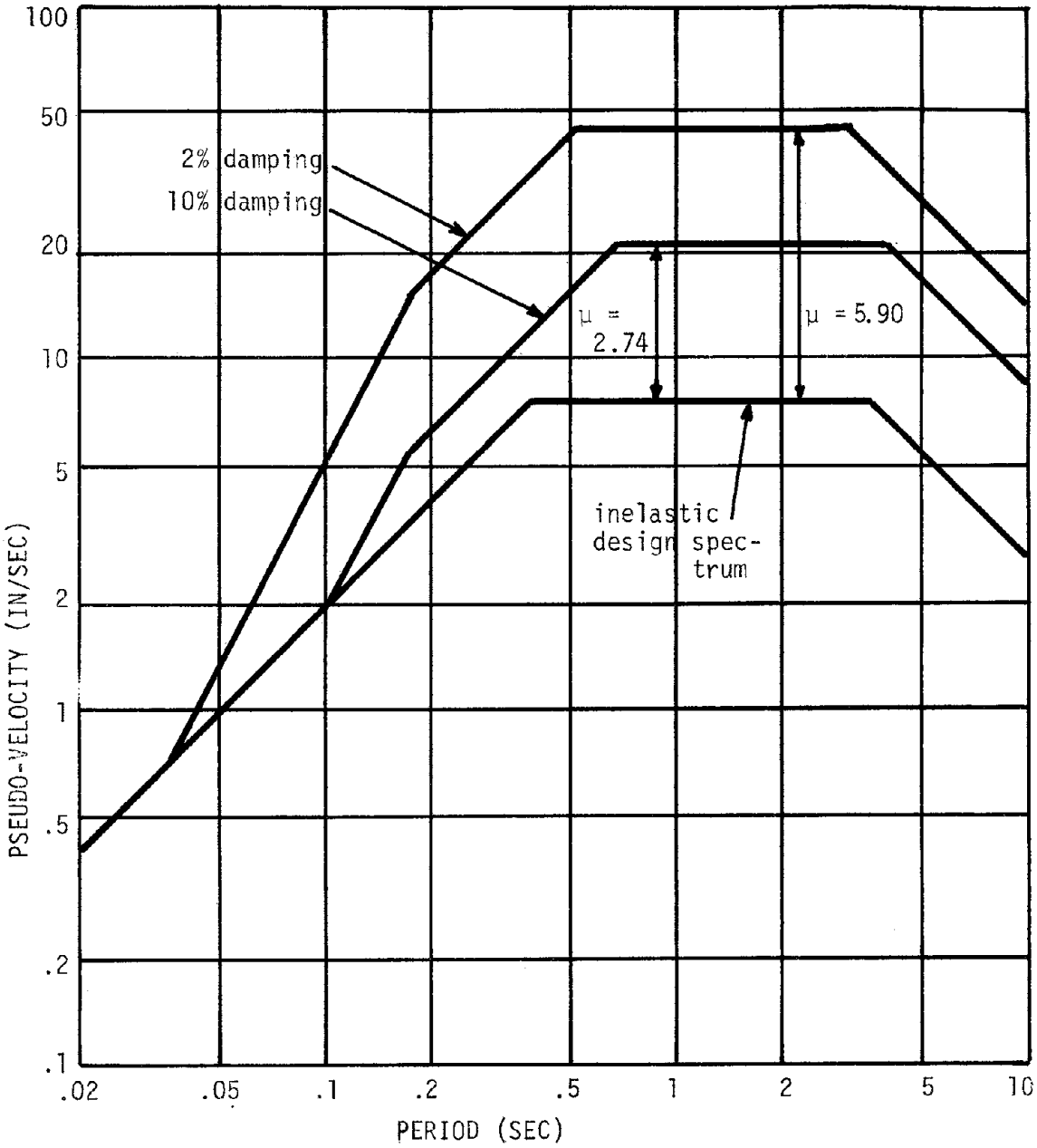

FIGURE 4.33 - ELASTIC SPECTRA, DAMPING = 2% and 10% - INELASTIC DESIGN SPECTRUM

local ductilities compared to the design ductility in the original design for 5% damping, and a ductility of 4. Only lower-story girder ductilities and the exterior column ductility at the sixth floor (maximum ductility = 4) exceeded the design ductility by an appreciable amount. On the other hand, the ductilities determined for the equivalent 2% design were less than the design ductility at all locations. Haviland (12) has reported that the design ductility level has little effect on the relationship between the level of response and the design ductility. Thus, the above results suggest that the previously determined strength factors may be too large for low damping values. It is even possible that use of the Newmark-Hall inelastic spectrum to design for lower damping levels produces conservative unfactored designs.

4.4.3 Earthquake Intensity

Earthquake intensity was varied in the analyses presented in this section to determine if general uniformity of ductility would be maintained in the event that the 10-story structure was subjected to a motion of greater or less intensity than the design motion. Accordingly, the acceleration record of artificial earthquake #R2 was multiplied by 1/2 and by 2. The ductility distributions resulting from subjecting the frame to 1/2 x R2 and 2 x R2 are shown in figures 4.34 and 4.35. These figures should be compared with figure 4.11, which shows ductility response to the design motion. No yielding occurred in the columns located in the second and third stories under the action of 1/2 x R2, and column ductilities in general were less than 2.0. Uniformity of ductility distribution in columns and girders was excellent under the action of

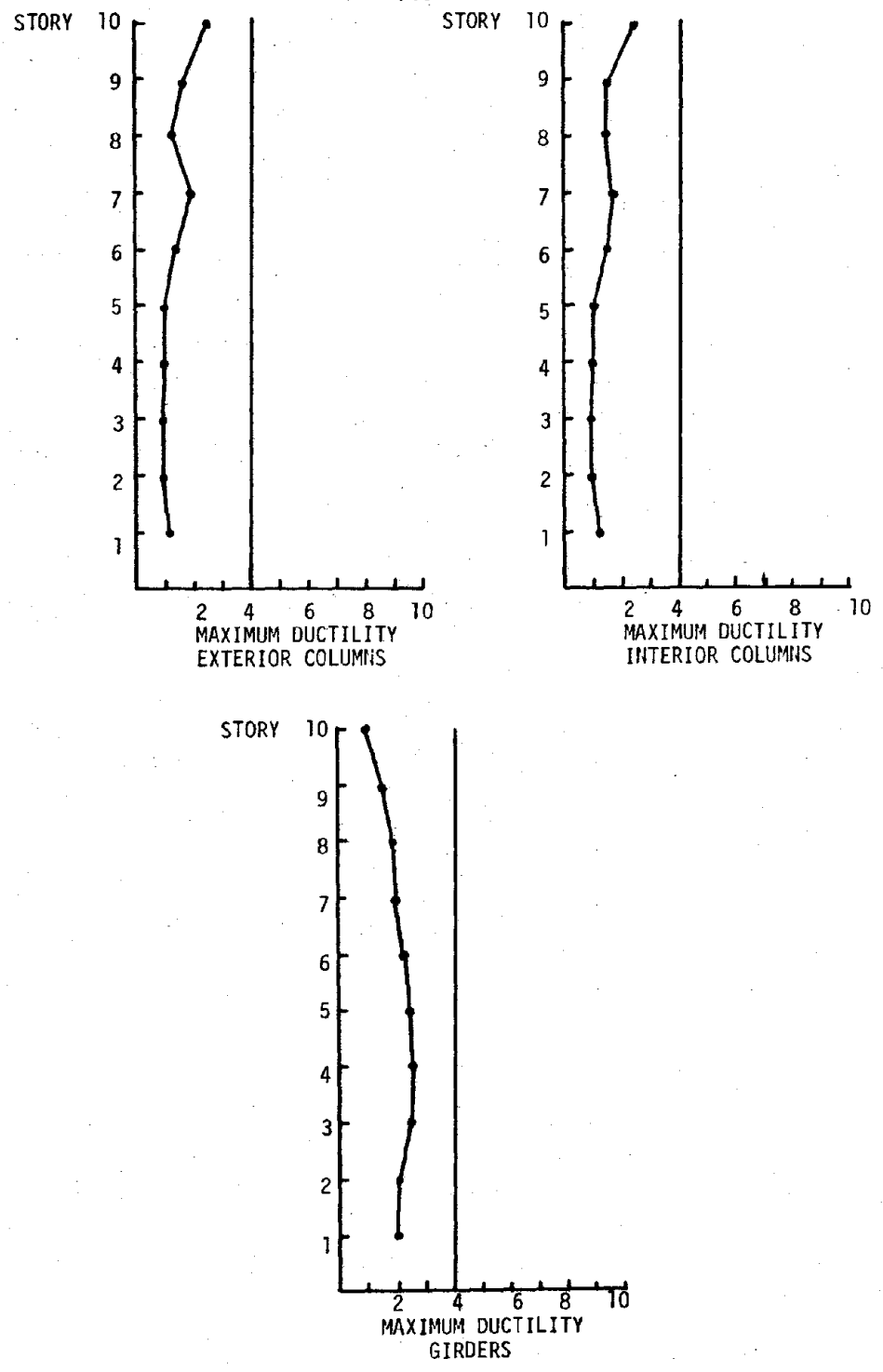

FIGURE 4.34 - MAXIMUM DUCTILITY - 10-STORY FRAME - EARTHQUAKE INTENSITY 1/2 x R2

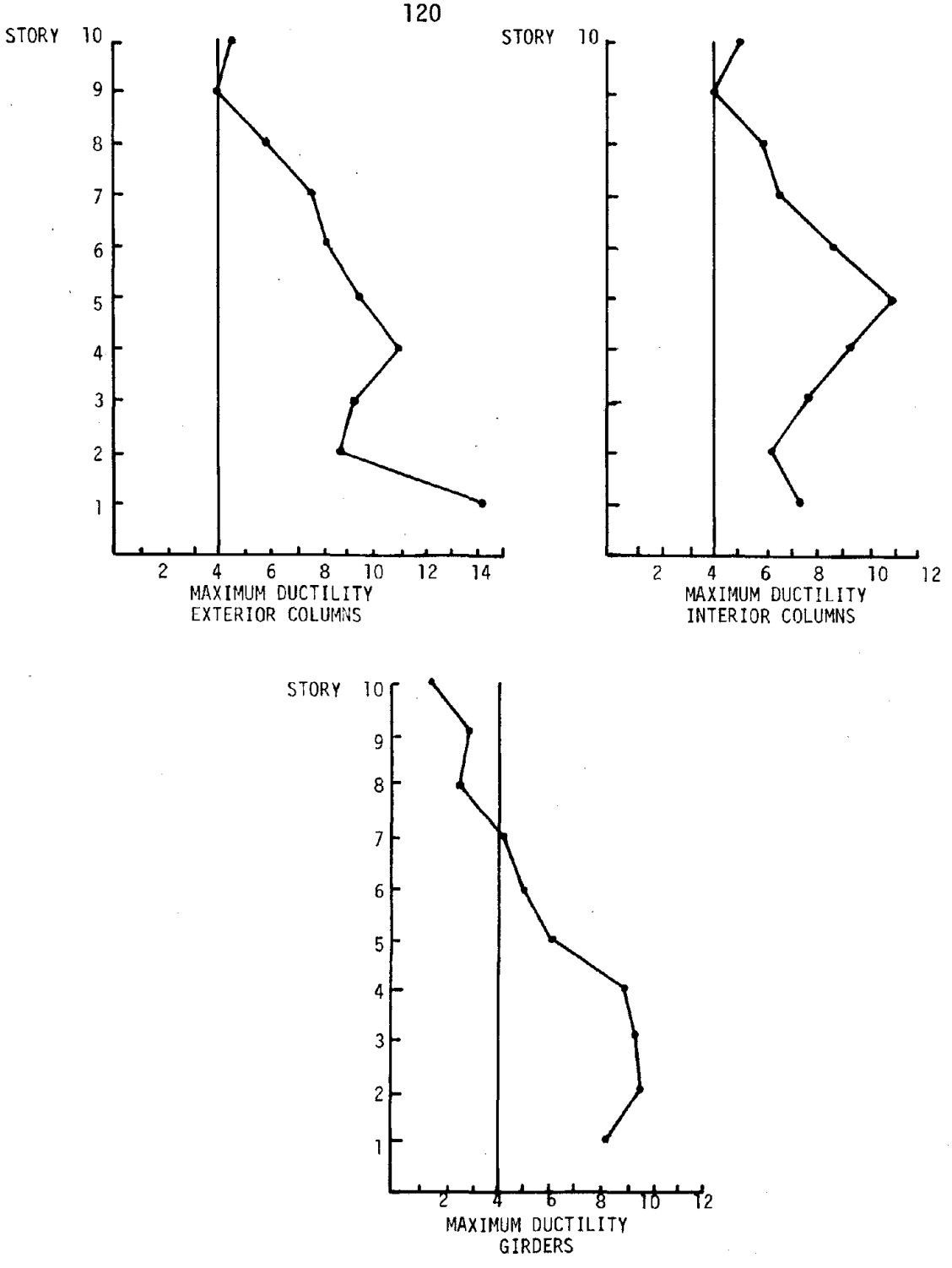

FIGURE 4.35 - MAXIMUM DUCTILITY - 10-STORY FRAME - EARTHQUAKE INTENSITY 2 x R2

1/2 x R2. The ductilities corresponding to an earthquake with twice the intensity of the design earthquake were not uniform over height. Ductility was greatly increased in lower stories, but remained near the design level in upper stories. The story displacements and forces shown in figure 4.36 and figure 4.37 indicate the expected trends. Displacements and forces increased with earthquake intensity.

Figure 4.38 shows the elastic response spectra corresponding to ground motion having intensity one half and twice R2 for 5% critical damping. In a manner similar to that described in Section 4.4.2, it was determined that the same frame would have resulted from designs for intensities of 1/2 x R2 and 2 x R2 and maximum ductilities of 2.0 and 8.0 respectively. The ductilities determined for 1/2 x R2 in fact were generally between 1.0 and 2.0. However, ductilities due to 2 x R2 were not uniform, and in several locations exceeded 8.0 by a substantial amount. These results indicate that use of the inelastic spectrum to design for smaller earthquake intensity could produce acceptable seismic response with the application of the strength factors determined in Section 4.2. However, it appears that strength factors would have to be varied more with height and perhaps increased in magnitude to control the distribution of inelastic response to earthquakes of increased intensity.

4.4.4 Conclusions

1) Ductility level and distribution is heavily dependent upon the details of individual earthquake motions.

2) The level of damping assumed in analysis does not seriously affect the uniformity of maximum ductility distribution.

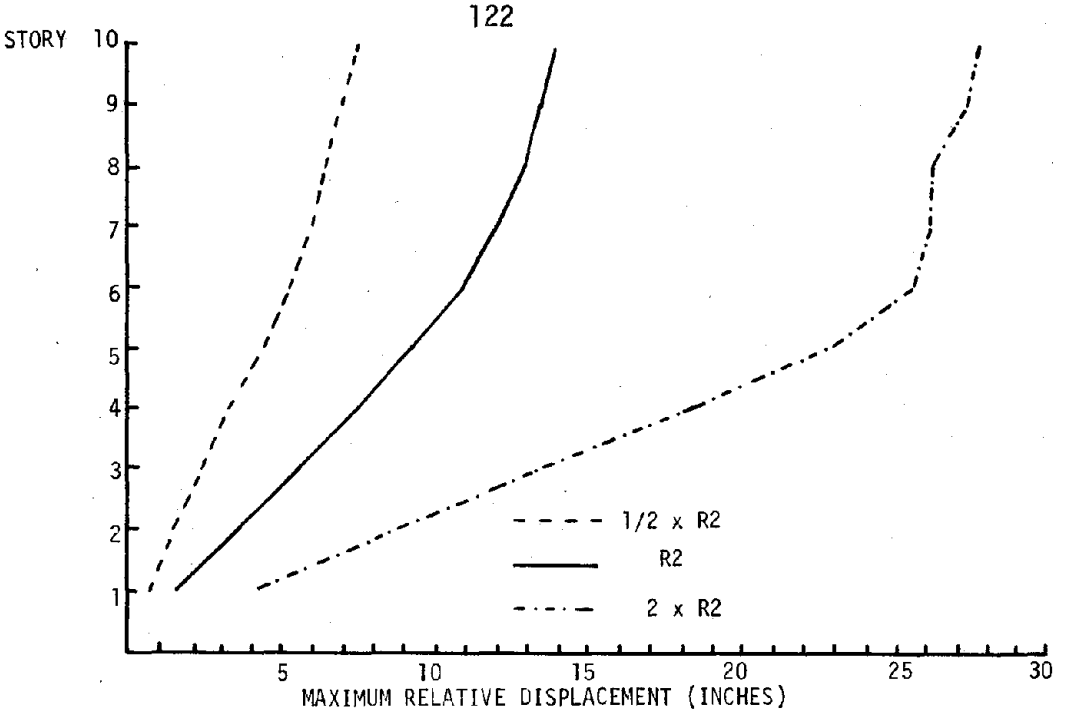

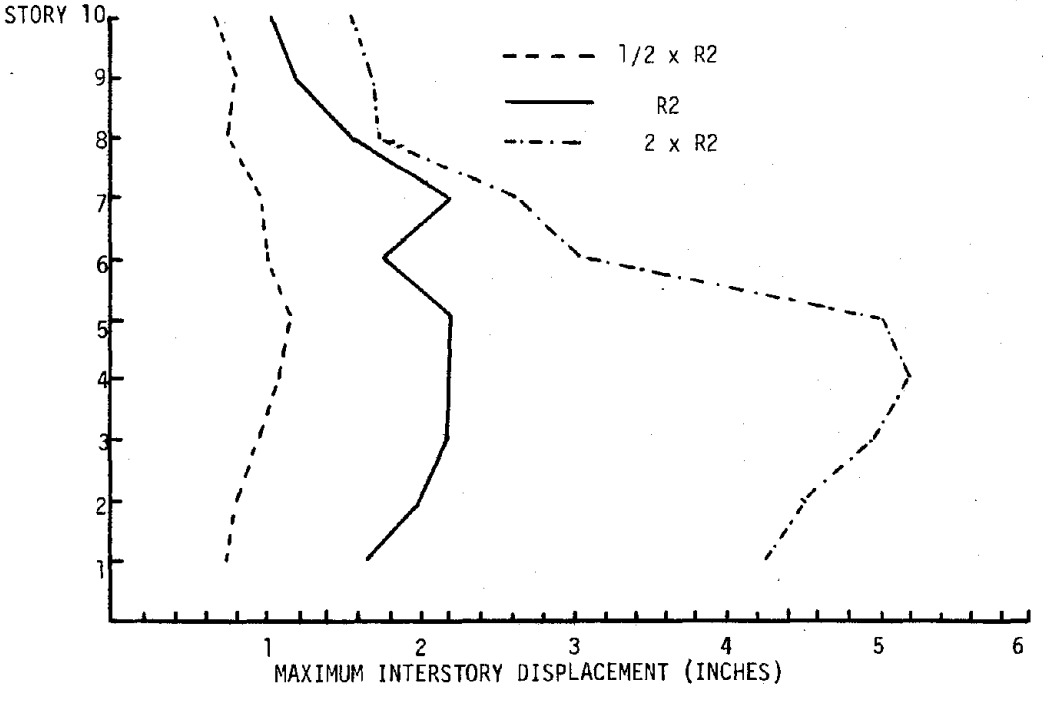

FIGURE 4.36 - MAXIMUM RELATIVE DISPLACEMENT, MAXIMUM INTERSTORY DISPLACEMENT - 10-STORY FRAME - EARTHQUAKE INTENSITY = 1/2 x R2, 1 x R2, 2 x R2.

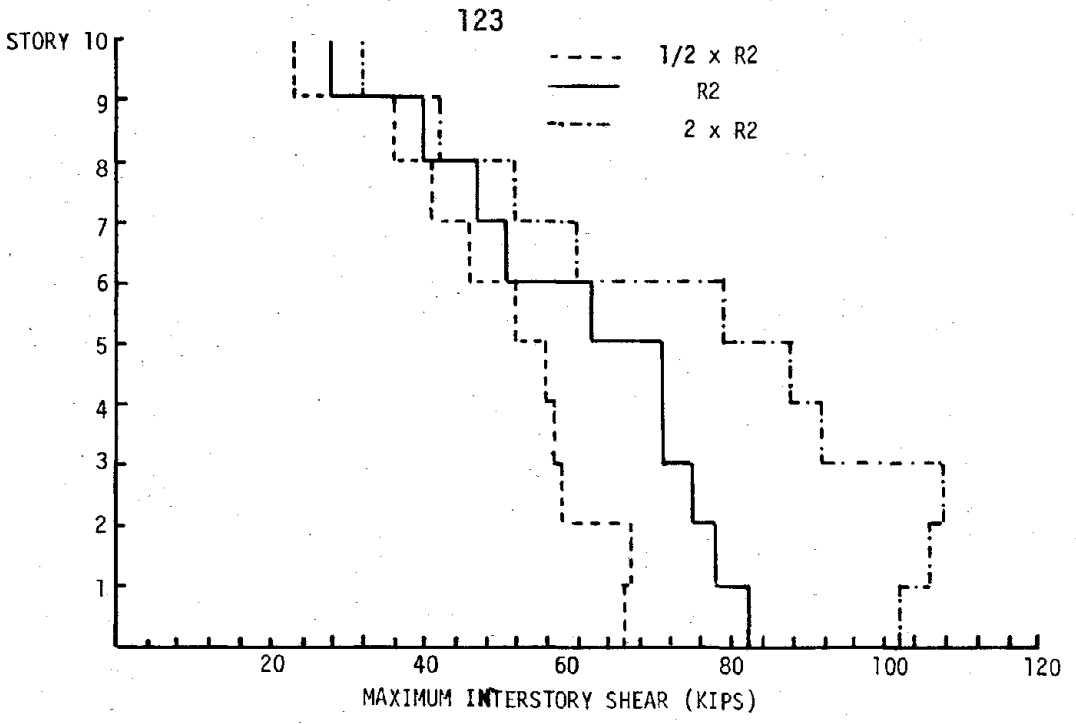

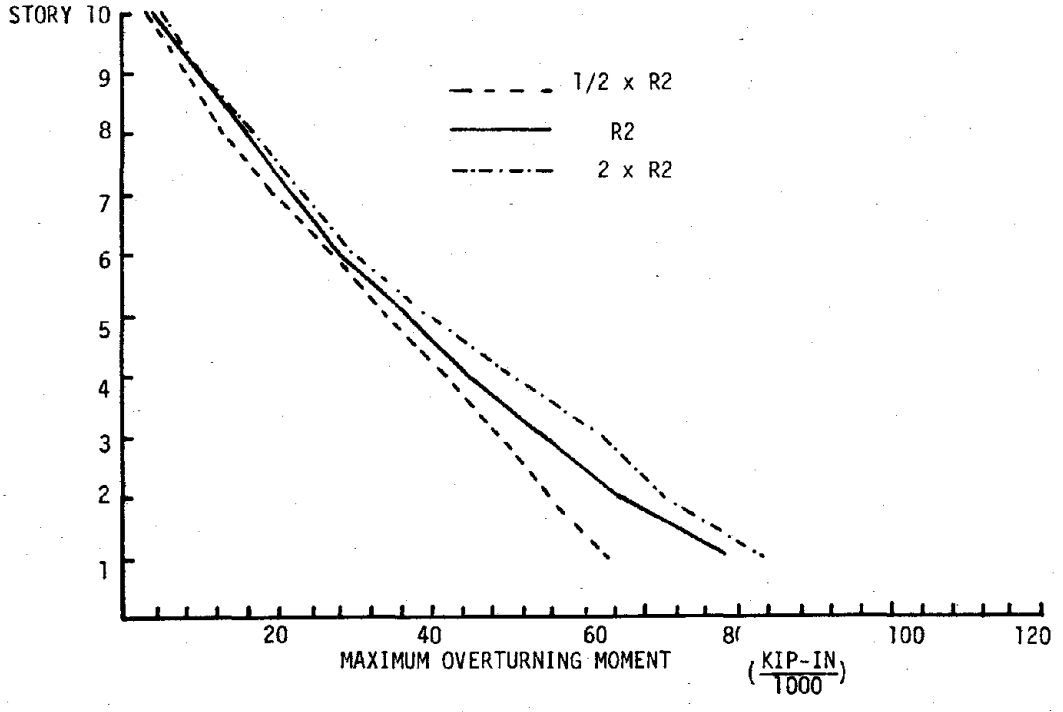

FIGURE 4.37 - MAXIMUM INTERSTORY SHEAR, MAXIMUM OVERTURNING MOMENT - 10-STORY FRAME - EARTHQUAKE INTENSITY = 1/2 x R2, 1 x R2, 2 x R2.

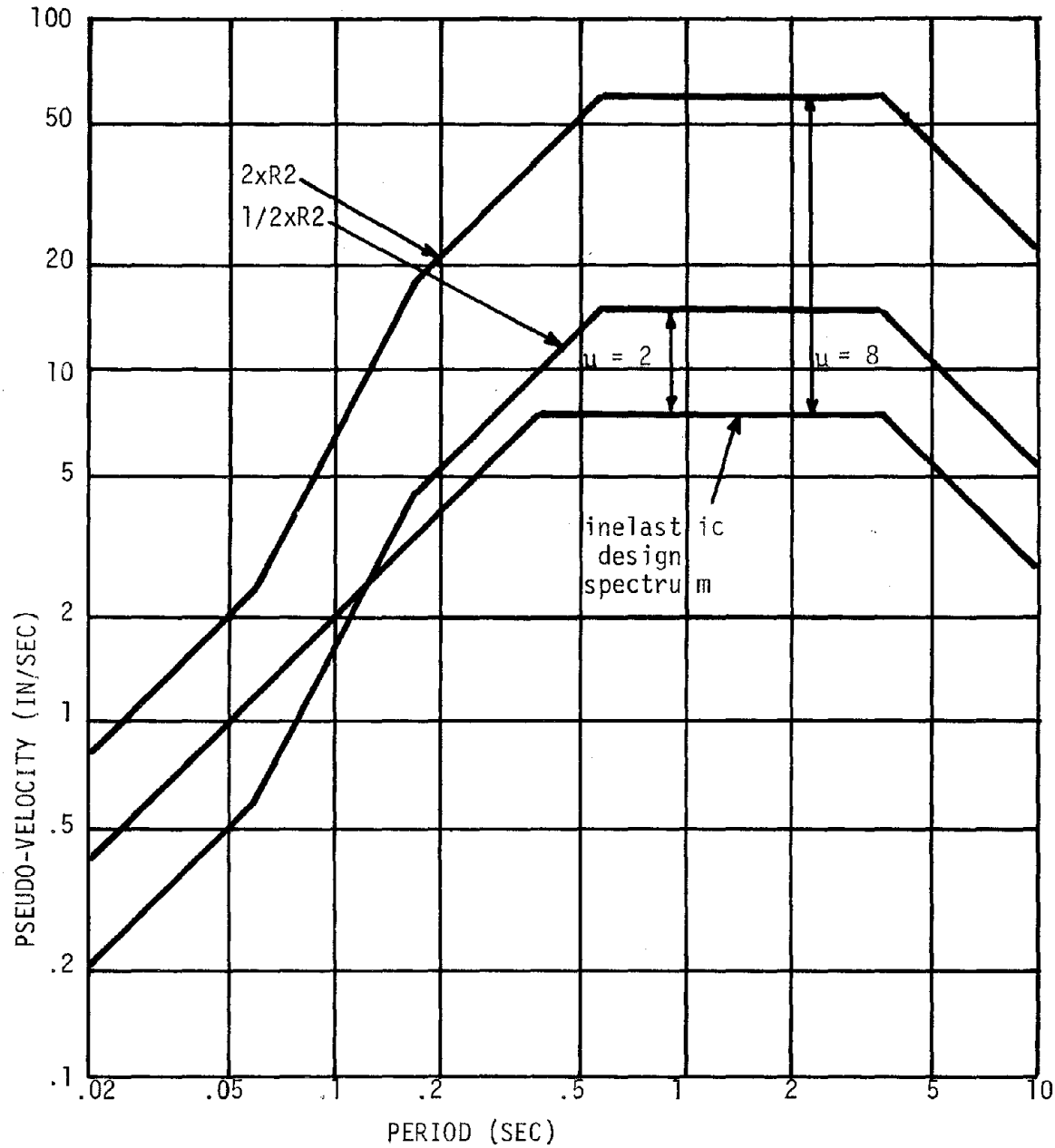

FIGURE 4.38 - ELASTIC SPECTRA, INTENSITY = 1/2 x R2 AND
2 x R2 - INELASTIC DESIGN SPECTRUM

3) It is possible that use of the Newmark-Hall inelastic spectrum to design for smaller levels of damping results in unfactored designs which are less unconservative than the design for 5% damping. More research is necessary to determine the effect of assumed design damping on response.

4) Ductility response to earthquakes having an intensity equal to 1/2 the design intensity remains uniform and assumes an expected level which is one half the design ductility. Response to earthquakes having twice the intensity of the design earthquake is characterized by much greater ductility values in lower-story members than in upper-story members.

5) The results of Section 4.4.3 indicate that strength factors necessary to control ductility response to design earthquakes of greater intensity would have to be larger and would have to vary more with height than the factors determined in Section 4.2.

4.5 EVALUATION OF THE INELASTIC SEISMIC DESIGN PROCEDURE

It is apparent from the results reported in Section 4.1 that straightforward application of the inelastic design procedure using an inelastic design spectrum which is detailed in Chapter 2 results in local member ductilities which exceed the desired values. Four possible factors which could contribute to the discrepancy between local ductilities and design ductility are suggested below. A discussion of each factor follows.

1) The calculated elastic response spectra of the simulated motions used in the time integration analysis of each frame may not match the target elastic spectrum from which the inelastic design spectrum was obtained at the periods of greatest importance.

2) The rules used to determine the Newmark-Hall inelastic design spectrum may be unconservative.

3) Predicting inelastic response of a multi-degree-of-freedom systems (MDOFS) by combining modal responses (SRSS) determined through the use of an inelastic spectrum, a procedure which cannot be justified theoretically, may be unconservative.

4) Use of elastic modal properties (periods, damping, participation factors) to determine total inelastic response from individual modal responses according to SRSS may be unconservative because of changes which occur in effective modal properties with the onset of extensive yielding in structural members.

Table 4.5 summarizes the results of efforts aimed at determining which of the factors listed above is responsible for the unconservative nature of the inelastic design procedure. The percent difference between the elastic target spectrum and the calculated elastic response spectra of motions #1, #2 and #3 of the fundamental period of the 4-story frame (T_1 = 0.967 sec.) and the difference between the target spectrum and the calculated spectra of motions #R1, #R2 and #R3 at the fundamental periods of the 10-story and 16-story frames (T_1 = 2.322 sec. and T_1 = 2.935 sec. respectively) are tabulated in table 4.5. It is apparent that in most instances the match between target and calculated spectra is good (difference of less than $\pm$ 10%). The two large differences (-12.79% and -20.21%) were a result of calculated responses which were less than the predicted response (indicated by the minus percentage). Thus it can be concluded that the discrepancies between local ductilities determined by

TABLE 4.5 - SDOF SYSTEM AND MAXIMUM LOCAL AND AVERAGE DUCTILITIES - UNFACTORED DESIGN

			DUCTILITY								
	Earth-quake	% Difference Elastic Spectra	Elasto-Plastic SDOFS	Bilinear SDOFS (5% Second Slope)	Maximum Local		Maximum Story Average		Average All Columns	Average All Girders	Average All Members
					Columns*	Girders	Columns	Girders			
4-Story T_1=.967	#1	- 1.94	3.496	3.371	11.697	3.490	8.152	2.997	7.240	1.825	4.919
	#2	- 4.02	3.209	2.938	12.175	2.891	7.283	1.996	6.297	1.568	4.270
	#3	-20.21	6.110	5.004	15.701	5.633	8.310	4.036	7.403	2.111	5.135
10-Story T_1=2.322	#R1	- 2.49	3.745	3.620	16.376	10.196	9.566	9.420	7.666	3.779	6.000
	#R2	+ 8.74	5.743	4.324	11.893	7.084	8.152	6.311	6.579	3.151	5.110
	#R3	+ 4.75	5.885	3.761	12.210	7.500	7.536	6.761	6.047	2.858	4.680
16-Story** T_1=2.935	#R1	-12.79	5.395	5.083							
	#R2	- 3.93	3.660	3.515							
	#R3	- 9.21	4.173	3.588							

* Maximum at section other than base of first-story column where rigid base-foundation connection exists.

** No analysis of unfactored design available.

time integration analysis and design ductility were not due to the use of artificial earthquakes which do not satisfy design conditions.

The rules used to derive the inelastic design spectrum were briefly examined as follows. The properties of elasto-plastic and bilinear (5% second slope) single-degree-of-freedom systems (SDOFS) having elastic natural periods equal to the fundamental period of each frame were calculated. The maximum resistance of each SDOFS was specified as necessary to ensure that the yield displacement of the SDOFS matched the design yield displacement given by the inelastic acceleration spectrum. Inelastic time integration analysis (22) was used to determine the maximum response of the 4-story frame SDOFS to motions #1, #2 and #3 and of the 10-story and 16-story frame SDOFS to #R1, #R2 and #R3. Maximum ductility defined as the ratio of total to yield displacement for each SDOFS is listed in table 4.5. The inelastic spectrum is intended to predict the response of elasto-plastic SDOFS, and an examination of the elasto-plastic SDOFS which were analyzed reveals maximum ductilities which exceeded the design ductility ($\mu = 4$) by as much as 50% (maximum ductility of 6.11). The maximum ductilities of the bilinear SDOFS, which are of greater interest here because of strain hardening assumed in the analysis of all frames, were reasonably close to the design ductility (maximum ductility of 5.083). Thus, although the rules used to determine the inelastic spectrum do not result in a reliable prediction of response of elasto-plastic SDOFS, they appear to be reasonable when strain hardening is included in the analysis of the system under consideration.

The remainder of table 4.5 tabulates maximum local ductilities and averages of local ductilities determined from inelastic time integration

analysis of the 4-story and 10-story frames. No analyses were made of the unfactored 16-story frame design (see Section 4.1.3). The columns in table 4.5 labeled maximum local ductility report maximum local column ductility occurring at any column end section other than an end section located at the base of the frame where a rigid base-foundation connection exists, and the maximum ductility occurring at any girder cross section. The column maximum ductilities for the six artificial motions range from 11.697 to 16.376; girder ductilities range from 2.891 to 10.196. The average of the maximum ductilities occurring at the eight column end sections in each story and the average of the ductilities occurring at the six girder cross sections in each story were computed and are listed in tables 4.6 and 4.7. The largest of these "story" averages is tabulated in table 4.5 for each motion. The last three columns of table 4.5 list the average of ductilities occurring at all column end sections, the average of all girder ductilities, and the average of the ductilities occurring in all members of the 4-story and 10-story frames.

If the results tabulated in table 4.5 are examined closely, the following facts are revealed. As expected the maximum local ductilities, indicating the greatest amount of inelastic behavior occurring at any end section, are larger than the average values by a significant amount. The average values decrease as more end sections are used to compute average values; however, even the average of local ductility occurring at all end sections exceeds the ductility calculated for the corresponding SDOFS in response to the same motion.

Veletsos and Vann (25) in a study of the inelastic response of multi-degree-of-freedom shear beam type systems to seismic disturbances concluded

TABLE 4.6 - AVERAGE DUCTILITY 4-STORY FRAME

	Earthquake #1		Earthquake #2		Earthquake #3	
STORY	COLUMNS	GIRDERS	COLUMNS	GIRDERS	COLUMNS	GIRDERS
1	8.152	2.997	5.604	1.996	7.880	4.036
2	7.867	1.706	7.040	1.686	8.310	1.794
3	7.263	1.503	7.283	1.507	7.955	1.524
4	5.676	1.093	5.262	1.082	5.466	1.090
	Average of all Columns	Average of all Girders	Average of all Columns	Average of all Girders	Average of all Columns	Average of all Girders
	7.240	1.825	6.297	1.568	7.403	2.111
	Average of All Members		Average of All Members		Average of All Members	
	4.919		4.270		5.135	

TABLE 4.7 - AVERAGE DUCTILITY 10-STORY FRAME

	Earthquake # R1		Earthquake # R2		Earthquake # R3	
STORY	COLUMNS	GIRDERS	COLUMNS	GIRDERS	COLUMNS	GIRDERS
1	8.877	9.420	6.642	6.311	5.989	6.761
2	9.465	8.400	6.178	6.172	5.832	5.712
3	9.106	7.301	7.707	5.867	7.536	4.722
4	9.566	4.092	8.152	3.975	7.121	2.441
5	7.208	2.050	7.694	2.527	5.412	2.046
6	7.444	1.729	7.702	1.968	6.653	2.101
7	7.072	1.451	6.301	1.488	6.258	1.472
8	5.765	1.318	6.182	1.276	5.871	1.296
9	7.952	1.207	5.379	1.132	6.078	1.172
10	4.206	0.825	3.856	0.798	3.718	0.812
	Average of All Columns	Average of All Girders	Average of All Columns	Average of All Girders	Average of All Columns	Average of All Girders
	7.666	3.779	6.579	3.151	6.047	3.858
	Average of All Members		Average of All Members		Average of All Members	
	6.000		5.110		4.680	

that extensive yielding occurring in the base spring of such systems results in a change in the "apparent mode of vibration." This in turn results in an inelastic first mode participation factor which is greater than the elastic first mode participation factor. Suhendra (23) in backfiguring effective inelastic modal properties of MDOFS based on the results of time integration seismic analysis found that inelastic behavior causes greater increases in effective damping in lower modes than in higher modes. This suggests that higher modes may assume a greater importance in determining inelastic response than in determining elastic response. The studies of Veletsos and Vann and Suhendra indicate that assuming that elastic modal properties may be used in computing inelastic modal responses to determine total inelastic response can result in unconservative estimation of total response.

The following conclusions can be made from the results presented; however, they must be viewed with caution because of the limited number of frames which were studied.

1) The design of the three frames studied herein based on the use of an unmodified inelastic response spectrum is unconservative and results in local and average ductilities which exceed the design ductility.

2) The artificial earthquakes used in the time integration analyses and the rules used to derive the inelastic design spectrum do not introduce sufficient error to account for the unconservative design.

3) Based on conclusion 2), the observed averages of local ductilities, and the results reported by Veletsos and Vann and Suhendra, it can be concluded that the inelastic design procedure investigated in this thesis is unconservative because of the erroneous

assumption that elastic modal responses, based on elastic modal properties and determined from an inelastic response spectrum, can be combined by calculating SRSS values to determine total inelastic response.

CHAPTER 5 - SUMMARY OF CONCLUSIONS AND SUGGESTIONS FOR FURTHER RESEARCH

5.1 CONCLUSIONS

This report details an investigation designed to determine the reliability of an inelastic seismic design procedure based upon elastic modal analysis using an inelastic response spectrum. This was accomplished by computing the inelastic response to simulated earthquake motions, derived from the design response spectrum, of three steel moment-resisting frames. The important conclusions of this research are repeated below to summarize the results. It must be emphasized that these conclusions are subject to the limitations imposed by the analysis techniques used, the modelling assumptions made, and the small number of frames investigated.

1) The unmodified inelastic seismic design procedure based on an elastic modal analysis together with an inelastic response spectrum appears to be unconservative. Frames designed according to this procedure exhibit excessive inelastic behavior when subjected to simulated motions with calculated response spectra matching the design elastic response spectrum.

2) The inelastic seismic design procedure is unconservative primarily because the individual modal responses based on elastic modal properties cannot be combined according to SRSS to compute total inelastic response with sufficient accuracy.

3) Strength factors can be used to increase member capacity, determined according to the unmodified inelastic design procedure, to successfully control the level and distribution of inelastic behavior. Column strength factors should be nearly uniform over height with slight increases at the base of the frame and in upper stories below the roof level. Exterior column strength

factors should be larger than interior column strength factors. Girder strength factors should decrease over the height of the frame and should be taken as 1.0 in members in which necessary strength to resist uniform gravity loads dominates design. The inelastic response of exterior columns is more sensitive to changes in member strength than is the response of girders and interior columns. Thus, it is best to attempt to refine control of ductility distribution and level by modifying girder strength and interior column strength.

4) Spectral factors necessary to properly control inelastic behavior by increasing design forces determined by modal analysis using an inelastic response spectrum are generally uniform over height, but vary more in upper stories than do strength factors. Spectral design forces must be increased 1.5 to 1.7 times to obtain desired inelastic response under design loading conditions.

5) The P-Δ effect does not alter ductility response significantly. It is possible to successfully include the P-Δ effect in design through static analysis of the effect of P-Δ forces determined from a knowledge of frame mass and interstory displacement resulting from modal analysis.

6) The details of earthquake motions can seriously effect the distribution and, to lesser extent, the level of inelastic behavior.

7) The level of damping assumed in analysis does not greatly effect the distribution of maximum ductility response.

8) It is possible that the unmodified inelastic seismic design procedure for smaller levels of assumed damping (e.g., damping = 2% of critical) might be less unconservative than for the 5% level considered herein.

9) Increased earthquake intensity results in much greater increases in yielding in lower stories than in upper stories, suggesting

that greater variation in strength factors over height is necessary to control response to stronger motions. Decreased earthquake intensity results in continued uniform distribution of inelastic behavior at a reduced level.

5.2 SUGGESTIONS FOR FURTHER RESEARCH

The following are suggestions for continued research on the use of inelastic spectra in seismic design.

1) Research should be conducted to determine possible modifications to the Newmark-Hall inelastic design spectrum to generalize the strength factor approach used herein.

2) The effect of design damping and design earthquake intensity on inelastic response should be examined.

3) Application of the design procedures discussed in this report to reinforced concrete structures should be investigated. The moment capacities of reinforced concrete members can be more easily adjusted to obtain the best possible distribution of inelastic behavior.

In spite of the design difficulties demonstrated by this investigation, it is felt that there is great promise in the use of inelastic spectra in the seismic design of structures.

REFERENCES

1. American Institute of Steel Construction, Inc., Manual of Steel Construction, 7th Edition.

2. Anderson, J.C. and Bertero, V.V., "Seismic Behavior of Multistory Frames Designed by Different Philosophies," Earthquake Engineering Research Center Report No. EERC 69-11, University of California, Berkeley, California, October, 1969.

3. Anderson, J.C. and Gupta, R.P., "Earthquake Resistant Design of Unbraced Frames," Proceedings of the ASCE, Journal of the Structural Division, Vol. 98, No. ST11, November, 1972, pp. 2523-2539.

4. Applied Technology Council, An Evaluation of a Response Spectrum Approach to Seismic Design of Buildings, A Study Report for Center for Building Technology, Institute of Applied Technology, National Bureau of Standards, September, 1974.

5. Aziz, T.S., "Inelastic Dynamic Analysis of Building Frames," M.I.T. Department of Civil Engineering Research Report R76-37, Order No. 554, August 1976.

6. Berg, G.V., "Response of Multi-story Structures to Earthquake," ASCE Transactions, Vol. 127, 1962, Part I, pp. 705-720.

7. Biggs, J.M., Introduction to Structural Dynamics, McGraw-Hill, New York, 1964.

8. Clough, R.W. and Benuska, K.L., "Nonlinear Earthquake Behavior of Tall Buildings," Proceedings of the ASCE, Journal of the Engineering Mechanics Division, Vol. 93, No. EM3, June, 1967, pp. 129-146.

9. Clough, R.W., Benuska, K.L., Wilson, E.L., "Inelastic Earthquake Response of Tall Buildings," Proceedings of the Third World Conference on Earthquake Engineering, Vol. II, New Zealand, 1965, pp. 68-89.

10. Gasparini, D.A. and Vanmarcke, E.H., "Simulated Earthquake Motion Compatible with Prescribed Response Spectra," M.I.T. Department of Civil Engineering Research Report R76-4, Order No. 527, January 1976.

11. Goel, S.C. and Berg, G.V., "Inelastic Earthquake Response of Tall Steel Frames," Proceedings of the ASCE, Journal of the Structural Division, Vol. 94, No. ST8, August 1968, pp. 1907-1934.

12. Haviland, R.W., Biggs, J.M., Anagnostopoulos, S.A., "Inelastic Response Spectrum Design Procedures for Steel Frames," M.I.T. Department of Civil Engineering Research Report R76-40, Order No. 557, September 1976.

REFERENCES

(continued)

13. Hisada, T., Nakagawa, K., Izumi, M., "Earthquake Response of Idealized Twenty Story Buildings Having Various Elasto-Plastic Properties," Proceedings of the Third World Conference on Earthquake Engineering, Vol. II, New Zealand, 1965, pp. 168-184.

14. Isbell, J.E. and Biggs, J.M., "Inelastic Design of Building Frames to Resist Earthquakes," M.I.T. Department of Civil Engineering Research Report R74-36, Structures Publication No. 393, May, 1974.

15. Luyties, W.H., Anagnostopoulos, S.A., Biggs, J.M., "Studies on the Inelastic Dynamic Analysis and Design of Multi-Story Frames," M.I.T. Department of Civil Engineering Research Report R76-29, Order No. 548, July 1976.

16. Newmark, N.M. and Hall, W.J., "Procedures and Criteria for Earthquake Resistant Design," Building Practices for Disaster Mitigation, Building Science Series 46, National Bureau of Standards, February, 1973, pp. 209-236.

17. Newmark, N.M. and Rosenblueth, E., Fundamentals of Earthquake Engineering, Prentice-Hall, Inc., Englewood Cliffs, New Jersey, 1971.

18. Penzien, J., "Elasto-Plastic Response of Idealized Multi-Story Structures Subjected to a Strong Motion Earthquake," Proceedings of the Second World Conference on Earthquake Engineering, Vol. 2, Tokyo, Japan, 1960, pp. 739-760.

19. Piqué, J.R., "On the Use of Simple Models in Nonlinear Dynamic Analysis," M.I.T. Department of Civil Engineering Research Report R76-43, Order No. 559, September, 1976.

20. Roesset, J.M., Unpublished Users' Guide for the Computer Program APPLE PIE, M.I.T., Cambridge, Massachusetts.

21. Scaletti, H., Unpublished User's Guide for Static Analysis Program, M.I.T., Cambridge, Massachusetts.

22. Schumacker, E., "A Guide to the Use and Internal Flow of the Anagnostopoulos Program for Nonlinear Dynamic Analysis of Building," Seismic Design Decision Analysis, Internal Study Report No. 58, M.I.T. Department of Civil Engineering, June, 1975.

23. Suhendra, R., "Nonlinear Dynamic Response of Steel Frames," Thesis presented to the Massachusetts Institute of Technology, Cambridge, Massachusetts, in 1977, in partial fulfillment of the requirements for the degree of Master of Science.

REFERENCES

(continued)

24. Thomaides, S.S., "Earthquake Response of Systems with Bilinear Hysteresis," Proceedings of the ASCE, Journal of the Structural Division, Vol. 90, No. ST4, August, 1964, pp. 123-143.

25. Veletsos, A.S. and Vann, W.P., "Response of Ground-Excited Elasto-plastic Systems," Proceedings of the ASCE, Journal of the Structural Division, Vol. 97, No. ST4, April, 1971, pp. 1257-1281.

26. Walpole and Shepherd, "Elasto-Plastic Seismic Response of Reinforced Concrete Frame," Proceedings of the ASCE, Journal of the Structural Division, Vol. 95, No. ST10, October, 1969, pp. 2031-2055.

APPENDIX A

TABLE A1 - ELASTIC MODAL PROPERTIES - 4-STORY FRAME

	Mode 1	Mode 2	Mode 3	Mode 4
Period (Sec)	0.967	0.320	0.186	0.134
Story	Mode Shape	Mode Shape	Mode Shape	Mode Shape
4	1.4311	1.2121	-0.8278	-0.2987
3	1.2008	-0.2455	1.3965	0.8859
2	0.8061	-1.3347	-0.0766	-1.3417
1	0.3517	-0.9721	-1.2667	1.2507

TABLE A2 - ELASTIC MODAL PROPERTIES - FIRST FOUR MODES 10-STORY FRAME

	Mode 1	Mode 2	Mode 3	Mode 4
Period (Sec)	2.322	0.835	0.496	0.339
Story	Mode Shape	Mode Shape	Mode Shape	Mode Shape
10	0.9393	0.9918	-0.8914	-0.7442
9	0.8913	0.6531	-0.1226	0.4791
8	0.8094	0.1359	0.6945	0.8811
7	0.7280	-0.2509	0.8586	0.2007
6	0.6262	-0.5794	0.5450	-0.6694
5	0.5239	-0.7521	0.0256	-0.7994
4	0.4108	-0.7895	-0.4955	-0.2444
3	0.3034	-0.7009	-0.7592	0.4348
2	0.1966	-0.5112	-0.7143	0.7638
1	0.0954	-0.2656	-0.4198	0.5568

TABLE A3 - ELASTIC MODAL PROPERTIES - FIRST FOUR MODES
16-STORY FRAME

	Mode 1	Mode 2	Mode 3	Mode 4
Period (Sec)	2.935	1.112	0.659	0.460
Story	Mode Shape	Mode Shape	Mode Shape	Mode Shape
16	0.8110	-0.8674	-0.8354	0.7534
15	0.7801	-0.6888	-0.4062	0.0343
14	0.7308	-0.4015	0.1871	-0.6684
13	0.6816	-0.1514	0.5311	-0.7355
12	0.6210	0.1130	0.6963	0.3605
11	0.5634	0.3123	0.6493	0.1036
10	0.5019	0.4708	0.4465	0.4955
9	0.4442	0.5703	0.1835	0.6458
8	0.3871	0.6192	-0.0943	0.5466
7	0.3303	0.6236	-0.3381	0.2693
6	0.2733	0.5888	-0.5158	-0.0831
5	0.2194	0.5224	-0.5968	-0.3827
4	0.1672	0.4305	-0.5855	-0.5619
3	0.1196	0.3262	-0.4946	-0.5774
2	0.0745	0.2120	-0.3452	-0.4518
1	0.0362	0.1059	-0.1789	-0.2476